INFORMATION TO USERS

This manuscript has been reproduced from the microfilm master. UMI films the text directly from the original or copy submitted. Thus, some thesis and dissertation copies are in typewriter face, while others may be from any type of computer printer.

The quality of this reproduction is dependent upon the quality of the copy submitted. Broken or indistinct print, colored or poor quality illustrations and photographs, print bleedthrough, substandard margins, and improper alignment can adversely affect reproduction.

In the unlikely event that the author did not send UMI a complete manuscript and there are missing pages, these will be noted. Also, if unauthorized copyright material had to be removed, a note will indicate the deletion.

Oversize materials (e.g., maps, drawings, charts) are reproduced by sectioning the original, beginning at the upper left-hand corner and continuing from left to right in equal sections with small overlaps.

Photographs included in the original manuscript have been reproduced xerographically in this copy. Higher quality 6" x 9" black and white photographic prints are available for any photographs or illustrations appearing in this copy for an additional charge. Contact UMI directly to order.

ProQuest Information and Learning
300 North Zeeb Road, Ann Arbor, MI 48106-1346 USA
800-521-0600

University of Alberta

Development of a Micro-Scale Dynamic Model for Wear Simulation

by

Khaled Taher Elalem 

A thesis submitted to the faculty of Graduate Studies and Research in partial fulfillment of the requirements for the degree of Master of Science

In

Materials Engineering

Department of Chemical and Materials Engineering

Edmonton, Alberta
Fall 2000

University of Alberta

Library Release Form

Name of Author: Khaled Taher Elalem

Title of Thesis: Development of a Micro-Scale Dynamic Model for Wear Simulation

Degree: Master of Science

Year this Degree Granted: 2000

Kelalem

Khaled T. Elalem
404 10610-111Street
Edmonton, AB T5H 3E9

Date: Aug 30, 2000

University of Alberta

Faculty of Graduate Studies and Research

The undersigned certify that they have read, and recommend to the Faculty of Graduate Studies and Research for acceptance, a thesis entitled Development of a Micro-Scale Dynamic Model for Wear Simulation submitted by Khaled Taher Elalem in partial fulfillment of the requirements for the degree of Master of Science in Materials Engineering.

Dongyang Li

Dr. Dongyang Li, Supervisor

Ru Chongqing

Dr. Chongqing Ru

Phillip Choi

Dr. Phillip Choi

Date: Aug. 30, 2000

Abstract

Wear is a complex surface damage process. Although experiment is the prime approach in determination of wear behaviour of metals, the behaviour of a material may not be always explained since there could be several wear mechanisms involved simultaneously. Computer modeling provides an effective approach for fundamental understanding of wear process. However, many current models are built on tribological rules or assumptions, and therefore not always predictive. Efforts have been made to develop more effective models, which can be used to explore realistic wear processes. In this work, a micro-scale dynamic model (MSDM) was proposed to simulate wear of materials. The model was developed based on fundamental physical laws without employing empirical equations or tribological rules. In this model, a material system is discretized and represented using a discrete lattice. Each lattice site represents a small volume of the material. During wear, a lattice site may move under the influence of external force and the interaction between the site and its adjacent sites. The site-site interaction depends on the mechanical properties of the material, such as the elastic modulus, yield strength, work-hardening and fracture strength. The movement and trajectory of lattice sites during wear were determined using Newton's law of motion. A bond can be broken when the total accumulated plastic strain exceeds the fracture strain. A site or a cluster of sites is worn away if all bonds connecting the site or the cluster to its neighbors are broken. This model was applied to single-phase and composite materials abraded under dry sand/rubber-wheel abrasion condition. In order to justify the model, finite element analysis was conducted to determine stress/strain in the contact region in

comparison with the MSDM simulation. Wear tests were also performed to evaluate wear resistance of various materials in comparison with modeling. Good agreement between the simulation and experimental results has been found.

University of Alberta

Dedication

Special thanks to my family and friends for their support and encouragement.

Acknowledgment

I would first like to thank my supervisor, Dr D. Y. Li for his constant guidance and advice throughout this endeavour. His useful suggestions and innorative ideas have been of great assistance to me in completing this project.

I would also like to thank the Department of Chemical and Materials Engineering staff for their help and assistance, especially Barton Bob, Jack Gibeau, Bob Scott, and Bob Konzuk for their technical support in conducting the experimental work and in using the computer laboratory facilities.

My special thanks are due to my colleagues, Carolina Diaz and Demetri Giannitsios for their friendship and all the memorable experiences during our graduate education.

Finally, I am grateful for financial support from the Natural Science and Engineering Research Council of Canada (NSERC), Syncrude Canada Ltd. and Alberta Science and Research Authority (ASRA).

Table of Contents

Chapter 1 - Introduction and Literature Review

1.1. General introduction to wear 2

- Wear phenomena 2

- Experimental techniques for abrasive wear testing 6

1.2. Wear Modeling Approaches 9

a) Macro-Models 9

b) Atomistic-Models 11

c) Objective of this work - Development of a new computational wear model 12

1.3. The Dry Sand/Rubber-Wheel Abrasion Testing 15

Reference list for Chapter 1 17

Chapter 2 - Research Paper, A Microscale Dynamical Model for Wear Simulation

2.1. Introduction 21

2.2. Description of the Micro-Scale Dynamic Model 23

2.2.1 Interaction between lattice sites 24

2.2.2 The movement of a lattice site 26

2.2.3. Simulation of material response to external force 27

2.3. Application of the MSDM approach to an Abrasion Process 28

2.4. Conclusions 38

Reference list for Chapter 2 40

Table of Contents (continued)

Chapter 3 - Research Paper, Dynamical Simulation of an Abrasive Wear Process

3.1. Introduction 43

3.2 Results and Discussion 45

- Description of the Micro-Scale Dynamic Model (MSDM) 45

- Modeling an Abrasive Wear Process 49

3.3. Conclusions 56

Reference list for Chapter 3 57

Chapter 4 - Research Paper, Dynamic Simulation of Abrasive Wear of Composite Materials

4.1. Introduction 60

4.2. Model Description 63

- Interaction between Lattice Sites 64

- The Movement of a Lattice Site 68

4.3. Application of the MSDM approach to Study Abrasive Wear of Composites 69

4.4. Conclusions 73

Reference list for Chapter 4 75

Chapter 5 - Research Paper, Variations in wear loss with respect to load and sliding speed under dry sand/rubber wheel abrasion condition: a modeling study

5.1. Introduction 78

5.2. Results and Discussions 80

Table of Contents (continued)

-The MSD model 80

5.2.1. Effect of Load on Wear 81

5.2.2. Effect of Sliding Speed on Wear 86

- Remark Comments 90

5.3. Conclusions 90

Reference list for Chapter 5 92

Chapter 6 - General Discussion and Conclusions

6.1. Summary of the research results presented in different papers 94

6.2. Some technical details of the model that are not given in the papers 96

6.2.1. Flow chart 96

6.2.2. Interaction between ceramic and metal phases 97

6.2.3. Determination of the time interval (Δt) 99

6.2.4. Simplification of the force on a sand particle from the rubber wheel 101

6.2.5. Interaction between sand and metal (surface interaction) 101

6.2.6. Discussion on mechanical properties used in the model 103

-The force coefficient, k 103

-The tensile properties 103

6.3. Future work 104

6.4. Conclusions 105

Appendix 107

List of Tables

Table 2-1. Mechanical properties of the materials 34

Table 2-2. Chemical compositions of the AR steels (wt.%) 34

Table 3-1. Mechanical properties of the materials 53

Table 5-1. Mechanical properties of the materials 81

List of Figures

Figure 1-1. The dump truck box is subjected to abrasive wear 2

Figure 1-2. A bucket wheel used in mining Canadian tar sands, suffering from abrasive wear 3

Figure 1-3. Erosive wear of hardened steel (x50) 3

Figure 1-4. Three common abrasion processes 5

Figure 1-5. Schematic illustration of three common methods for abrasive wear tes testing and testers in the wear/surface laboratory at University of Alberta 7

Figure 1-6. FEM analysis of asperity interaction during sliding wear 7

Figure 1-7. Crack propagation simulated using the MD method 13

Figure 1-8. Rubber wheel tester used in the present work 16

Figure 2-1. The linear approximation of a stress-strain curve 25

Figure 2-2. Illustration of the vectors used in equation (4) 27

Figure 2-3. Schematic of a standard abrasive wear test (ASTM G65) 29

Figure 2-4. The pressure distribution between the rubber wheel and the specimen surface 31

Figure 2-5. The relation between the relative volume loss and the applied load 33

Figure 2-6. Relative volume losses of copper, steel and molybdenum 36

Figure 2-7. (a) Relative volume losses of three AR steels predicted using the MSDM approach, and (b) experiment results 37

Figure 3-1. The linear approximation of a stress-strain curve 47

Figure 3-2. Schematic of a standard abrasive wear test (ASTM G65) 49

Figure 3-3. The pressure distribution in the contact region 50

Figure 3-4(a). Strain distribution obtained using the MSDM 52

List of Figures (continue)

Figure 3-4(b). Strain distribution obtained using a commercial FEM package (ANSYS) 53

Figure 3-5. Relative volume losses of aluminum, copper, stainless steel and steel predicted using the MSDM 55

Figure 3-6. Volume losses of aluminum, copper, stainless steel and steel (experiment) 56

Figure 4-1. Schematic illustration of a standard abrasion test (ASTM G65) 64

Figure 4-2. The linear approximation of a stress-strain curve 66

Figure 4-3. Relative wear losses of Aluminum and 20%SiC-Al alloy composite with respect to the applied load 71

Figure 4-4. Sample microstructure (20%SiC-Al alloy) 71

Figure 4-5. Relative volume loss against the volume fraction of SiC particles under a relative load L=2 72

Figure 4-6. The effect of carbide size on the relative volume loss (under relative load L=2) 73

Figure 5-1. Rubber wheel test equipment 79

Figure 5-2. The effect of applied load on wear (modeling) 82

Figure 5-3. The effects of load on wear losses (experimentally) 83

Figure 5-4. The percentage of site loss of an abrasive sand particle (a) under a low load (L=1), and (b) under a high load of (L=3), given by modeling 84

Figure 5-5. (a) original sand, (b) worn sand after wear test under a load of 25N, and © worn sand after wear test under a higher load of 150N. The sliding speed=4 m/s (adapted from ref. [6]) 86

Figure 5-6. The effect of sliding speed on wear (modeling) 87

Figure 5-7. The effect of sliding speed on wear (experimentally) 88

Figure 5-8. The damage to sand particle given by modeling (a) at low sliding speed (RSS=1), and (b) at a higher sliding speed (RSS=5) 89

List of Figures (continue)

Figure 6-1. Flow chart of the MSDM 96

Figure 6-2. Illustration of typical tensile curve of ceramic and metal materials 97

Figure 6-3. Variation in wear loss verses Δt 100

Figure 6-4. Sand-Metal interaction 102

List of Abbreviations and Symbols

MSDM	Micro-Scale Dynamic Model
FEM	Finite Element Methods (Analysis)
MD	Molecular Dynamics
W	the weight loss of a material
L	the normal contact force
d	the slid distance
H	hardness of the material
K	wear coefficient for a specific material
t	time
Δt	time interval
l_o	the unit length of the lattice or the bond length in stress-free condition
l	bond length after the deformation
E	the slope of the stress-strain curve of the material
$\vec{F}$	the total force applied to the lattice site
f	force between a pair of adjacent sites
n	the number of sites adjacent to a specific site
$\vec{v}$	the velocity of a site
$\vec{r}$	the position of a site
P_{max}	the maximum pressure
a	one half of the contact region between the rubber wheel and the specimen

List of Abbreviations and Symbols (continued)

E_R	the elastic modulus of the rubber wheel
R	the radius of the wheel
m	mass of the lattice site
Δl	total deformation of the bond
Δlc	deformation of the ceramic bond
Δl_m	deformation of the metal bond
Δl_y	deformation of metal at yielding
$f_{(c,m)}$	the force on the ceramic site
$f_{(m,c)}$	the force on metal site
Ec	elastic modules of ceramic
E_{me}	elastic modulus of metal
E_{mp}	plastic modulus of metal
ε_y	yield strain of the metal
ε_c	strain of ceramic
ε_m	strain of metal
σ	stress
σ_y	yield strength
σ_T	tensile strength
Ω	plastic deformation

Chapter 1

Introduction and Literature Review

1.1 General introduction to wear

-Wear phenomena

Wear is defined by the American Society for Testing and Materials (ASTM) [1] as 'the damage to a solid surface, generally involving the progressive loss of material, due to relative motion between two moving surfaces'. Such a process is complicated, involving time-dependent deformation, failure and removal of materials at the counter face [2]. Wear occurs in a wide variety of operations. The following are a few examples of wear in industry.

Figure 1-1. The dump truck box is subjected to abrasive wear

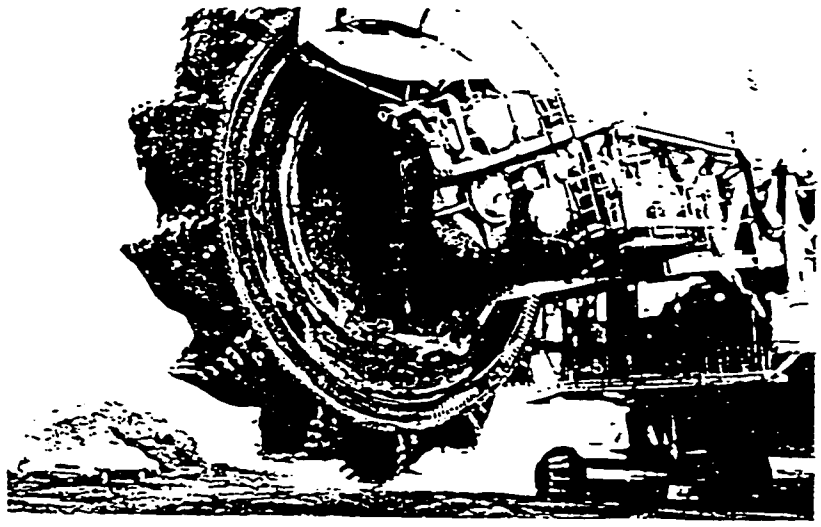

Figure 1-2. A bucket wheel used in mining Canadian tar sands, suffering from abrasive wear

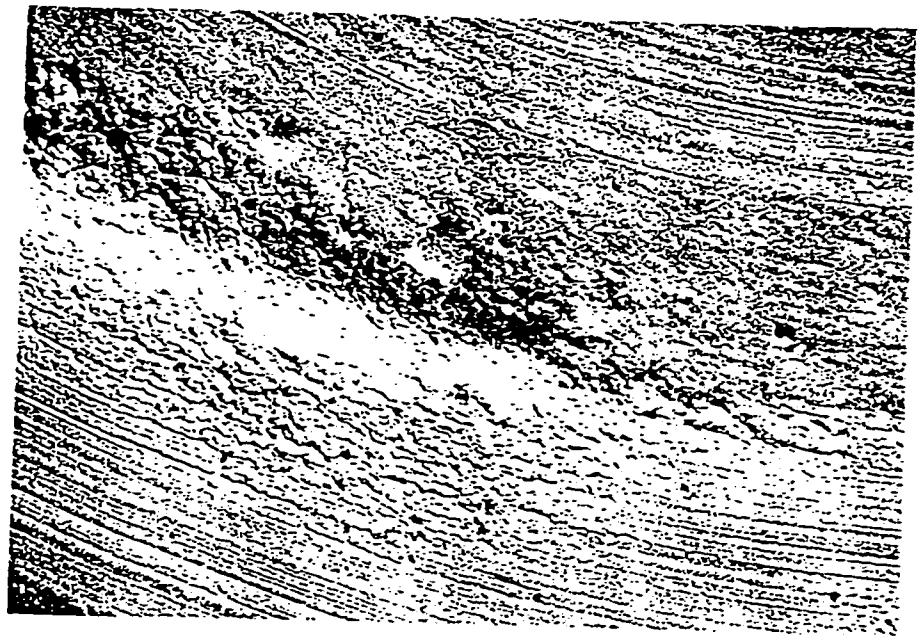

Figure 1-3. Erosive wear of hardened steel (x50)

Wear is often the major factor limiting the service life and the performance of machine components. Although it is a surface destructive process, wear may lead to total failure of a mechanical component or even the entire system [3]. In many industries, repairing and replacing worn parts significantly increase the production cost. The capital loss due to wear and friction is very large. In north America, it has been estimated that wear and friction cost Canada in excess of $ 5 billion/year and cost the United States more than $ 100 billion per annum [3,4].

Wear may occur in different modes such as abrasion, erosion, adhesive wear and corrosive wear, among which abrasion is the most common mode in industry. Abrasive wear is defined as 'The action of a hard, sharp material cutting through the surface of a softer material' [5]. Figure 1-4 schematically illustrated three common abrasion processes. Abrasive wear takes about 30% of total wear loss and the cost of this wear mode is very high which is in the range of 1 ~ 4 % of the gross national product of an industrialized nation [5]. The effect of abrasion is particularly evident in the agriculture, mining, and mineral processing industries, which involve earth moving and handling of dirt, rock, and minerals [3]. The abrasion rate depends on the characteristics of each surface, the presence of abrasives between the surfaces in contact, the speed of contact, and environmental influences [6-8].

Wear of a material is strongly affected by its mechanical properties and the wear condition. Hardness is considered to be the main mechanical parameter. The relation between wear and mechanical properties may be described approximately by the Archard equation [5]:

$$W = K.\frac{L.d}{H} \tag{1.1}$$

where, W is the weight loss of a material, L is the normal contact force, d is the slid distance, H is the hardness of the material, and K is a wear coefficient for a specific material. As indicated, wear loss increases as the contact force and the slid distance increase, respectively. Harder materials have lower wear losses than softer ones.

- Low-stress abrasion

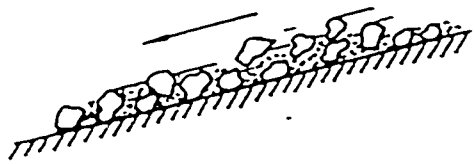

- Two-body abrasion

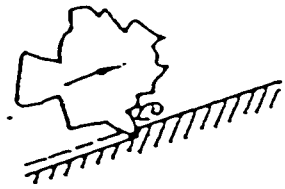

- Three-body abrasion

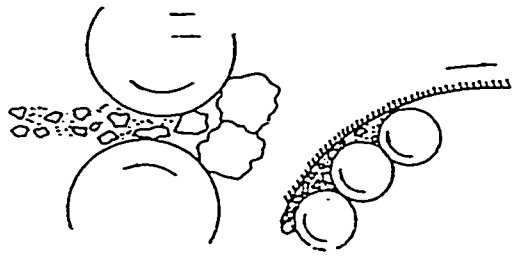

Figure 1-4. Three common abrasion processes

The mechanical properties of a material are strongly affected by its microstructure and corresponding properties of individual phases, e.g., the reinforced phase and the matrix of a composite. Hogmark et al. [9] and Sato and Mehrabian [10] showed a decrease in wear rate of an Al alloy when hard particles were added to the matrix. If the reinforcing particles are soft, the wear rate will increase as the volume fraction of the soft particles increases. In addition, the interfacial bonding is also critical [11]; when the strength of bonding between the matrix and the reinforcing phase decreases; an increase in the wear rate of the matrix would result.

- Experimental techniques for abrasive wear testing

There are many wear testers used to evaluate wear resistance of materials [12-16]. Figure 1-5 illustrates several wear test rigs commonly used for evaluation of abrasive wear in industry.

Dry sand/rubber-wheel tester is widely used in industry particularly for mining, oilsand petroleum and agriculture industries to evaluate abrasive wear of materials under low constant stress. During this test, a target specimen is pressed against a rotating wheel under a normal force and a flow of abrasive sand passes through the gap between the specimen and the rubber wheel. The target specimen is thus abraded and the volume loss is a measure of the abrasion resistance of the material. The slurry-pot tester is also often used to evaluate abrasion. A specimen can be rotated in dry sand or slurry, and abraded by the medium.

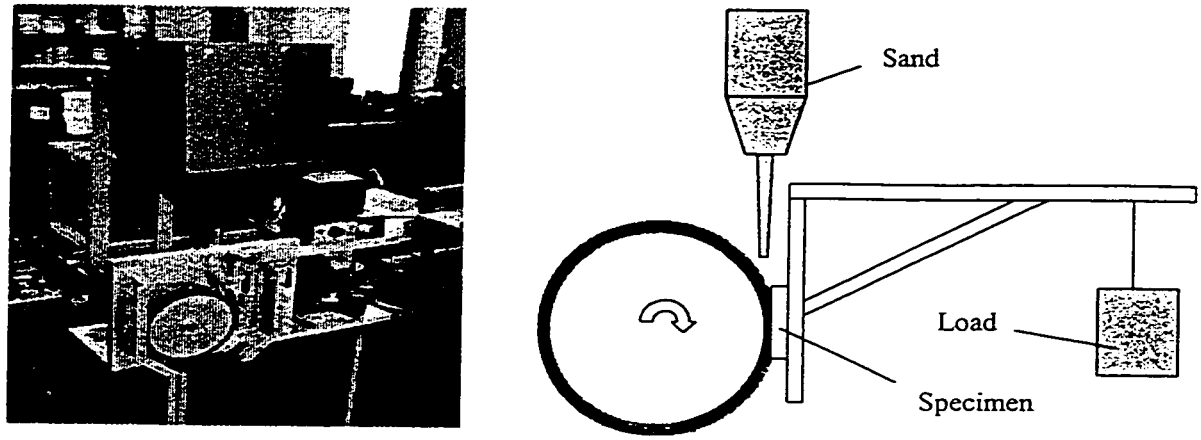

(a) Dry sand/rubber wheel abrasion tester

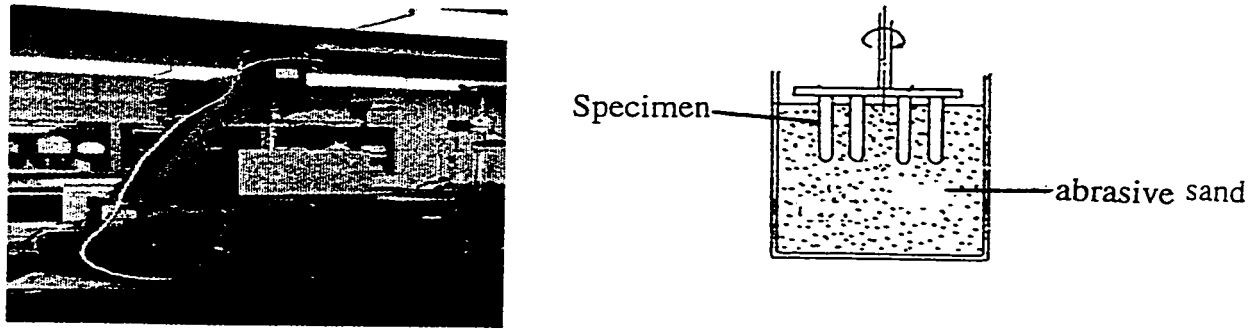

(b) Slurry-pot tester

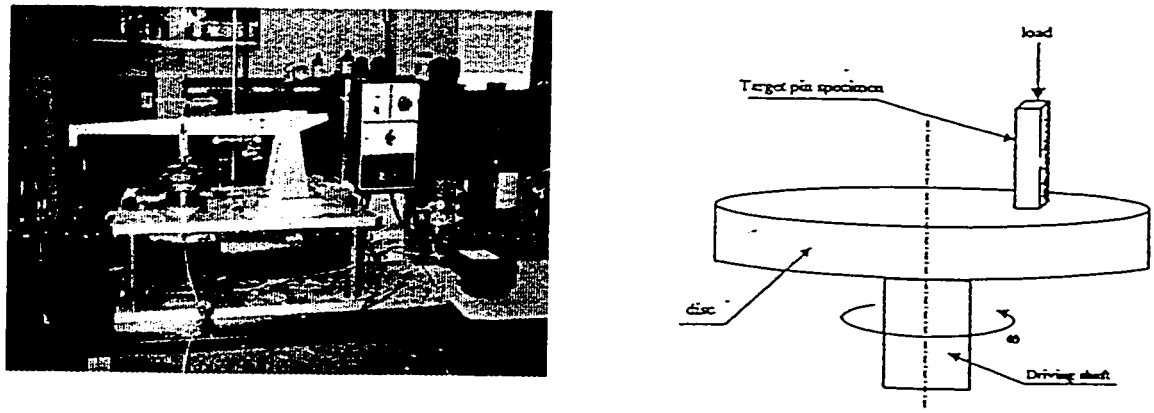

(c) Pin-on-disc wear tester

Figure 1-5. Schematic illustration of three common methods for abrasive wear testing and testers in the wear/surface laboratory at University of Alberta

Pin-on-Disc tester is another rig used to evaluate abrasive wear and friction properties of solid materials and coatings under dry or lubricated contact conditions. During this test, a pin specimen is pressed onto a rotating disc. The volume/weight loss of the pin specimen or the disc is a measure of the wear resistance of that material (pin or disc) against the other one (disc or pin). The applied load and sliding speed are variable.

However, a specific wear process can be very complicated, which may involve several wear mechanisms and the synergistic interaction between these mechanisms may make the obtained information difficult to be explained. In order to understand the wear mechanism and provide guidelines for materials design, selection and modification for specific applications, other approaches are also being developed to study wear phenomena.

One approach used to study wear phenomena is computer simulation. Computer simulation provides an effective and economical approach, which allows for the investigation of the effects of different factors on wear behavior of materials [17,18]. The advantage of this approach is that computational "experiments" could be performed under various controllable conditions, and effects of each parameter, e.g., microstructure, strain hardening and Young's modulus, on wear could be studied separately. A good computer model can be a powerful tool to explore the wear mechanism and to predict the performance of materials under different wear conditions.

1.2. Wear Modeling Approaches

There are many computer models proposed to simulate wear processes in different situations [19-42]. These models can be classified into two groups: Macro-modeling and Atomistic modeling.

a) Macro-Models:

Earlier mechanical models were developed to simulate wear and friction by using different techniques [19-22]. These models have different capabilities and can be used to investigate phenomena relevant to wear processes. For instance, one of the representative techniques is the finite element approach (FEM). The FEM approach [23-29] is widely used to analyze the contact mechanics of multi-asperity surfaces and to determine effects of important parameters on the deformation characteristics during wear process. The FEM analysis is performed by applying a fine mesh to descritize a specimen. The specimen is represented using many small blocks or elements. The strain and displacement of an individual element is described by a set of equations. The equations for each individual element can be joined into a large set of equations that describe the whole system. By solving this set of algebraic matrix equations, the stress/strain distribution can be determined under certain boundary conditions. If the strain reaches a critical value for fracture, the material fails in the place where the critical strain is reached. However, the FEM may not provide information in detail about the nucleation and propagation of cracks because of its statistical failure criteria. The FEM is usually

used to solve elastic/plastic contact problems in 2-dimensional and 3-dimensional spaces. Figure 1-6 gives an example of FEM analysis of asperity interaction during sliding wear.

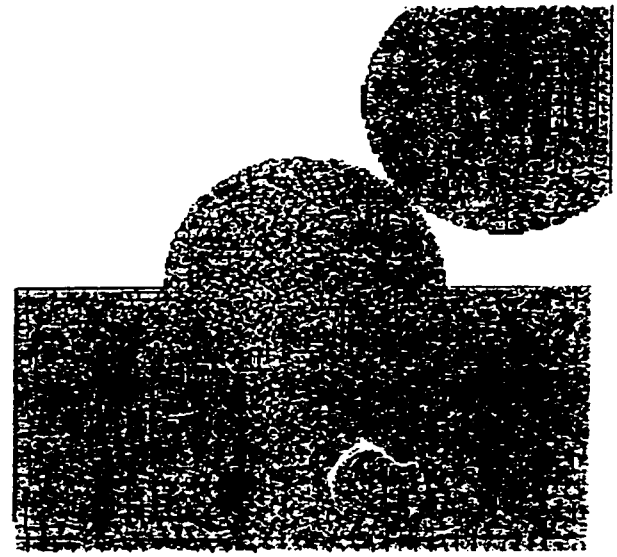

Figure 1-6. FEM analysis of asperity interaction during sliding wear

Nevertheless, the finite element method has been used to simulate wear and solve contact problems by identifying the location and magnitude of the maximum stress that is associated with the highest probability of failure [23-29] .

In addition to its limitation in determination of failure process, the FEM analysis is also restricted to the simulation of a limited number of asperities in contact. Since the analysis of the rough surfaces in contact involves many asperities, a large number of mesh elements are required and this makes the finite element approach unfeasible [43].

There are many other macro-models proposed to simulate erosion [30,31], sliding friction and wear [34,35], and sliding at elevated temperature [38]. These models provide information that is consistent with experimental observations. However, many models

were developed under some assumptions, based on existing tribological rules, or incorporated with empirical equations such as Archad wear equation [5]. This, more or less, weakens their predictive function. Furthermore, these macro-models only take into account the average mechanical properties of heterogeneous materials (e.g. multiphase and composite materials). Therefore, these models are not suitable for characterizing wear behavior of materials in fine detail such as the microstructural effect on wear. As a matter of fact, many models were proposed for mechanical design rather than for prediction of material performance [17]. Most of these models only deal with static situations. Therefore, these macro-models are developed for application of existing tribological theories to mechanical design rather than for fundamentally exploring wear mechanism and predicting wear behavior of materials.

b) Atomistic-Models:

Efforts have been made to develop more fundamental models for studying tribological phenomena and wear behaviour of materials, such as the Molecular Dynamics simulation (MD) [39,40]. MD technique deals with the motion and trajectory of individual atoms or molecules due to an applied force, and can be used to predict various dynamic processes at atomic or nano-meter level. Figure 1-7 presents a MD simulation example of crack propagation under a tensile stress. MD technique is a powerful computational method, which significantly advances the understanding of material behavior and relevant processes such as fracture and interfacial failure. In this method, Newton's law of motion is used to determine the movement and the location of an atom in a given system. Using this technique, wear behaviour of metals could be simulated on atomic level. When an

atom is under a force, its motion and trajectory are determined by the Newton's law of motion,

$$\vec{F} = m\frac{d^2\vec{r}}{dt^2} \tag{1.2}$$

where, m is the mass of the atom. $\vec{F}$ is the total force on the atom.

Molecular dynamics simulation is a powerful tool based on fundamental physics laws. MD technique may well characterize friction and wear processes at nanometer scale, when appropriate atomistic potentials are used. However, it is difficult to directly apply MD approach to a micro/macroscopic wear process because of the limited capability of current computing facilities [2]. Molecular Dynamic method is usually used to simulate a process involving 10^3~10^4 atoms. However, to simulate a bulk materials as small as 1 μm^3, one has to deal with 10^9~10^{10} atoms. Although faster parallel computers may allow the MD simulation of a system involving 10^8 atoms, it is not feasible to model wear behaviour of a realistic system that involves many micro/macroscopic factors such as the microstructural inhomogeneity and contact geometry, which has to be modeled using a large number of atoms.

c) Objective of this work - Development of a new computational wear model

The existing wear modeling approaches have provided useful tools for exploration of wear mechanisms and mechanical system design. However, these approaches have, more or less, some limitations as mentioned earlier. Great efforts are being continuously

made to improve these models through optimizing computing algorithm and incorporating with fundamental physical laws. The objective of this work is to develop

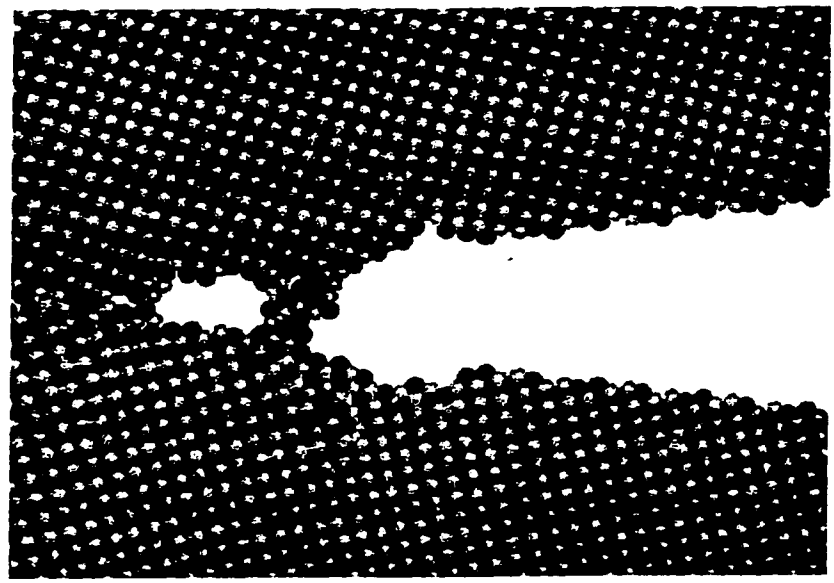

Figure 1-7. Crack propagation simulated using the MD method

an effective computational model that overcomes the constraints of the currently available models.

In this work, we proposed a new dynamic approach with the intention to overcome the limitations of both the macro-models and the atomistic approaches [23-40]. This, so-called Micro-Scale Dynamic Model (MSDM), was developed to simulate wear processes and to predict material performance during wear processes. This tentative model was proposed for dynamic wear simulation at microscopic level with the aim of building a bridge between the atomistic simulation technique and the macro models. This

model was built on Newton's law of motion, similar to the MD approach, but it can handle a significantly large system.

In this model, a material system is discretized and represented using a discrete lattice. During a wear process, a lattice site can move under the influence of external force and the interactions between the site and its adjacent sites. The site-site interaction is dependent on the mechanical properties of the material, such as elastic modulus, plastic behavior, work-hardening and the fracture strength. Newton's second law is used to determine the motion of a lattice site. The strain between a pair of sites is recoverable if it is within the elastic region of the material, otherwise a plastic strain is caused. The bond between a pair of sites is broken when the plastic strain exceeds a critical value for fracture. A site or cluster of sites is worn away if all bonds connecting the site and its adjacent sites are broken. Good agreement between the modeling and experimental work has been found. This model has demonstrated its capability for material ranking and exploration of wear mechanisms. This approach (MSDM) is based on simple fundamental equations, flexible and easy for further development towards a complete approach for wear prediction. The current work is focused on modeling of abrasive wear under dry sand/rubber-wheel abrasion test condition [6,15]. This model has provided the capability for investigation of different parameters that influence the wear behavior of different materials, including mechanical properties of the target material and the abrasive sand, abrasive sand shape, applied load, sliding speed, volume fraction of reinforcing phase in composites, etc.

1.3. The Dry Sand/Rubber-Wheel Abrasion Testing

The developed computer model (MSDM) was applied to simulate the wear under dry sand/rubber-wheel abrasion condition. The dry sand/rubber-wheel abrasion test specified by ASTM [15] is commonly used to evaluate the abrasive wear and rank materials, particularly for the oilsand, mining and agriculture industries [44]. This apparatus has been shown in figure 1-5 and enlarged picture of the rubber wheel-specimen contact area is shown in figure 1-8. During the test, a specimen is pressed against the rim of a rotating rubber wheel; sand particles are fed into the gap between the wheel and specimen and they abrade the specimen under the applied force. The weight loss of a specimen after testing is measured and converted to volume loss, which is a measure of the wear resistance of the material. This test is performed to evaluate material resistance to "low stress scratching abrasion" [6,15], particularly useful for ranking materials that are subjected to low stress abrasion in service: e.g. mining equipment, oil sand handling, agriculture tools, chutes and hoppers in ore processing plant, and construction equipment. Good correlation is generally found between the test results and field experience [45,46].

Wear is a complex process and wear behaviour of different materials varies with respect to the testing condition such as the applied load, the sliding speed, and the abrasive sand. It has been shown that discrepancy may exist between the experimental and field test and inaccurate or misleading information could be generated [47].

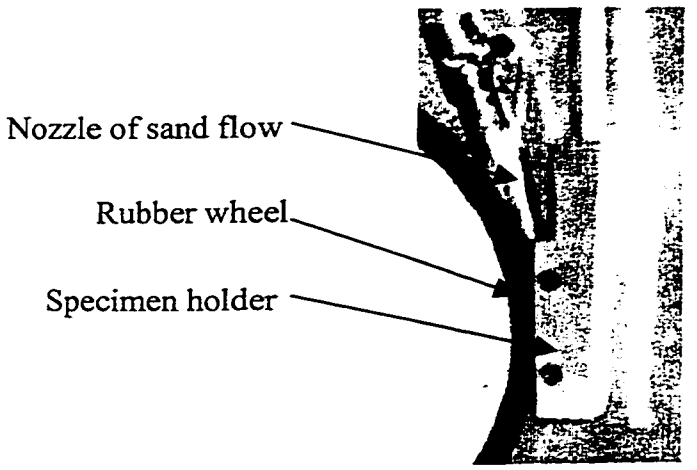

Figure 1-8. Rubber wheel tester used in the present work

Although the dry sand/rubber-wheel abrasion tester is widely used in industry, it is difficult to obtain information about wear mechanisms involved, and some phenomena can not be explained without using other approaches. Using computer modeling to simulate this abrasive process under controllable conditions may allow one to take a closer look at the abrasion process, to explore the wear mechanism and to help to rank the materials appropriately in terms of the wear resistance.

In this work, the developed model (MSDM) was applied to abrasive wear under the dry sand/rubber wheel condition as an example, with the aim at 1) justifying the capability of this new computer model and 2) exploring wear mechanisms that may not be explained by experimental testing.

Reference List for Chapter 1

[1] Standard terminology related to erosion and wear; Annual Book of Standards, 3.o2, ASTM, Philadelphia, PA, 1993.

[2] D. Y. Li, K. Elalem, M. J. Anderson and S. Chiovelli, "A microscale dynamical model for wear simulation" , Wear, 225-229, (1999), 380-386.

[3] Ernest Rabinowicz, Friction and Wear of Materials, 2nd ed., John Wiley & Sons, Inc., (1995).

[4] Associate community on tribology, NRC Canada, report no. 26556, (1986).

[5] *ASM Handbook*, ASM international, USA, 18, (1992), 184-190 & 801-811

[6] A.N.J. Stevenson and I.M. Hutchings, Wear, 195 (1996), 232-240.

[7] G. Huard et al., Proc. Int. Conf. On Wear of Materials, ASME, New York, (1987), 689-699.

[8] R.D. Haworth, Jr., Trans, ASM, 41 (1949) 819-869.

[9] S. Hogmark, S., O., Vingh and S. Fridstoik, Wear, 31, (1975), 39.

[10] Sato, A., and Mehrabian, R., Met Trans., USA, 7B, (1976), 443.

[11] B. N. Keshavaram, P. K., Rohatgi, and R. Asthana, Wear of materials, 19, 133-145.

[12] M. Matsunaga, Y. Ito, and H. Kobayashi, Wear of Materials, ASME, (1979), 336-342.

[13] Wear Testing with a Pin-on-disk Appaaratus,," G 99, Annual Book of ASTM standars, ASTM, (1990).

[14] D. K. Shetty, J. T. Stropki, and I. G. Wright, Preprint No. 84--AM-3A, ASLE, (May, 1984).

[15] A.W. Ruff, ASM International, Materials Park, OH, USA, (1997), 22.

[16] Y. L., G. T. Burstein, I. M. Huteching, Wear,181-183 (1995) 70-79.

[17] Ling F. F. and Pan C.H.T. (Eds.) Approaches to Modeling of Friction and Wear, Springer-Verlag, New York, NY, (1988).

[18] Ludema K.C. and Bayer R.G. (Eds.) Tribological Modeling for Mechanical Designers, ASTM STP 1105, American Society for Testing and Materials, Philadelphia, (1991).

[19] A.A. Polycarpou and A. Soom, Wear, 181-183, (1995) 32-41.

[20] N. Axen and S. Jacobson, Wear, 174, (1994), 187-199.

[21] S.J. Cho, B.J. Hockey, B.R. Lawn and S.J. Bennison, and J. Am. Ceram. Soc., 72 (1989) 1249-1252.

[22] Haiyan Liu and Stephen M. Hsu, Wear, 195, (1996), 169-177.

[23] K. Shimizu, T. Noguchi, H. Seitoh, and E. Muranaka, Wear, 233-235 (1999), 157-159.

[24] F. A. Akyuz, and J. E. Merwin, AIAA Journal, 6, (1968), 1825-1831.

[25] K. Komvopoulos and D. H. Choi, Journal of Tribology, 114, (1992), 823-831.

[26] P. Põdra and S. Andersson, Wear, 224, (1999), 13-21.

[27] H. Sui, H. Pohl, U. Schomburq, G. Upper, and S. Heine, Wear, 224, (1999), 175-182.

[28] F.E. Kennedy, Jr, and L.P. Grotelueschen, J. of Appl. Mech., 51, (1984), 687-689.

[29] N. Ohmae, ASME Paper 86-Trib-25 (1986).

[30] P. Hancock, J.R. Nicholls and D.J. Stephenson, Surf. Coat. Technol, 32, (1987), 285.

[31] J.R. Nicholls and D.J. Stephenson, Wear, 186-187, (1995), 64-77.

[32] Kien K. Wong and Hector McI. Clark, Wear, 160, (1993), 95-104.

[33] S. Turenne and M. Fiset, Wear, 162-164, (1993), 679-687.

[34] A.A. Polycarpou and A. Soom, Wear, 181-183, (1995), 32-41.

[35] N. Axen and S. Jacobson, Wear, 174, (1994), 187-199.

[36] S.J. Cho, B.J. Hockey, B.R. Lawn and S.J. Bennison, J. Am. Ceram. Soc., 72, (1989), 1249-1252

[37] Haiyan Liu and Stephen M. Hsu, Wear, 195, (1996), 169-177.

[38] Jiaren Jiang, F.H. Stott and M.M. Stack, Wear, 181-183, (1995), 20-31.

[39] Mark O. Robbins and J. Krim, MRS Bulletin, 23, (1998), 23-26.

[40] J.A. Harrison, S.J. Stuarat, and D.W. Brenner, Atomic-Scale Simulation of Tribological and related Phenomena, Handbook of Micro/Nanotribology (1998)

[41] W. Zhong and D. Tomanek, Phys. Rev. Lett., 64, (1990), 30-54.

[42] S.M. Hsu, M.C. Shen and A.W. Ruff, Tribology International, 30, No. 5, (1997), 377-383.

[43] Xuefeng Tian and Bharat Bhushan, Journal of Tribology, 118, (1996), 33-42.

[44] M. Scholl, Conf. On wear of materials, Wear, 203-204, (March 1997), 57-64.

[45] P.A. Swanson, Proc. Int. Conf. On Wear of Materials, ASME, New York, (1977), 148-157.

[46] P.A. Swanson, Tribology: wear test selection for design and application, ASTM, Philadelphia, PA, (1983), 80-99.

[47] X. Ma, R. Liu, and D. Y. Li, Wear, 2000, in press.

Chapter 2

Research Paper

A Microscale Dynamical Model for Wear Simulation

Published in Wear, Vol. 380-386, 1999, pp. 225-229

2.1. Introduction

Wear is a complicated process, which involves time-dependent deformation and removal of material at the counterface. Experimentally, one can measure the wear loss and investigate the wear mechanism by analyzing worn surfaces using, for instance, scanning electron microscopy (SEM). However, a wear process might involve several wear mechanisms and the synergistic interaction between these mechanisms may make the obtained information difficult to interpret and use. It is recognized that computer modeling allows "computational experiments" to be performed under controllable conditions and the effect of each parameter on wear can be studied separately. Therefore, computer modeling provides an effective method complementary to experimental techniques for fundamental understanding of wear mechanisms and for prediction of material performance during wear processes.

There are numerous computer models proposed to simulate tribological processes [1,2]. For instance, earlier mechanical models were developed to simulate friction and wear by employing slip line theory [3], the upper-bound method [4], and the FEM approach [5,6]. Recent examples are given by modeling erosion [7-10], sliding friction and wear [11-14], and sliding at elevated temperature [15]. By taking into account different factors such as the temperature effect on oxidation or corrosion, these models provide information that is consistent with experimental observations. However, many models were developed under some assumptions or they are based on existing tribological rules, or they incorporate empirical equations. These, more or less, weaken

their predictive function. Furthermore, these macro-models only take into account the average mechanical properties of heterogeneous materials (e.g., multiphase and composite materials). This makes them not suitable for characterizing wear behavior of materials in finer detail such as the influence of microstructure on wear. As a matter of fact, many models were proposed for mechanical design rather than for prediction of materials performance [2]. Therefore, they involve the application of existing tribological theories to mechanical design, and are not developed for fundamentally exploring wear mechanisms and predicting wear behavior of materials.

Efforts have been made to develop more fundamental models for studying tribological phenomena and material response to external forces, such as Molecular Dynamics simulations (MD) [16-23] and first-principles techniques [24]. The MD technique is one of the most powerful approaches. It deals with the motion and trajectory of individual atoms or molecules, and can be used to predict precisely various dynamic processes at the atomic or nanometer level. This technique significantly advances our understanding of material behavior and relevant processes. The MD technique may well characterize friction processes at the nanometer scale, when appropriate atomistic potentials are used. However, it is difficult to apply the MD approach directly to a micro/macroscopic wear process because of the limited capability of current computing facilities. The Molecular Dynamic method is usually used to simulate a process involving $10^3 \sim 10^4$ atoms. However, to simulate a bulk material as small as 1 μm^3, one has to deal with $10^9 \sim 10^{10}$ atoms. Although the faster parallel computers may allow the MD simulation of a system involving 10^8 atoms, this requires significantly long computing

times. It is therefore not realistic to model wear behavior of a realistic system that involves many micro/macroscopic factors such as microstructural inhomogeneity and contact geometry, which have to be modeled using a large number of atoms.

In order to build a bridge between atomistic simulation techniques and macro-models, a tentative model is proposed for dynamic simulation of wear processes at the microscopic level. The authors attempt to build this model based on fundamental physical laws with the capability of predicting wear behavior of engineering materials. In this model, a material system is discretized and represented using a discrete lattice. This should not be confused with the usual use of the term "lattice" when referring to crystal. Each lattice site represents a small volume of the material. A wear process is simulated by modeling the movement of each site using Newton's equation of motion. The force on each lattice site includes the contribution from the external force and the interaction between the site and its neighbors, which is dependent on the mechanical properties of the material. Preliminary simulation has demonstrated that this model can provide information that is consistent with experimental observations.

2.2. Description of the Micro-Scale Dynamic Model

The present simulation is performed in a two-dimensional space. In this model, a given specimen is descretized using a square lattice, each site of which represents a small volume of the material. The interaction between a pair of adjacent sites is dependent on the mechanical properties of the material. Under the influence of external forces during a wear process, a lattice site may move and its motion is determined by the external force

and by the interaction between this site and its neighbors. Final positions of all lattice sites reflect the response of the material to the external forces, thus providing information on its wear performance.

2.2.1 Interaction between lattice sites

The interaction between two adjacent sites is dependent on the mechanical properties of the material, such as the elastic modulus, the yield stress, the tensile strength, the ductility and work-hardening. The force between a pair of adjacent sites is proportional to the deformation of the bond between these two adjacent sites,

$$f = k \cdot \Delta l \tag{1}$$

where, $\Delta l = l - l_\circ$ is the deformation of the bond, $l_\circ$ is the unit length of the lattice or the bond length in stress-free condition, and l is the bond length after the deformation. Again, the term "bond" does not refer to the usual use of the term for a chemical bond between atoms. The corresponding strain is equal to $\varepsilon = \Delta l / l_\circ$. The coefficient, k, in eq.(1) is a force coefficient that characterizes the interaction between a pair of sites. The k-value is equal to $E \cdot l_\circ$, where E is the slope of the stress-strain curve of the material. When the deformation Δl is within the elastic region, E is the elastic modulus. To simplify the simulation, we use two values for E and linearly approximate the stress-strain curve as illustrated in figure 2-1. In the elastic region, $E = E_e = \sigma_y / \varepsilon_y$, where σ_y and ε_y are the yield stress and yield strain, respectively; while in the plastic region, $E = E_p = (\sigma_T - \sigma_y) / (\varepsilon_T - \varepsilon_y)$, where σ_T and ε_T are the tensile strength and the

corresponding strain. When the force between a pair of sites is within the elastic region, the corresponding deformation is recoverable; otherwise plastic deformation will be involved. Since E_p is the slope of the stress-strain curve in the plastic region, its value reflects the work- hardening of the material. It should be pointed that, during a wear process, the initially square lattice is distorted because of plastic deformation. This leads to changes in orientation of the lattice bonds. In this initial model, however, only isotropic materials are considered.

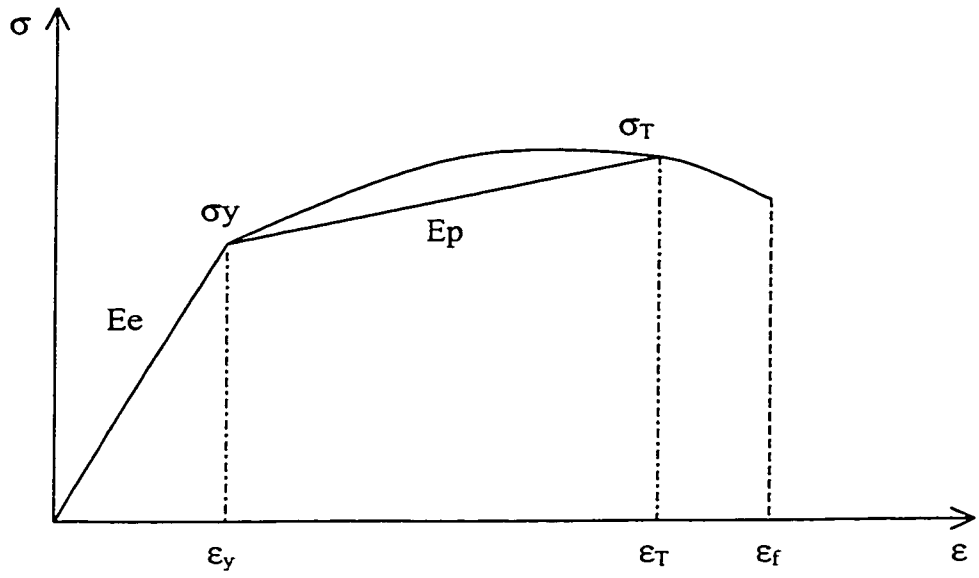

Figure 2-1. The linear approximation of a stress-strain curve

Therefore, the absolute value of the force due to the stretching or contracting of a bond does not change with the reorientation of the bond. In addition, in this model, lattice inhomogeneities such as grain boundary and second phases are not taken into account, which may influence the bond strength.

2.2.2 *The movement of a lattice site*

When a lattice site is under the influence of a force, its motion and trajectory are determined by Newton's law of motion,

$$\vec{F} = m\frac{d^2\vec{r}}{dt^2} \tag{2}$$

where, m is the mass of a lattice site, which actually represents the mass of a unit cell (with its volume equal to l_o^2 in 2-D space). $\vec{F}$ is the total force applied to the lattice site. This force is the sum of the forces caused by deformations of all bonds that connect the site and its adjacent sites. The magnitude of each force is proportional to the bond deformation as expressed by eq.(1). If the site is on the surface, the load on the site includes the external force. When a lattice site, e.g., site p, shifts from its initial position, the resulting force on site p is expressed as

$$\vec{F}_p = \sum_q^n k \cdot \Delta\vec{l}(p,q) + \vec{f}_p \tag{3}$$

where, n is the number of sites adjacent to this site, and

$$\Delta\vec{l}(p,q) = \vec{l}(p,q) - \vec{l}_o(p,q) = [\vec{r}(q) - \vec{r}(p)] - \vec{l}_o(p,q) \tag{4}$$

is the deformation vector. The vectors in equation (4) are illustrated in figure 2-2. $\vec{f}_p$ is the external force on site p if this site is on surface. If site p is not a surface site, $\vec{f}_p$ is equal to zero. When the total force, $\vec{F}_p$, is known, one may determine the velocity of site p and its next position after a time interval Δt,

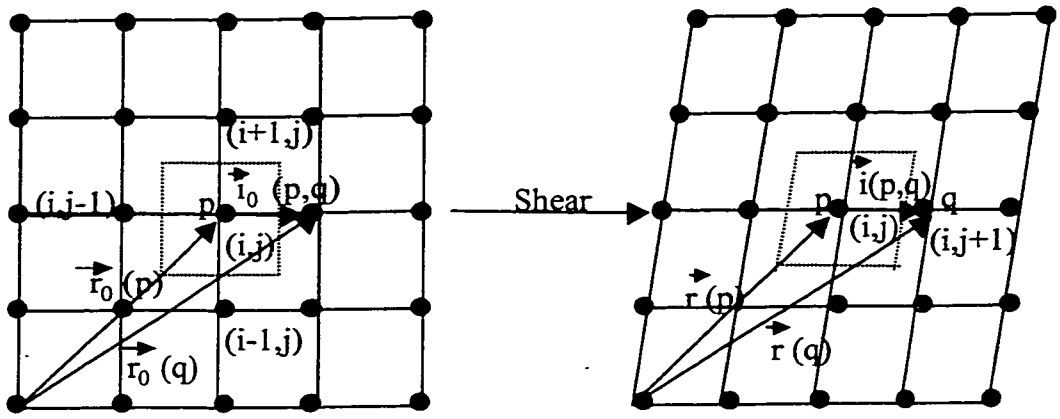

Figure 2-2. Illustration of the vectors used in equation (4)

$$\vec{v}(p) = \vec{v}_{\circ}(p) + \frac{1}{m}\vec{F}(p)\Delta t \tag{5}$$

$$\vec{r}(p) = \vec{r}_{\circ}(p) + \vec{v}(p)\Delta t \tag{6}$$

where, $\vec{v}_{\circ}(p)$ is the velocity of site p at the time t, while $\vec{v}(p)$ is the velocity at time $t+\Delta t$. $\vec{r}_{\circ}(p)$ is the position vector of site p at time t, while $\vec{r}(p)$ is the new position of site p at time $t+\Delta t$. In such a way, one may determine the force on this site at $t+\Delta t$ based on its new position and thus predict the next changes in velocity and position of the site. In figure 2-2, a bulk metal is discritized and each node represents a concentrated mass of the material.

2.2.3. *Simulation of material response to external force*

During a wear process, material at the counterface is worn away by abrasive particles or by sliding asperities. The wear process may be simulated in the following way. We first discretize a bulk material using a discrete lattice as described earlier. The

external force at the contact results in displacement of surface sites. New velocities and positions of the surface sites after a time step Δt can be determined using Newton's law of motion. The resultant deformation generates a new force on each lattice site, which determines the next changes in velocity and position of the site. Within the elastic region, i.e. $\Delta l / l_\circ \leq \varepsilon_y$, the displacement of a site is recoverable. If $\Delta l / l_\circ > \varepsilon_y$, plastic deformation occurs, resulting an irreversible residual strain, $\Delta\varepsilon_p = (\Delta l / l_\circ - \varepsilon_y)$. As a result, the length of the stress-free bond, $l_\circ$, changes to $l_\circ' = l_\circ(1+\Delta\varepsilon_p)$. If a bond experiences a number of plastic deformation events and the accumulated plastic deformation reaches its critical value for fracture (ε_f), this bond is then broken. A site or a cluster of sites is worn away if all bonds connecting the site or the cluster to its adjacent sites are broken. In such a way, one may predict how many lattice sites are removed from the bulk material during the wear process. Since the bond between a pair of adjacent sites is related to mechanical properties of the material, the wear loss is therefore dependent on the mechanical properties.

2.3. Application of the MSDM approach to an Abrasion Process

The MSDM approach was applied to modeling an abrasion process that is similar to the rubber-wheel abrasion test described in ASTM G65 [25,26]. This test is widely used to rank wear-resistant materials under low stress condition. During this process, abrasive particles pass through the gap between the rubber wheel and the specimen, abrading the specimen surface (see figure 2-3). The mass loss of a tested material is

dependent on the mechanical properties of the tested material and the abrasive particles as well as the wear conditions, such as the applied load and the rubber-wheel hardness. In order to evaluate wear behavior of a material during this abrasion process, two-dimensional modeling was performed in the following way.

The specimen and the abrasive particle were discretized using a square lattice with the unit length equal to l_o. A 200×50 lattice was used to map the cross-section of the material under wear attack. Each lattice site of a sand particle has a mass m_s. The bond between a pair of sand sites was characterized by $k_s = E_s l_o$ and the fracture strength as well as the fracture strain of the sand, where E_s is the elastic modulus of the sand. Since sand particles are not ductile, they experience little plastic deformation before fracture. For a metallic specimen, each lattice site has a mass m_m, and the bonds between adjacent sites are characterized by $k_m = E_m l_o$ as well as by the yield stress, the yield

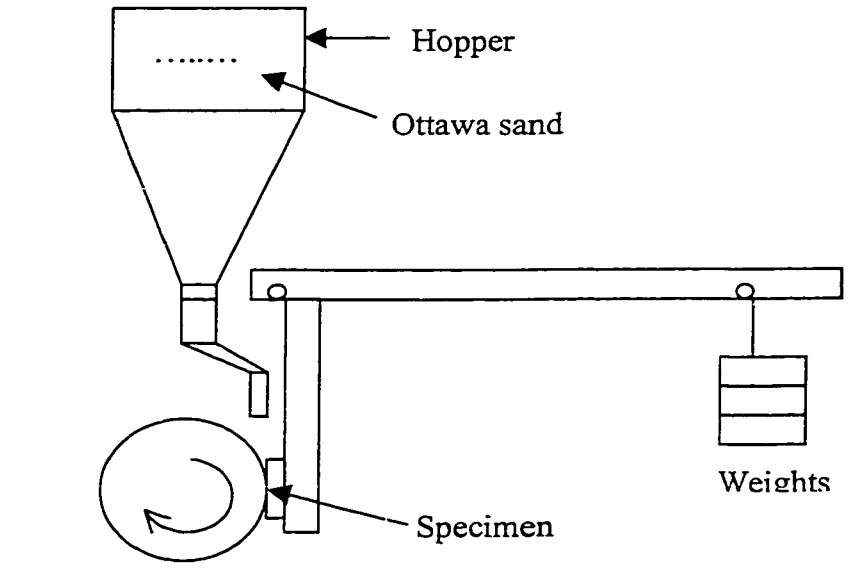

Figure 2-3. Schematic of a standard abrasive wear test (ASTM G65)

strain, the tensile strength, and the ductility.

When a sand particle gets into the gap between the rubber wheel and the specimen, the rubber wheel grasps the sand particle and presses it onto the specimen. The sand particle then moves along with the wheel and scratches the specimen surface, thus resulting in material loss. In this simulation, the horizontal velocity of a sand particle included two components: an average velocity component and a deviation velocity. The average velocity component was equal to ωR, where ω and R are the angular velocity and the radius of the rubber wheel, respectively. This average velocity component was retained by the horizontal interaction between the rubber wheel and the sand, which pushed the sand forwards along with the rubber wheel. The deviation velocity component resulted from the interaction between the sand and the specimen, which made the overall horizontal velocity deviate from the average velocity that was equal to ωR. A sand particle also gained a vertical velocity under the pressure from the rubber wheel. According to Hertzian theory [27], when a rubber cylinder is in contact with a hard plane, the contact pressure may have an elliptical distribution

$$P(x) = P_{\max}\sqrt{1-\frac{x^2}{a^2}} \tag{7}$$

where $P_{\max}$ is the maximum pressure and a is one half of the contact region between the rubber cylinder and the specimen (see figure 2-4). The contact region is increased with an increase in the applied load, F, which is the contact force per unit length of the cylinder

$$a = \sqrt{\frac{4R}{\pi E_R}F} \tag{8}$$

where E_R is the elastic modulus of the rubber wheel and R is the radius of the wheel. The maximum pressure is at the center of the contact area, expressed as

$$P_{max} = \frac{2F}{\pi a} = \sqrt{\frac{E_R}{\pi R} F} \tag{9}$$

Under such a pressure, a sand particle experiences a vertical force that is elliptically distributed along the moving path of the particle. In the simulation, when a sand particle gets into the contact region, all sites of a sand particle that are in contact with the rubber wheel will bear the force from the wheel. The sand particle moves forward and the vertical force on sites of the particle in contact with the rubber wheel will change elliptically along the moving path. The force can be transferred to sites that are away from the sand-wheel contact area and then to the sand-specimen interface, causing the wear loss.

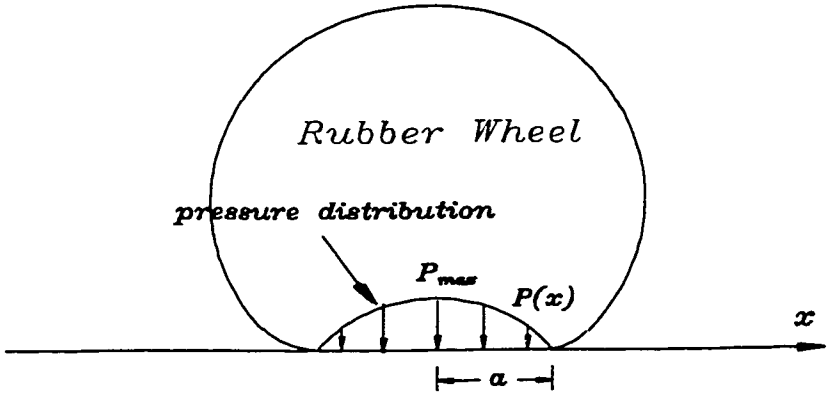

Figure 2-4. The pressure distribution between the rubber wheel and the specimen surface.

Since the interaction between a pair of sand sites and that between a pair of material sites are different, the effective force coefficient for a pair of material and sand

sites is required. This coefficient can be calculated by letting the forces on both sites be equal, that is

$$f_s = k_s \Delta l_s^{'} = k_m \Delta l_m^{'} = f_m \tag{10}$$

where, $\Delta l_s^{'}$ and $\Delta l_m^{'}$ are the half deformations of a sand bond and a material bond, respectively. The total deformation between the sand site and the material site is therefore equal to.

$$\Delta l = \Delta l_s^{'} + \Delta l_m^{'} \tag{11}$$

Since the interaction between the sand site and the material site is equal to either f_s or f_m, by using equations (10) and (11), we have

$$f = \bar{k} \Delta l = \frac{k_s k_m}{k_s + k_m} \Delta l \tag{12}$$

Thus, we obtain the effective force coefficient, $\bar{k} = \frac{k_s k_m}{k_s + k_m}$, for characterizing the interaction between a sand site and a material site.

Modeling was performed to investigate the load effect on wear loss. In this preliminary 2-D simulation, the abrasive particles had a square shape and size equal to $300 \times 300 \mu m^2$. The sliding velocity was equivalent to 0.5m/s and the time step was chosen as $\Delta t = 0.0001$ second. A monolayer of abrasive particles was considered between the rubber wheel and the specimen. The maximum value of applied load, Fm, corresponds to the maximum contact range, $2a = 3.0cm$. Relative wear losses (relative to the maximum wear loss under Fm) caused by the normal load in the range from 0*Fm to 1.0*Fm were obtained. This modeling predicts the relation between the applied load and

the wear loss. An approximately linear relationship in this load range was obtained as figure 2-5 illustrates. The points in the figure were obtained from the simulation. Since the system was not large enough, these points somehow deviated a little from a line. However, the general trend of the linear relationship is obvious. As demonstrated by Stevenson and Hutchings [25], there indeed existed a linear relationship between wear loss and the applied load during a rubber-wheel abrasion testing. The model agrees well with their observation.

This model was applied to evaluating wear losses of copper, steel, and molybdenum, three typical materials representing relatively soft, medium, and hard materials, respectively. Three similar materials, AR steels, were also studied to evaluate the capability of the MSDM approach for predicting wear performance of materials that have similar mechanical properties. Mechanical properties of these materials are listed in table 2-1, and compositions of the AR steels are listed in table 2-2.

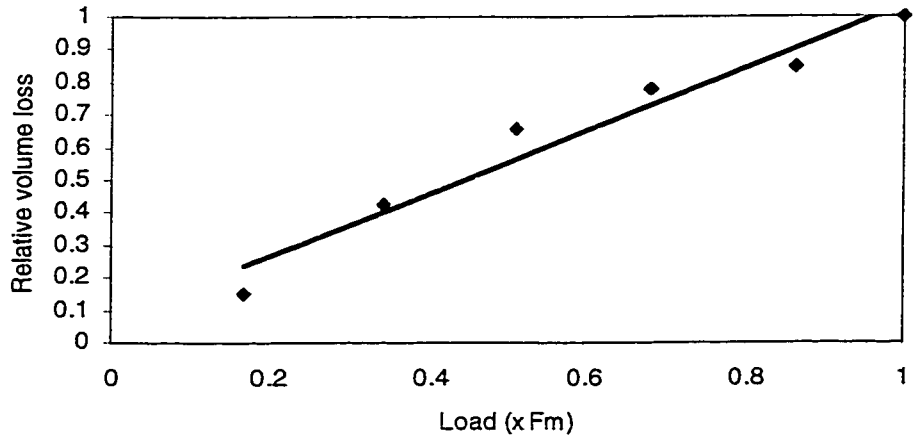

Figure 2-5. The relation between the relative volume loss and the applied load

The critical value for fracture, ε_f, was determined from bulk material property, which corresponds to the elongation (%).

Table 2-1 Mechanical properties of the materials under study

Material	Modulus E_e (GPa)	Yield stress σ_y (MPa)	Tensile strength σ_T (MPa)	Elongation (%) ε_f
Copper	110	69	200	45
Steel	207	180	380	25
Molybdenum	310	565	655	35
AR Steel #1	207	1055	1240	17
AR Steel #2	207	1276	1449	18
AR Steel #3	207	1040	1530	15
Sand	430	862	862	0.2

Table 2-2 Chemical compositions of the AR steels (wt.%)

Content / Material	C	Mn	P	S	Si	Ni	Cr	Mo	others
AR Steel #1	0.16	1.28	0.015	0.005	0.32	-	-	-	-
AR Steel #2	0.32	1.1	0.005	0.002	0.23	-	0.50	-	0.04-0.08Al, 0.01-0.02Ti
AR Steel #3	0.25	0.85	-	-	0.32	3.5	1.45	0.28	-

In this modelling, it was assumed that the failure of a bond was only caused by tension, or precisely speaking, only caused by the elongation of the bond when it exceeded the critical ε_f for fracture, no matter how complex the local stress is.

Relative wear losses of copper, steel, and molybdenum were evaluated by the modeling and illustrated in figure 2-6, which demonstrates that copper has the highest wear loss, followed by the steel, and then molybdenum. This result is consistent with the general trend of wear behavior of these materials as given in reference [28]. The modeling also well distinguished the three AR steels in terms of wear performance. Figure 2-7(a) presents the modeling results, which illustrates that AR steel #1 has the highest wear loss, and AR steel #3 has the lowest wear loss. Wear losses of these AR steels were experimentally measured using an ASTM G65 rubber-wheel tester by the wear laboratory in the Syncrude Research Center. Figure 2-7(b) illustrates the experimental result. One may see that the result of modeling is consistent with the experimental measurement.

The present simulation shows that this model can not only predict the wear performance of different type materials (e.g., Cu, Steel, and Mo) that have very different mechanical properties, but can also distinguish similar materials such as the AR steels whose mechanical properties are close. Therefore the MSDM can give the accuracy that allows us to be able to predict the wear behavior of similar materials. This is helpful for evaluating the effects of minor or non-radical modifications made to existing materials for improved performance. The MSDM method based on fundamental physical laws thus

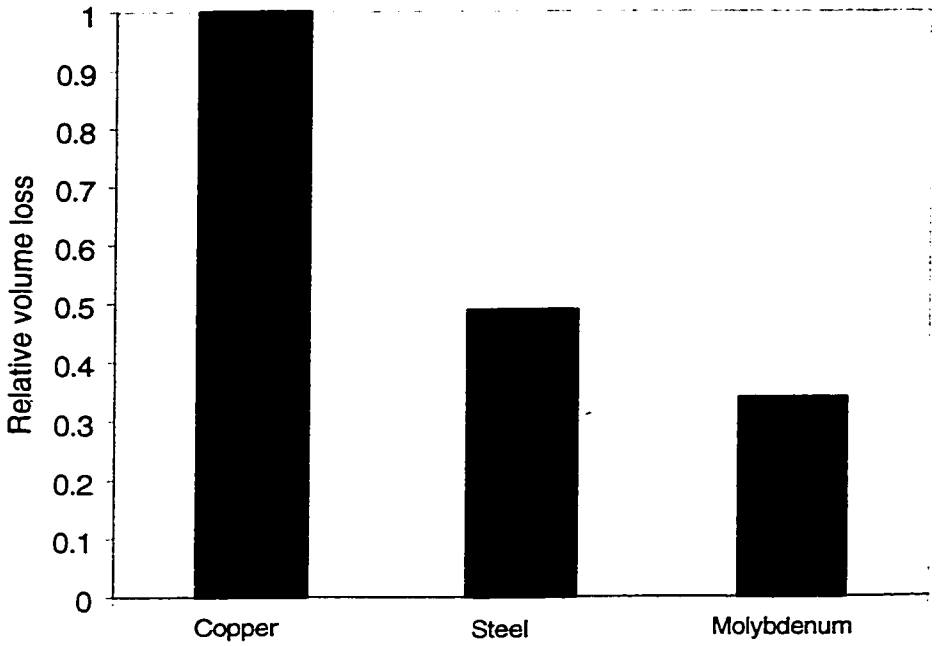

Figure 2-6. Relative volume losses of copper, steel and molybdenum.

provides an effective approach to the characterization of wear processes and the prediction of material performance. It should be pointed out that the present simulation is very preliminary and only gives qualitative results. Some factors are ignored in this preliminary 2-dimensional modeling. For instance, in the present modeling, the wear loss was caused by square-shaped sand particles, and the distributions of sand shape and size were not taken into account. These would actually influence the wear loss. Besides, the temperature rise of the specimen due to friction was ignored.

Although the temperature rise may not be large (e.g., ~24°C, see [25]), the hardness of the rubber wheel can, more or less, be influenced and this may change the wear loss. Another important parameter is the unit length of the grid for mapping the specimen.

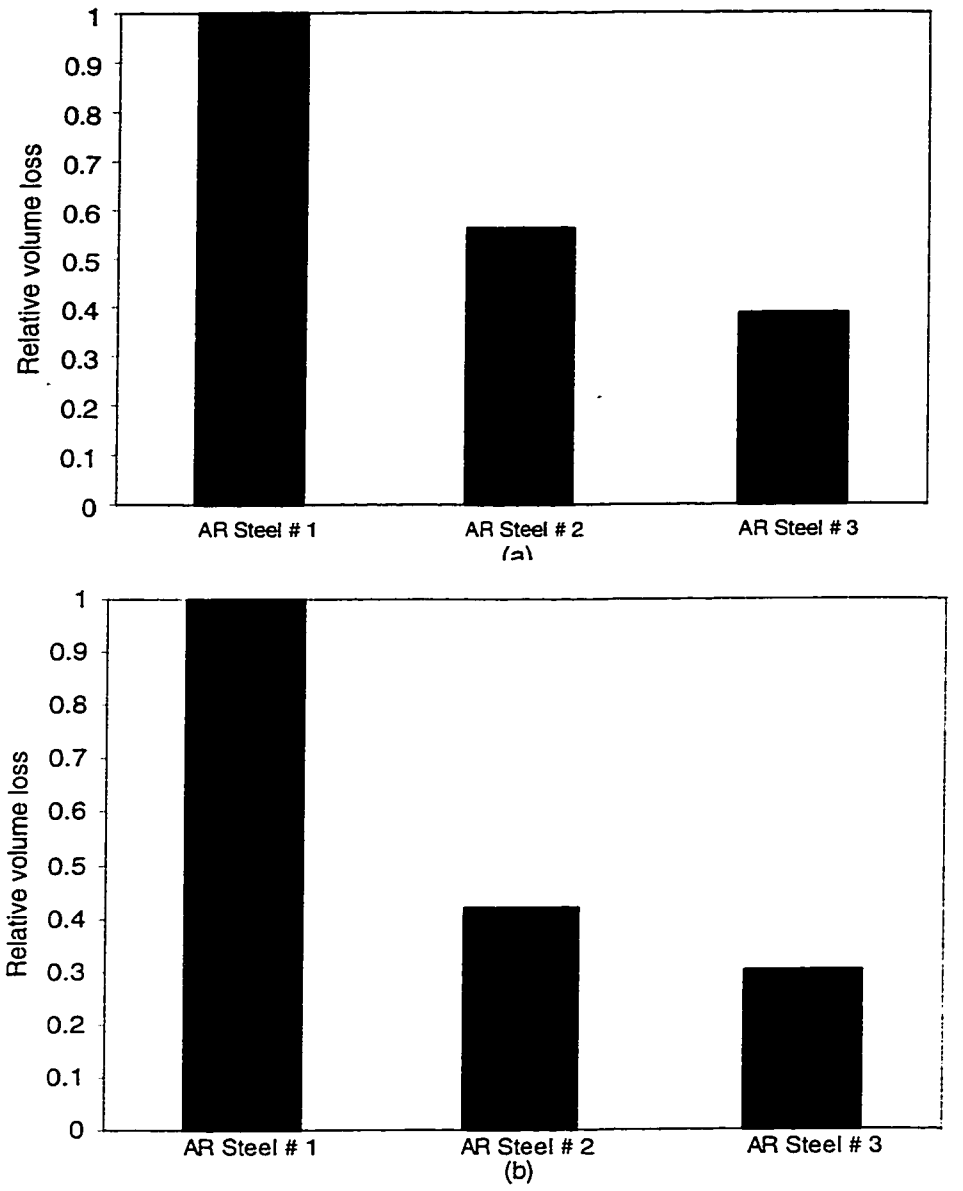

Figure 2-7. (a) Relative volume losses of three AR steels predicted using the MSDM approach, and (b) experiment results.

In this preliminary simulation, we consider the materials as homogeneous materials and therefore used a grid with fairly large unit length ($l_o = 150\mu m$) to map the specimen in order to save computing time. This decreased the accuracy of the simulation, since the local stress and strain can not be well described if using a large l_o. This occurs because

the local strain distribution around a lattice site is approximated by the deformation of the bonds between the site and its four neighbours.

This approximation is acceptable only when the volume of a lattice site (i.e., $V=l_o^2$ in 2-D space) is small enough and a relatively large number of sites are used to map the material system. Therefore, one should obtain more accurate results when a smaller unit length is used. If the material is a multiphase or composite material, a grid with significantly smaller unit length must be used to reflect the microstructure effect on wear behavior. Further study is being conducted to improve the approach and quantify the simulation study.

2.4. Conclusions

A tentative model was developed to characterize the wear process and predict material performance at the microscopic level, based on mechanical properties of the material. This model provides a simple approach, flexible and easy to apply. In this model, a material system is mapped onto a discrete lattice, each of which represents a small volume of the material. Under the influence of an external force a lattice site may move, controlled by Newton's law of motion. The force on the lattice site is dependent on the external force and the interaction between the site and its neighbours. Preliminary simulation was conducted to study a Rubber-Wheel (ATSM G65) abrasion process. It is demonstrated that this model correctly predicts the relation between the applied load and the wear loss. The wear performance of a number of materials, including copper, ordinary

steel, molybdenum, and several AR steels, was also predicted. The simulation is consistent with experimental observations.

Acknowledgement

The authors are grateful for financial support from Syncrude Canada Ltd. and the Natural Science and Engineering Research Council of Canada (NSERC).

Reference List for Chapter 2

1. F.F. Ling and C.H.T. Pan (ed.), Approaches to Modeling of Friction and Wear (Proc. Of the Workshop on the Use of Surface Deformation Models to Predict Tribology Behavior), Springer-Verlag, New York, 1986.
2. Kenneth C Ludema and Raymond G. Bayer (ed.), Tribological Modeling for Mechanical Designers, ASTM, Baltimore, USA, 1991.
3. J.M. Challen and P.L.B. Oxley, Wear, 53 (1979) 229-243.
4. B. Avitzur, C.K. Huang and Y.D. Zhu, Wear, 95 (1984) 59-77.
5. F.E. Kennedy and L.P. Grotelueschen, J. of Appl. Mech., 51 (1984) 687-689.
6. N. Ohmae, ASME Paper 86-Trib-25 (1986).
7. P. Hancock, J.R. Nicholls and D.J. Stephenson, Surf. Coat. Technol, 32 (1987) 285.
8. J.R. Nicholls and D.J. Stephenson, *Wear*, 186-187 (1995) 64-77.
9. Kien K. Wong and Hector McI. Clark, *Wear*, 160 (1993) 95-104.
10. S. Turenne and M. Fiset, Wear, 162-164 (1993) 679-687.
11. A.A. Polycarpou and A. Soom, *Wear*, 181-183 (1995) 32-41.
12. N. Axen and S. Jacobson, *Wear*, 174 (1994) 187-199.
13. S.J. Cho, B.J. Hockey, B.R. Lawn and S.J. Bennison, *J. Am. Ceram. Soc.*, 72 (1989) 1249-1252
14. Haiyan Liu and Stephen M. Hsu, *Wear*, 195 (1996) 169-177.
15. Jiaren Jiang, F.H. Stott and M.M. Stack, *Wear*, 181-183 (1995) 20-31.
16. Mark O. Robbins and J. Krim, *MRS Bulletin*, 23 (1998) 23-26.

17. M.S. Tomassone, J.B. Sokoloff, A. Widom and J. Krim, *Phys. Rev. Lett.*, 79 (1997) 4798.

18. U. Landman, W.D. Luedtke, and J. Gao, *Langmuir*, 12 (19) (1996) 4514.

19. D.A. Rigney and J.E. Hammerberg, *MRS Bulletin*, 23 (1998) 32-36.

20. Judith A. Harrison and Scott S. Perry, *MRS Bulletin*, 23 (1998) 27-31.

21. J.A. Harrison, R.J. Colton, C.T. White and D.W. Brenner, *Phys. Rev.* B46 (1992) 9700.

22. J.N. Glosli and G.M. McClelland, *Phys. Rev. Lett.*, 70(13) (1993) 1960.

23. M.R. Soren, K.W. Jacobsen and P. Stoltze, *Phys. Rev.* B53(1996)2101.

24. W. Zhong and D. Tomanek, *Phys. Rev. Lett.*, 64(1990)3054.

25. A.N.J. Stevenson and I.M. Hutchings, Wear, 195(1996) 232-240.

26. A.W. Ruff, in Friction And Wear Testing, ASM International, Materials Park, OH, USA, 1997, P.22.

27. S.P. Timoshenko and J.N. Goodier, Theory of Elasticity, 3rd ed., McGraw-Hill, New York, 1970.

28. Ernest Rabinowicz, Friction and Wear of Materials, John Wiley & Sons, Inc., New York, 1965, P.170.

Chapter 3

Research Paper

Dynamical Simulation of an Abrasive Wear Process

Published in Journal of Computer-Aided Materials Design, Vol. 6, 1999, pp. 185-193

3.1. Introduction

Wear is a complex process of surface damage by, e.g., sliding against another surface or solid particle impingement. Wear resistance of a material is determined by measuring its weight or volume loss after being worn. However, it is often difficult to explain the wear behavior of a material and identify the predominant factors that causes the most of the damage, since several wear mechanisms might be involved under a particular wear condition. Computer simulation provides an effective and economical approach, which allows us to conduct computational wear experiments under controllable conditions. Effects of different factors on the wear performance of the material could thus be distinguished.

There are numerous computer models proposed to simulate wear processes [1-3]. In general, the current models can be classified into two groups. One group is performed on macro-levels. Earlier models were developed, for example, employing the slip line theory [4,5], upper-bound method [6,7], and the finite element method [8-10]. The FEM approach has been widely used to analyze two-dimensional and three-dimensional elastic/plastic contact problems. The strain or stress distribution in a contact region can be determined using the FEM approach, thus facilitating the prediction of the material failure in the contact region. However, to deal with a realistic engineering surface, one has to treat a large number of mesh elements because of the existence of many surface asperities that always change during a wear process; this makes the finite element approach unfeasible [11]. Recent examples include modeling erosion [12,13], sliding friction and wear [14], and sliding at elevated temperatures [15]. There are many other

macro-models proposed to simulate wear processes [16-18]. However, many of the models are only suitable for specific situations; they may only work for particular pairs of materials, limited contact geometry, operating condition range, or particular environment [3]. In addition, many models were developed on some assumptions or based on existing tribological rules, or incorporated with empirical equations. This, more or less, weakens their predictive function. Furthermore, quite a number of macro-models only take into account the average mechanical properties of heterogeneous materials (e.g. multiphase and composite materials). This makes them not suitable for characterizing wear behavior of materials in fine details such as the microstructural effect on wear.

Another group of models are developed on fundamental physics laws, such as the Molecular Dynamics simulation (MD) [19,20] and first-principles techniques [21]. The MD technique may well characterize friction processes at nanometer scale, when appropriate atomistic potentials are used. However, it is difficult to directly apply the MD approach to a micro/macroscopic wear process because of the limited capacity of current computing facilities. For instance, to simulate a material system with its volume equal to 1 μm^3, one has to deal with $10^9 \sim 10^{10}$ atoms. The MD technique is usually used to handle 10^4 atoms, limited by the current computing capability. Obviously, it is difficult to apply the MD method to analyze a system on microscopic level, which may involve a significantly large number of atoms.

Great efforts have been continuously made to improve our ability to simulate wear and friction processes and progress in this area is being achieved. This paper presents a tentative dynamic approach, the so-called Micro-Scale Dynamic Model

(MSDM), for wear simulation and its application in studying an abrasive wear process. Several materials were investigated and a comparison between the result of the wear modeling and experimental observation was made. The model was also justified by applying it to the analysis of the volumetric strain distribution in a contact region with a comparison to a finite element analysis.

3.2 Results and Discussion

- Description of the Micro-Scale Dynamic Model (MSDM)

In this model, a given specimen is discretized using a square lattice or grid, each site of which represents a small volume of the material. This paper reports our result of 2-dimensional modeling. The model can be easily expanded to 3-dimensional space and performed in a similar way. During wear, a lattice site may move under the influence of the external force and the constraint by its neighbors. The interaction between two adjacent sites is dependent on the mechanical properties of the material. The force between a pair of adjacent sites is expressed as

$$f = k \cdot \Delta l \qquad (1)$$

where, $\Delta l = l - l_\circ$ is the deformation of the bond connecting these two sites, $l_\circ$ is the unit length of the lattice or the bond length in stress-free condition, and l is the bond length after the deformation. The corresponding strain is equal to $\varepsilon = \Delta l / l_\circ$. The coefficient, k, is a force coefficient that characterizes the interaction between a pair of sites. The k-value is equal to $E \cdot l_\circ$, where E is the slope of the stress-strain curve of the material and is expressed as

$$E = \begin{cases} E_e = \sigma_y / \varepsilon_y & \text{if} \quad \Delta l / l_\circ \le \varepsilon_y \\ E_p = (\sigma_T - \sigma_y) / (\varepsilon_T - \varepsilon_y) & \text{if} \quad \Delta l / l_\circ > \varepsilon_y \end{cases} \tag{2}$$

where ε_y and σ_y are the yield strain and yield stress, respectively. σ_T and ε_T are the tensile strength and corresponding strain. When the deformation Δl is within the elastic region, E is the elastic modulus, i.e. E_e. E_p is a linearly approximated slope of the stress-strain curve in the plastic region (see figure 3-1), and its value reflects the work-hardening of the material The interaction between a pair of sites is dependent on the change in length of the bond connecting these two sites no matter how the bond orientation changes.

For the present simulation, lattice inhomogeneities such as grain boundary and second phases are not taken into account, which may influence the bond strength. For a heterogeneous material, e.g., composite, the site-site interaction is influenced by the difference in mechanical properties between different phases and the interfacial bonding strength. Such a case has been considered in another paper [22].

When a lattice site is under a force, its motion and trajectory are determined by Newton's law of motion,

$$\vec{F} = m \frac{d^2 \vec{r}}{dt^2} \tag{3}$$

where, m is the mass of the lattice site or a unit cell (with its volume equal to $l_\circ^2$ in 2-D space). $\vec{F}$ is the total force applied to the lattice site. This force is the sum of the forces

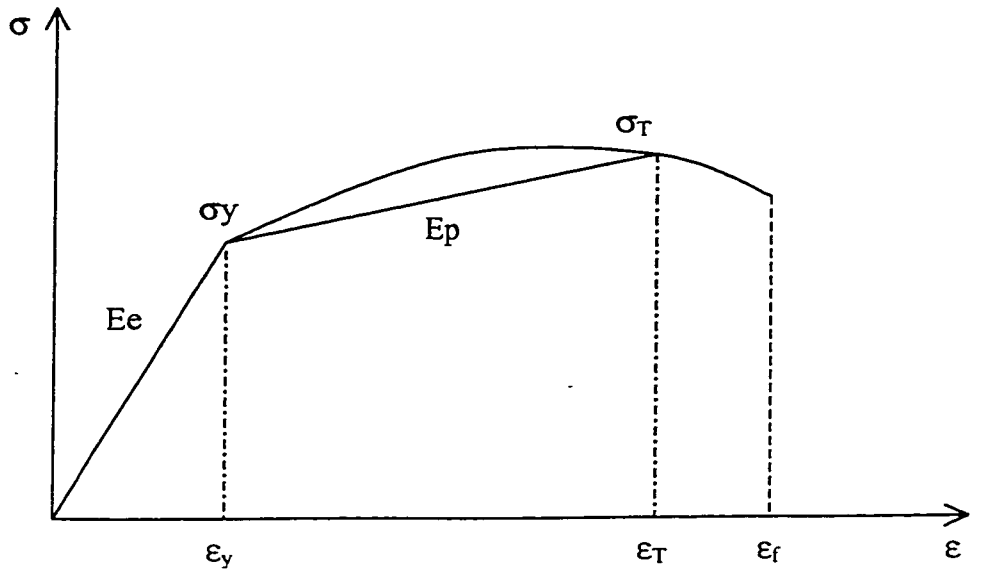

Figure 3-1. The linear approximation of a stress-strain curve

caused by deformations of all bonds that connect the site and its adjacent sites. The magnitude of each force is proportional to the bond deformation as expressed by eq.(1). If the site is on the surface, the load on the site includes the external force. When a lattice site, e.g., site p, shifts away from its initial position $\vec{r}_\circ(p)$, the resulting force on site p is expressed as

$$\vec{F}_p = \sum_q^n k \cdot \Delta\vec{l}(p,q) + \vec{f}_p \tag{4}$$

where, n is the number of sites adjacent to this site, and

$$\Delta\vec{l}(p,q) = \vec{l}(p,q) - \vec{l}_\circ(p,q) = [\vec{r}(q) - \vec{r}(p)] - [\vec{r}_\circ(q) - \vec{r}_\circ(p)] \tag{5}$$

is the deformation vector. $\vec{r}(q)$ and $\vec{r}(p)$ are the position vectors of sites q and p, respectively. $\vec{f}_p$ is the external force on site p if this site is on surface. If site p is not a

surface site, $\vec{f}_p$ is equal to zero. When the total force, $\vec{F}_p$, is known, one may determine the velocity of site p and its next position after a time interval Δt,

$$\vec{v}(p) = \vec{v}_\circ(p) + \frac{1}{m}\vec{F}(p)\Delta t \tag{6}$$

$$\vec{r}(p) = \vec{r}_\circ(p) + \vec{v}_\circ(p)\Delta t \tag{7}$$

where, $\vec{v}_\circ(p)$ is the velocity of site p at the time t, while $\vec{v}(p)$ is the velocity at time $t+\Delta t$. $\vec{r}_\circ(p)$ is the position vector of site p at time t, while $\vec{r}(p)$ is the new position of site p at time $t+\Delta t$. In such a way, one may determine the force on this site at $t+\Delta t$ based on its new position and thus predict the next changes in velocity and position of the site.

During a wear process, material at the surface layer is worn away, for instance, by abrasive particles or by sliding asperities. The wear process may be simulated in the following way. A bulk material is discretized first using a discrete lattice as described earlier. The external surface force results in displacement of sites in the surface layer. New velocities and positions of the sites after a time step Δt can be determined using Newton's law of motion. The resultant deformation generates a new force on each lattice site, which determines the next changes in velocity and position of the site. Within the elastic region, i.e. $\Delta l / l_\circ \le \varepsilon_y$, the displacement of a site is recoverable. If $\Delta l / l_\circ > \varepsilon_y$, plastic deformation occurs, resulting an irreversible residual strain, $\Delta\varepsilon_p = (\Delta l / l_\circ - \varepsilon_y)$. As a result, the length of the stress-free bond, $l_\circ$, changes to l. If a bond experiences a number of plastic deformation events and when the accumulated plastic deformation reaches its critical value for fracture (ε_f), this bond is then broken. A site or a cluster of

sites is worn away if all bonds connecting the site or the cluster to its adjacent sites are broken. Since the bond between a pair of adjacent sites is related to mechanical properties of the material, the wear loss is therefore dependent on the mechanical properties.

- Modeling an Abrasive Wear Process

The model was applied to an abrasive wear process that is similar to the case of rubber-wheel abrasion (ASTM 65) [23,24]. The set up of the rubber-wheel test is illustrated in figure 3-2.

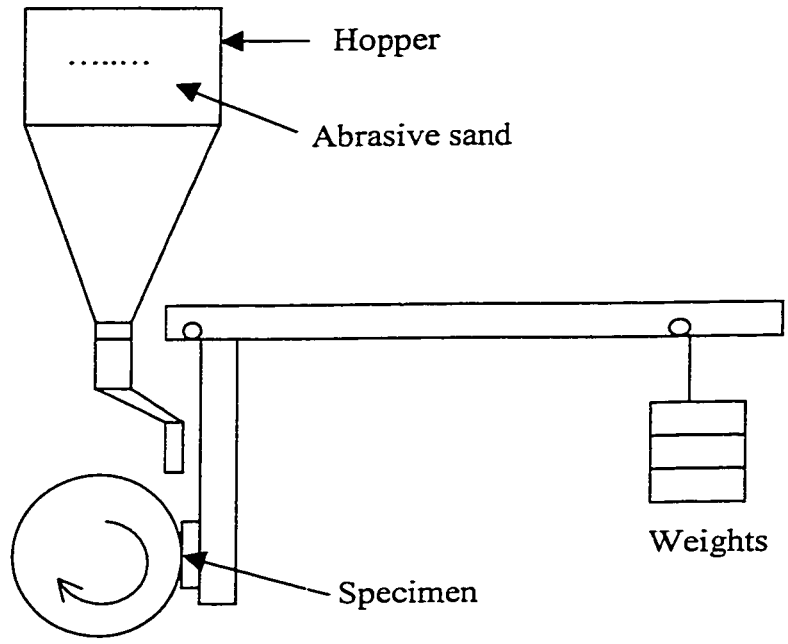

Figure 3-2. Schematic of a standard abrasive wear test (ASTM G65)

A flow of sand particles passes through the gap between the rubber wheel and the surface of a specimen. The vertical pressure on the sand particles in the contact area between the rubber wheel and the specimen distributes elliptically as illustrated in figure 3-3. A sand particle is also pushed by the rubber wheel to move horizontally, thus scratching the specimen surface and resulting in wear. In order to simplify the modeling, a sand particle was assumed to have an initial horizontal velocity equal to the rotation speed of the rubber wheel at its edge, i.e. $v_{in} = R\omega$; where ω is the angular speed of the rubber wheel and R is the wheel radius.

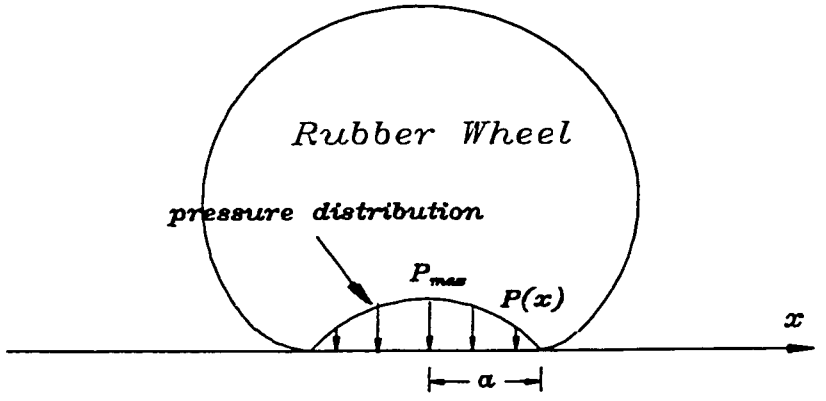

Figure 3-3. The pressure distribution in the contact region

The velocity of a sand particle changed when its movement was obstructed. In the modeling, a sand particle was also discretized and represented using a discrete lattice or grid. The velocity of a lattice site of the sand particle is therefore expressed as $\vec{v} = \vec{v}_{in} + \vec{v}'$, where $\vec{v}'$ is the variation in velocity of the sand site when it was in contact

with the specimen surface. The total velocity of a lattice site of a sand particle was also determined by the Newton's law of motion.

In order to make sure that the MSDM approach can provide correct information of the contact stress/strain, a simple test was made by analyzing the volumetric strain in a contact region where a sand particle is simply pressed onto the contact surface. For the present 2-D modeling, the distribution of the volumetric strain $e = \varepsilon_1 + \varepsilon_2 = \Delta V / V$ was analyzed using the MSDM approach. If in 3-D space, the volumetric strain should be expressed as $e = \varepsilon_1 + \varepsilon_2 + \varepsilon_3 = \Delta V / V$. Here, $\varepsilon_1, \varepsilon_2$ and ε_3 are the principal strain components. Figure 3-4(a) illustrates the distribution of the volumetric strain in the contact region. One may see that the zone right below the contact area is compressively strained while the surrounding region is tensile strained. This volumetric strain distribution was also analyzed using the finite element method. The FEM analysis was conducted using a commercial package (ANSYS) that was performed in 2-dimensional space. In the FEM analysis, square elements were used with fully constrained boundary except the top edge that was exposed to external stress. Figure 3-4(b) illustrates the FEM result; one may see that the FEM result is consistent with the MSDM analysis and this consistency demonstrates the capability of the MSDM approach for determining the contact strain state. It should be mentioned that this MSDM analysis was performed on a lattice with 100×50 nodes and the resolution is therefore not high. One may expect a more accurate result if the system is discretized using a larger number of nodes.

The MSDM approach can correctly describe the strain state in a contact region, justified by the comparison between the MSDM result and the FEM analysis. When the contact strain is correctly determined, then the wear of material can be predicted. The MSDM

model was used to evaluate wear losses of an Al alloy (Al 6061), a copper alloy (Cu 110), a hot rolled steel (HR steel), and stainless steel 304 (304SS). In the modeling, it was assumed that the failure of a bond occurred when this bond was elongated and its length exceeded the critical value for fracture (ε_f), no matter how complex the local stress is. Mechanical properties of these materials were obtained by tensile testing using a universal testing machine (Instron 8516) and the results are listed in table 3-1.

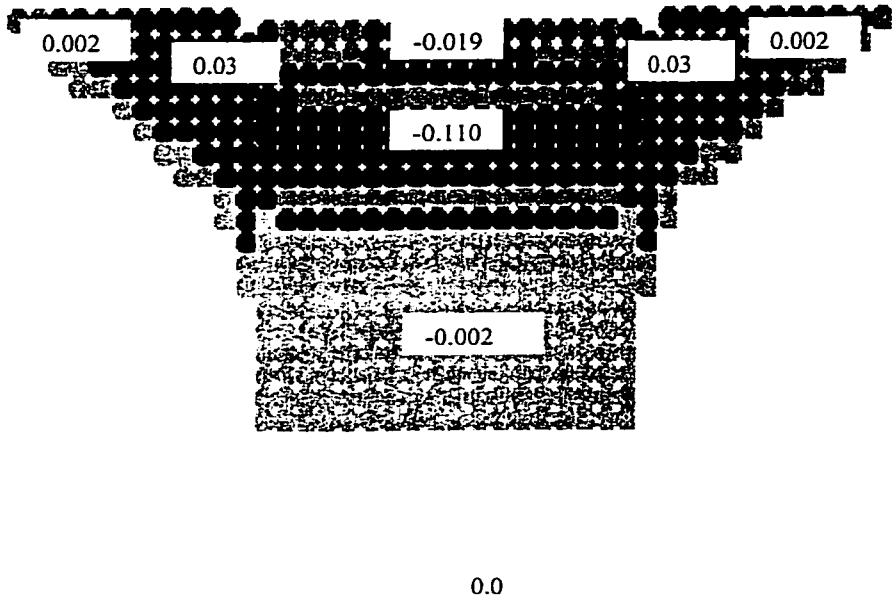

Figure 3-4 (a). Strain distribution obtained using the MSDM

Table 3-1. Mechanical properties of the materials under study

	E (GPa)	σ_y (MPa)	σ_T (Mpa)	Elongation (%)
Al 6061	66	300	349	15
Cu 110	107	278	302	17
304 SS	194	270	670	39
HR Steel	211	340	418	36

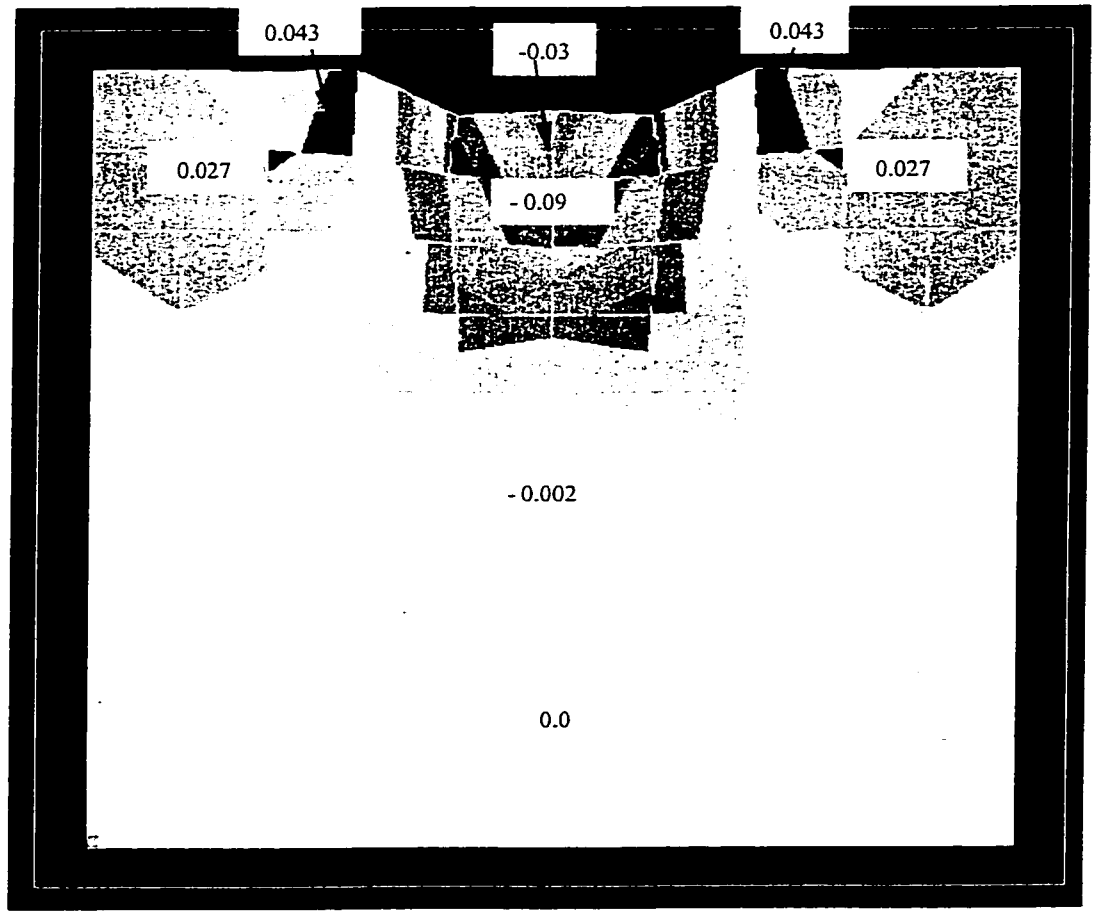

Figure 3-4 (b) Strain distribution obtained using a commercial FEM package (ANSYS)

Based on the mechanical properties, relative wear losses of the Al alloy, Cu alloy, HR steel, and 304 stainless steel were predicted using the MSDM approach. Silica sand was chosen as the abrasive particles and its mechanical properties were obtained from literature [25]. The simulation result is shown in figure 3-5. The result of the simulation demonstrates a linear relationship between the wear loss and the applied load. These materials are also ranked based on the simulation result. As shown, the aluminum alloy has the highest wear loss, followed by the copper alloy, stainless steel, and then the HR steel.

In order to justify the validity of the modeling, wear losses of these four materials were measured using an ASTM G65 Rubber-wheel tester. For each material, five specimens were tested under five different loads at the speed =80 rpm. Each abrasion process lasted 10 minutes. Weight loss of each specimen was measured and converted into the volume loss. The result of the experiment is presented in figure 3-6, which illustrates the linear relationship between the wear loss and the applied load as well as the rank of the materials. The experimental result is consistent with that predicted by the MSDM modeling. It should be mentioned that during this abrasive wear process, the specimen temperature may increase. However, the temperature rise during this abrasion process may not be significant [23], since the system is relatively open and the sand flow always carries fresh sand particles passing through the gap between the rubber wheel and the specimen surface. Therefore, the temperature variation could not considerably influence the mechanical properties of the tested materials and thus their wear performance.

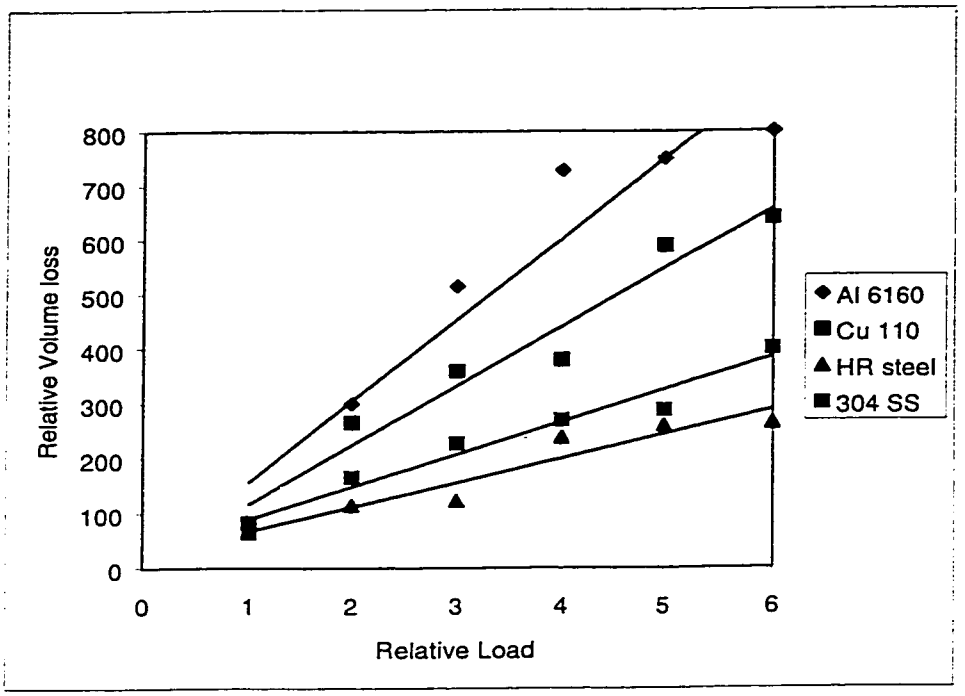

Figure 3-5. Relative volume losses of aluminum, copper, stainless steel and steel predicted using the MSDM

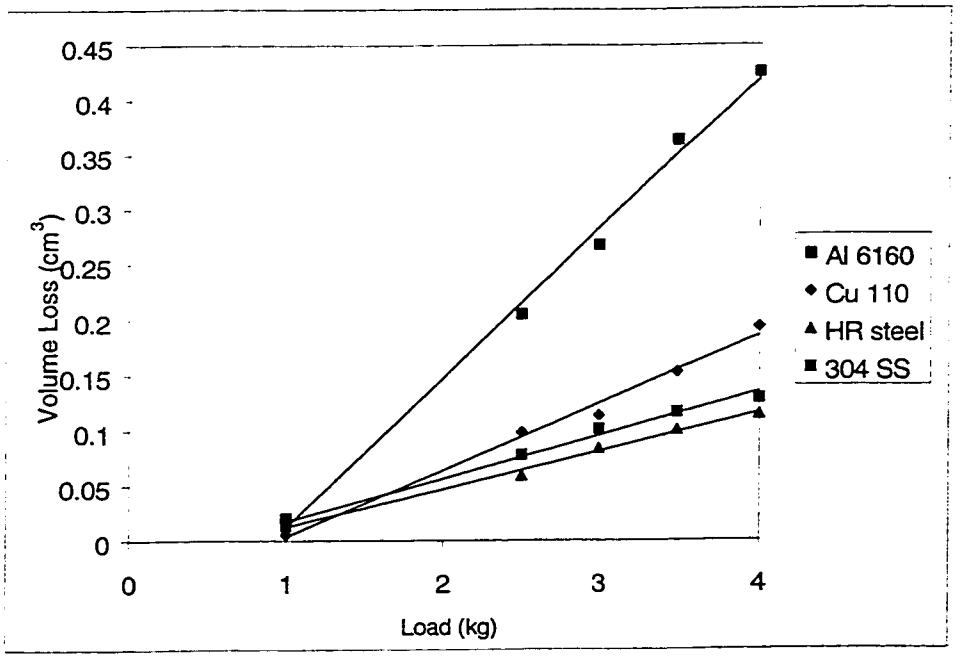

Figure 3-6. Volume losses of aluminum, copper, stainless steel and steel (experiment)

3.3. Conclusions

A dynamic model was developed to simulate wear processes and predict wear performance of materials at the microscopic levels. This model is simple, flexible and easy to apply. In the model, a material system is discretized and mapped onto a discrete lattice or grid, each of which represents a small volume of the material. Under the influence of external force and the constraint from its neighbors, a lattice site may move obeying the Newton's law of motion. Preliminary simulation was conducted to study a Rubber-Wheel (ASTM G65) abrasion process. Four materials including an Al alloy, a Cu alloy, a hot-rolled steel and, stainless steel 304 were studied, employing the MSDM approach. The simulation is consistent with performed experiment using an ASTM G65 tester. The model was further justified by the comparison of the volumetric strain distribution in a contact region predicted by the MSDM approach with that predicted using the FEM method.

Acknowledgement

The authors are grateful for financial support from the Natural Science and Engineering Research Council of Canada (NSERC) and Syncrude Canada Ltd.

Reference List for Chapter 3

1. Ling, F. F. and Pan, C.H.T. (Eds.), Approaches to Modeling of Friction and Wear, Springer-Verlag, New York, NY, 1988.
2. Ludema K.C. and Bayer R.G. (Eds.) Tribological Modeling for Mechanical Designers, ASTM STP 1105, American Society for Testing and Materials, Philadelphia, 1991.
3. Hsu, S.M., Shen, M.C. and Ruff, A.W., Tribology International, 30, No.5 (1997) 377.
4. Challen, J.M. and Oxley, P.L.B., Wear, 53 (1979) 229.
5. Green A. P., Proc. R. Soc. London, Ser. A, 228 (1955) 191.
6. Avitzur, B., Huang, C.K. and Zhu, Y.D., Wear, 95 (1984) 59.
7. Edwards C. M. and Halling J., J. Mech. Eng. Sci., 10 (1968) 101.
8. Komvopoulos, K. and Choi, D.H., J. Tribology, 114 (1992) 823.
9. Põdra, P. and Andersson, S., Wear, 224 (1999) 13.
10. Hai, S., Pohl, H., Schomburq, U., Upper, G. and Heine, S., Wear, 224 (1999) 175.
11. Xuefeng, T. and Bharat, B., J. Tribology, 118 (1996) 33.
12. Hancock, P., Nicholls, J.R. and Stephenson, D.J., Surf. Coat. Technol., 32 (1987) 285
13. Nicholls, J.R. and Stephenson, D.J., Wear, 186-187 (1995) 64.
14. Polycarpou, A.A. and Soom, A., Wear, 181-183 (1995) 32.
15. Jiaren, J., Stott, F.H. and Stack, M.M., Wear, 181-183 (1995) 20.
16. Wong, K.K. and Clark, H.M., Wear, 160 (1993) 95.
17. Turenne, S. and Fiset, M., Wear, 162-164 (1993) 679.
18. Haiyan, L. and Hsu, S.M., Wear, 195 (1996) 169.

19. Robbins, M.O. and Krim, J., MRS Bulletin, 23 (1998) 23.

20. Harrison, J.A., Stuarat, S.J. and Brenner, D.W., Atomic-Scale Simulation of Tribological and related Phenomena, Handbook of Micro/Nanotribology, 1998.

21. Zhong, W. and Tomanek, D., Phys. Rev. Lett., 64 (1990) 30.

22. Elalem, K. and Li, D.Y., Proc., the International Conference on Powder Metallurgy & Particulate Materials ($PM^2TEC'99$), Vancouver, Canada (1999) 'in press'.

23. Stevenson, A.N.J. and Hutchings, I.M., Wear, 195(1996) 232.

24. Ruff, A.W., ASM International, Materials Park, OH, USA, (1997) 22.

25. Callister, W.D., J. Materials Science and Engineering an Introduction, John Wiley & Sons, Inc., (1997) 401.

Chapter 4

Research Paper

Dynamic Simulation of Abrasive Wear of Composite Materials

Presented and published in Proceedings, the International Conference on Powder Metallurgy & Particulate Materials, (TM^2Tec99), Vancouver, Canada, 1999, Vol.3 part 11, pp. 3-12

4.1. Introduction

Wear is a complicated process, involving time-dependent deformation and removal of material at the contact area. Although experiment is the prime approach for evaluating wear of materials, it is costly and has some limitations for exploring the wear mechanism on micro/meso-scopic levels. A wear process may involve several wear mechanisms and the simultaneous action of these mechanisms may make the obtained information difficult to explain. In recent decades, computer modeling has become a powerful approach for wear study. Computer simulation provides an effective and economical technique, allowing us to study effects of different factors on wear behavior of materials under controllable conditions. The effect of each parameter involved in a wear process could thus be studied separately.

Numerous models have been proposed for simulating various wear processes. However, many proposed models are not generally recognized, since they are limited to specific conditions, e.g., only suitable for particular material pairs, limited contact geometry and operating condition, or particular environments [1] Current wear models generally fall into two classes: macro-modeling and atomistic modeling. The first class contains the so-called macro-models, where mechanical models were developed to simulate wear by, for example, employing the slip line theory [2,3] and the upper-bound method [4,5]. Perhaps one of the most widely used models is the finite element method (FEM) [6,7,8]. The FEM modeling is carried out by applying a fine mesh to discretise a specimen, and then solving and calculating the strain when the two surfaces are in contact. If the strain exceeds a critical value for a cell of the mesh, this cell is

disconnected from the rest of the specimen. The finite element method has been used to solve 2-dimensional and 3-dimensional elastic/plastic contact problems. However, in order to solve realistic wear problems, a large number of mesh elements are required to deal with the changing surface geometry. For 3-D rough surface contact problems with many asperities involved, the requirement of a large number of mesh elements makes the finite element approach unfeasible [9]. There are also many other types of macro-models, proposed to deal with erosion, oxidative wear, and corrosive wear under particular conditions. However, many models were developed under some assumptions or based on existing tribological rules, or incorporated with empirical equations. This, more or less, weakens their predictive function. Furthermore, many macro-models are static in nature and only take into account the average mechanical properties of heterogeneous materials (e.g. multiphase and composite materials). They are therefore not suitable for characterizing dynamic wear behavior of materials on finer levels, such as the microstructure effect on wear. As a matter of fact, a lot of macro-models were proposed for mechanical design rather than for prediction of material performance [10]. Therefore, these models were proposed for numerical application of the existing tribological theories in mechanical design rather than for fundamentally exploring wear mechanism and predicting wear behavior of materials.

The second class involves atomistic modeling of tribological phenomena and materials response to external forces, such as the Molecular Dynamics simulation (MD) [11]. MD technique deals with the motion and trajectory of individual atoms or molecules, and can be used to predict various dynamic processes at atomic or nanometre

levels. MD technique is one of the most powerful approaches, which significantly advances our understanding of material behavior and relevant processes. MD technique can well characterize friction process at nanometre scale, when appropriate atomistic potentials are used. However, it is difficult to directly apply MD approach to a micro/macroscopic wear process because of the limited capacity of current computing facilities. Molecular Dynamic method is usually used to simulate a process involving 10^3~10^4 atoms. However, to simulate a bulk materials as small as 1 μm^3, one has to deal with 10^9~10^{10} atoms. Although the fastest parallel computers may allow the MD simulation of a system involving 10^8 atoms, it is not realistic to model wear behaviour of a system involving many micro/macroscopic factors. For example, in order to investigate effects of the microstructure inhomogeneity and contact geometry on wear behavior of a material, a huge number of atoms have to be used.

Great efforts have being continuously made to improve the wear simulation technique. Recently, a tentative micro-scale dynamic model (MSDM) was proposed [12], taking advantages of both the macro-models and the MD approach. This dynamic model is developed to simulate wear processes at microscopic levels, with the aim of building a bridge between the atomistic simulation and the macro-level modeling. The MSDM model was developed on fundamental physical laws with the capability of predicting wear behavior of materials without any limitation to the surface geometry. This paper reports our preliminary research on the application of this model in investigating wear behavior of composites.

4.2. Model Description

The objective of this work is to apply the MSDM technique to modeling an abrasion process that is similar to the rubber-wheel abrasion test (ASTM G65, [Ruff, 1997]) for composite materials under different loads and volume fractions of the reinforcing particles. During this process, abrasive particles pass through the gap between the rubber wheel and the specimen, abrading the specimen surface (see figure 4-1). A sand particle is under pressure from zero to maximum and then back to zero, following an elliptical distribution along the moving path of the particle. The mass loss of a tested material is dependent on its mechanical properties and those of the abrasive sand as well as the wear condition.

The present simulation was performed in a two-dimensional space. In this model, a given specimen is discretised using a square lattice, each site or node of which represents a small volume of the material. A site is constrained by its neighbors and the interaction between a pair of adjacent sites is a function of mechanical properties of the material. During a wear process, a lattice site may move and its motion is determined by the external force and/or the interaction between this site and its neighbors. Final positions of all lattice sites reflect the response of the material to the external force, thus providing information on wear behavior of this material.

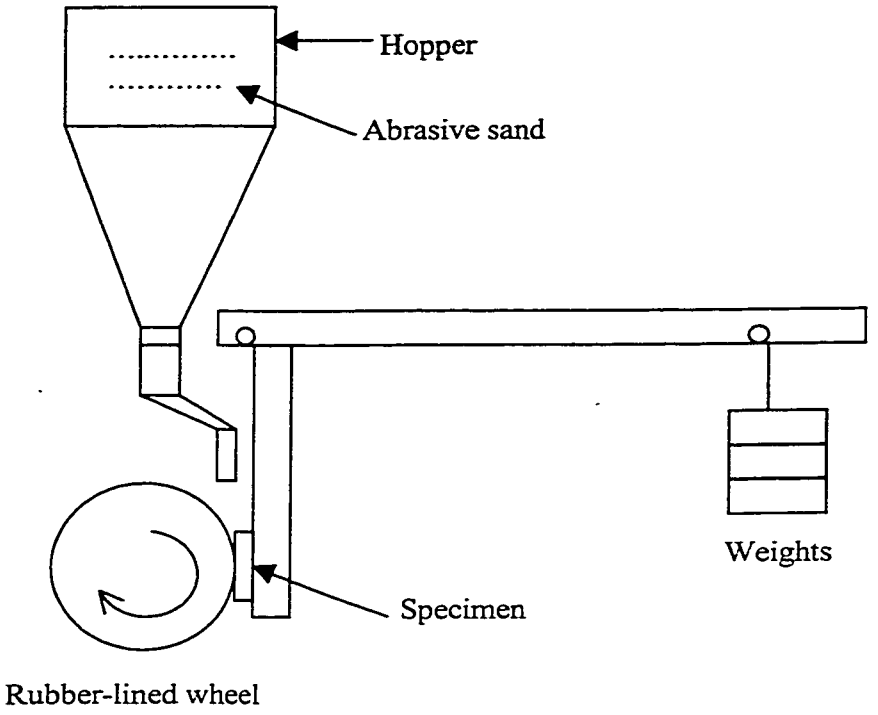

Figure 4-1. Schematic illustration of a standard abrasion test (ASTM G65)

- Interaction between Lattice Sites

As mentioned, in this MSDM model a lattice site may move under external forces and/or the interaction between adjacent sites. The interaction between two adjacent sites is dependent on mechanical properties of the material. In the case of a single-phase material, the force between a pair of adjacent sites is proportional to the deformation of the bond between these two sites, that is

$$f = k \cdot \Delta l \tag{1}$$

where, $\Delta l = l - l_{\circ}$ is the deformation of the bond, $l_{\circ}$ is the unit length of the lattice or the bond length in stress-free condition, and l is the bond length after the deformation. The

corresponding strain is equal to $\varepsilon = \Delta l / l_o$. The coefficient, k, in eq. (1) is a force coefficient that characterizes the interaction between a pair of sites. The k-value is equal to $E \cdot l_o$, where E is the slope of the stress-strain curve of the material. When the deformation Δl is within the elastic region, E is the elastic modulus. To simplify the simulation, we use two values for E and linearly approximate the stress-strain curve as illustrated in figure 4-2. In the elastic region, $E = E_e = \sigma_y / \varepsilon_y$, where σ_y and ε_y are the yield stress and yield strain, respectively; while in the plastic region, $E = E_p = (\sigma_T - \sigma_y) / (\varepsilon_T - \varepsilon_y)$, where σ_T and ε_T are the tensile strength and the corresponding strain. When the force between a pair of sites is within the elastic region, the corresponding deformation is recoverable; otherwise irreversible plastic deformation will be generated. Since E_p is the slope of the stress-strain curve in the plastic region, its value reflects the work-hardening of the material.

In the case of a composite material, the reinforcing particles are randomly generated in the matrix. There are three types of site-site interactions, for instance, in a ceramic/metal composite: metal-metal, ceramic-ceramic, and metal-ceramic interactions. The interaction between a pair of like sites, as that in a single-phase material, has been described earlier.

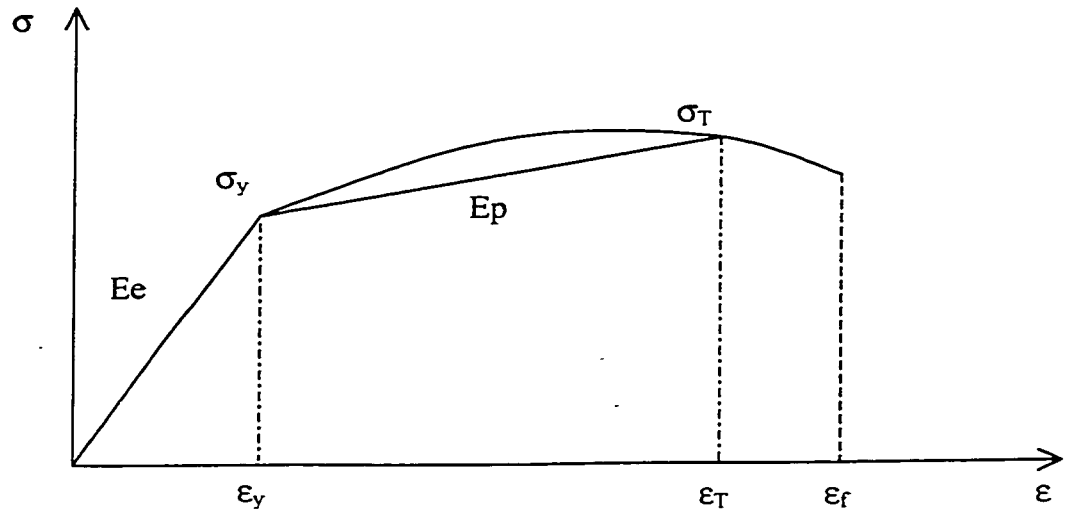

Figure 4-2. The linear approximation of a stress-strain curve

The interaction between a pair of unlike sites, if in elastic deformation range, may be represented as

$$\begin{cases} \Delta l = \Delta l_c + \Delta l_m \\ \Delta l_c = \Delta l / (1 + \dfrac{E_c}{E_{me}}) \\ \Delta l_m = \Delta l / (1 + \dfrac{E_{me}}{E_c}) \\ f(c,m) = f(m,c) = 2E_c \Delta l / (1 + \dfrac{E_c}{E_{me}}) \end{cases} \tag{2}$$

where $\Delta l = \Delta l_c + \Delta l_m$ is the change in length of a metal-ceramic bond. E_c and E_{me} are elastic moduli of the ceramic and metal, respectively. $f(c,m)$ is the magnitude of the force on the ceramic site due to the deformation of this metal-ceramic bond. $f(m,c)$ is

the magnitude of the force on the metal site which is equal to $f(c,m)$. If plastic deformation occurs, this unlike site-site interaction becomes

$$\begin{cases} \Delta l = \Delta l_c + \Delta l_m \\ \Delta l_c = [\Delta l - (1 - \dfrac{E_{me}}{E_{mp}})\Delta l_{my}] / (1 + \dfrac{E_c}{E_{mp}}) \\ \Delta l_m = \Delta l_{my}(1 - \dfrac{E_{me}}{E_{mp}}) + \Delta l_c \dfrac{E_c}{E_{mp}} \\ f(c,m) = f(m,c) = \{E_c[\Delta l - (1 - \dfrac{E_{me}}{E_{mp}})\Delta l_{my}] / (1 + \dfrac{E_c}{E_{mp}})\}2 \end{cases} \tag{3}$$

where Δl_{my} is the change in the bond length corresponding to the yield strain of the metal. E_{mp} is the modulus of the metal when it is in plastic deformation state. The equations (2) and (3) were derived by considering the force equilibrium between the pair of the ceramic and metal sites with the assumption that the cohesive strength of the ceramic/metal interface is high enough to withstand the deformation of the ceramic-metal bond without failure. In this case, a ceramic-metal bond is broken only when $2\Delta l_c / l_\circ \geq \varepsilon_{cf}$ or $2\Delta l_m / l_\circ \geq \varepsilon_{mf}$, depending on which condition is met first. Here, ε_{cf} and ε_{mf} are the fracture strains for the ceramic and the metal, respectively. However, if the cohesive strength of the ceramic-metal interface is not high, one may determine the failure of a ceramic-metal bond by taking into account the cohesive strength, σ_i, at the interface [13]. If $f(c,m) = f(m,c) \geq \sigma_i l_\circ^2$ before the condition, $2\Delta l_c / l_\circ \geq \varepsilon_{cf}$ or $2\Delta l_m / l_\circ \geq \varepsilon_{mf}$, is met, the ceramic-metal interface will fail. The cohesive strength of an

interface is dependent on the chemical cohesion and the structural mismatch between different phases as well as interfacial defects. Further study on this complicated issue is being conducted. In the present study, the cohesive strength of the interface was assumed to be high enough so that the failure of a ceramic-metal bond occurred only when the criterion, $2\Delta l_c / l_\circ \geq \varepsilon_{cf}$ or $2\Delta l_m / l_\circ \geq \varepsilon_{mf}$, was met.

- The Movement of a Lattice Site

When a lattice site is under the influence of a force, its motion and trajectory are determined by Newton's law of motion,

$$\bar{F} = m\frac{d^2\bar{r}}{dt^2} \tag{4}$$

where, m is the mass of the lattice site (with its volume equal to $l_\circ^2$ in 2-D space). $\bar{F}$ is the total force applied to the lattice site. This force is the sum of the forces caused by deformations of all bonds that connect the site and its adjacent sites. The magnitude of each force is proportional to the bond deformation as expressed by equation (1) for a single-phase material or by equations (2) and (3) for a composite material, respectively. If the site is on the surface, the load on the site includes the external force. When a lattice site, e.g., site p, shifts from its initial position, the resulting force on site p is expressed as

$$\bar{F}_p = \sum_q^n \bar{f}(p,q) + \bar{f}_p \tag{5}$$

where, n is the total number of sites adjacent to this site and q denotes a site adjacent to the site p. $\bar{f}(p,q)$ is the force on site p due to the deformation of the bond between sites p and q. $\bar{f}_p$ is the external force on site p if this site is on surface. If site p is not a

surface site, $\vec{f}_p$ is equal to zero. When the total force, $\vec{F}_p$, is known, one may determine the velocity of site p and its next position after a time interval Δt,

$$\vec{v}(p) = \vec{v}_\circ(p) + \frac{1}{m}\vec{F}(p)\Delta t \tag{6}$$

$$\vec{r}(p) = \vec{r}_\circ(p) + \vec{v}_\circ(p)\Delta t \tag{7}$$

where, $\vec{v}_\circ(p)$ is the velocity of site p at the time t, while $\vec{v}(p)$ is the velocity at time $t+\Delta t$. $\vec{r}_\circ(p)$ is the position vector of site p at time t, while $\vec{r}(p)$ is the new position of site p at time $t+\Delta t$. In such a way, one may determine the force on this site at $t+\Delta t$ based on its new position and thus predict the next changes in velocity and position of the site.

4.3. Application of the MSDM approach to Study Abrasive Wear of Composites

The MSDM model has been successfully applied to modeling abrasive wear of single-phase materials, in good agreement with experimental results [12,14]. This approach has been further justified by comparing the MSDM analysis of the strain distribution in a contact region with that obtained using the finite element method, when a sand particle is pressed onto a metal surface [14]. In the present work, the MSDM method was applied to investigate the wear performance of an aluminum alloy-matrix composite reinforced by SiC. In this modeling, the SiC-Al alloy interfacial bonding was assumed to be strong enough so that the failure of the bond occurred only when the local strain of the SiC site or that of the aluminum alloy site reaches its critical strain at

fracture (ε_f). Silicon carbide sand was chosen as the abrasive particle and a monolayer of abrasive particles between the rubber-wheel and a specimen was assumed.

In this modeling, the mechanical properties of aluminum alloy E_{me}=68GPa, E_{mp}=0.31GPa, ε_f=16%, σ_y=300MPa, were obtained from tensile testing and the mechanical properties of SiC, E_c=430GPa, ε_f=0.2%, σ_y=862MPa, were obtained from literature [15]. Relative wear loss of 20%SiC-Al alloy composite with respect to the applied load was simulated, and the result is illustrated in figure 4-3. It was demonstrated that the wear loss increased with an increase in the magnitude of the applied load. A linear relationship between the wear loss and the applied load was observed. This linear relationship agrees with general trend of material loss against load under the rubber-wheel abrasion condition [14,16].

The wear resistance of a MMC composite greatly depends on the volume fraction of the ceramic particles. In this modeling, several volume fractions of SiC particles were considered; they were 0%, 10%, 20% and 30%. In order to simplify the modeling, tetragonal shape was considered for the SiC particles. The spatial distribution of randomly created SiC particles in a sample is illustrated in figure 4-4. Relative wear losses of the composites with different SiC fractions were predicted, and the result is presented in figure 4-5. One may see that the SiC particles significantly enhanced the wear resistance of aluminum alloy, and the wear loss decreased with increasing the SiC fraction. This result agrees well with experimental observations [16].

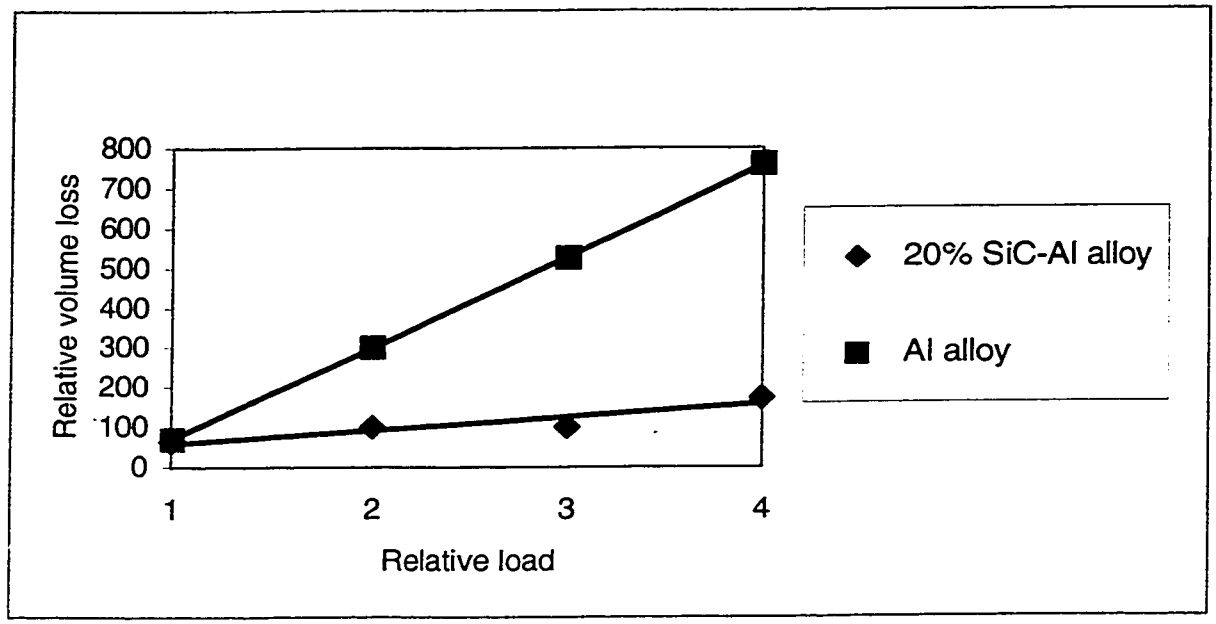

Figure 4-3. Relative wear losses of Aluminum and 20%SiC-Al alloy composite with respect to the applied load

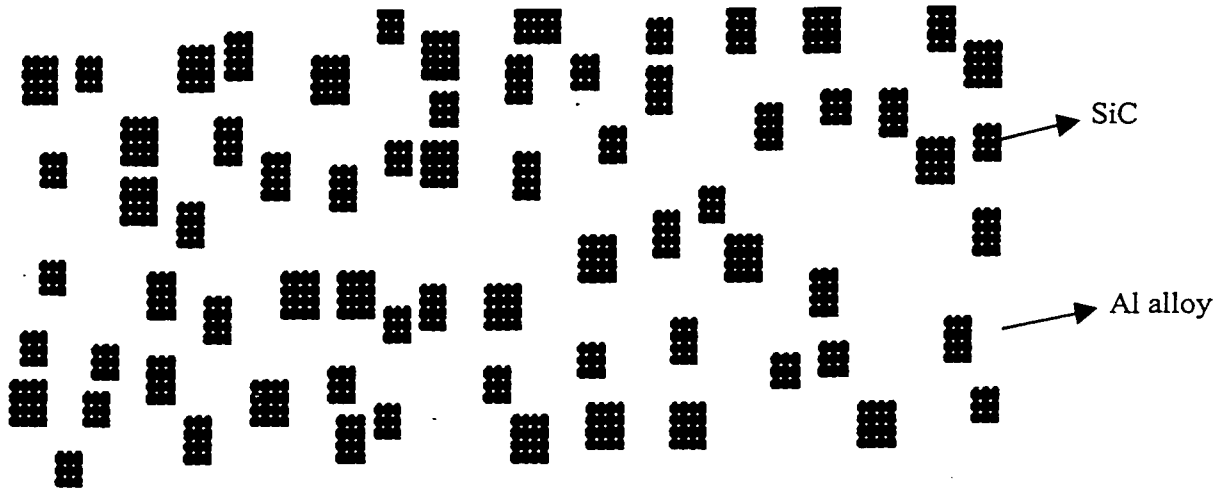

Figure 4-4. Sample microstructure (20%SiC-Al alloy)

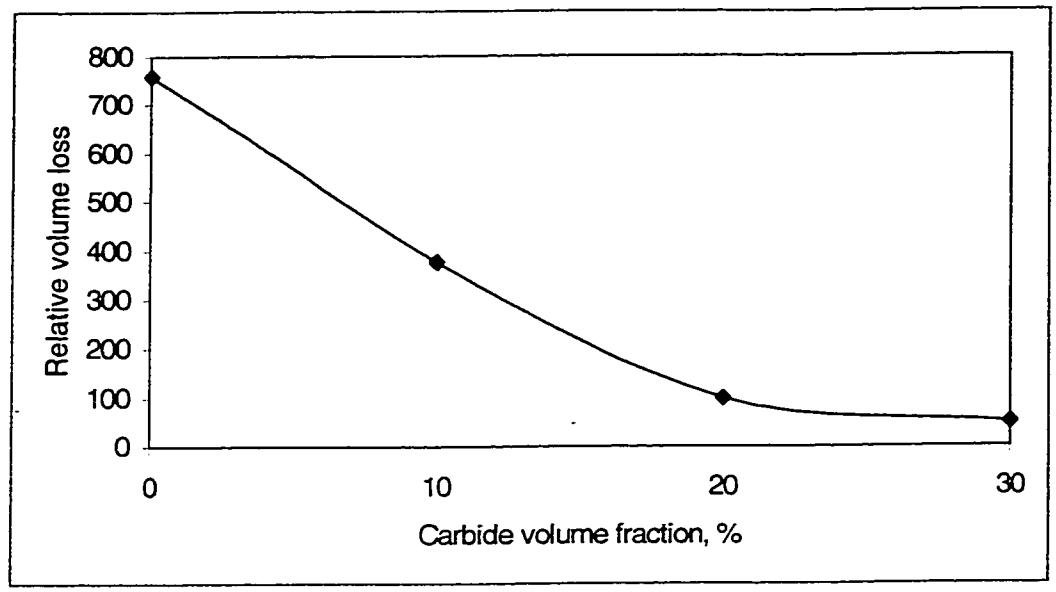

Figure 4-5. Relative volume loss against the volume fraction of SiC particles under a relative load L=2

The size of reinforcing particles in a MMC composite strongly influences the performance of the composite. The size effect of SiC particles on the wear performance of the SiC/Al alloy composite was also investigated. In this modeling, several sizes of reinforcing SiC particles were chosen, which were 1, 1.5, 2, 2.5, and 3 times as big as the average size of SiC particles shown in figure 4-4, respectively. The size of the abrasive sand particles used for the modeling was about two times bigger than that of the reinforcing SiC particles shown in figure 4-4. The simulation demonstrated that the larger the carbide size, the lower is the wear rate, as figure 4-6 illustrates. The simulated size effect is in agreement with the results obtained by other investigators [16].

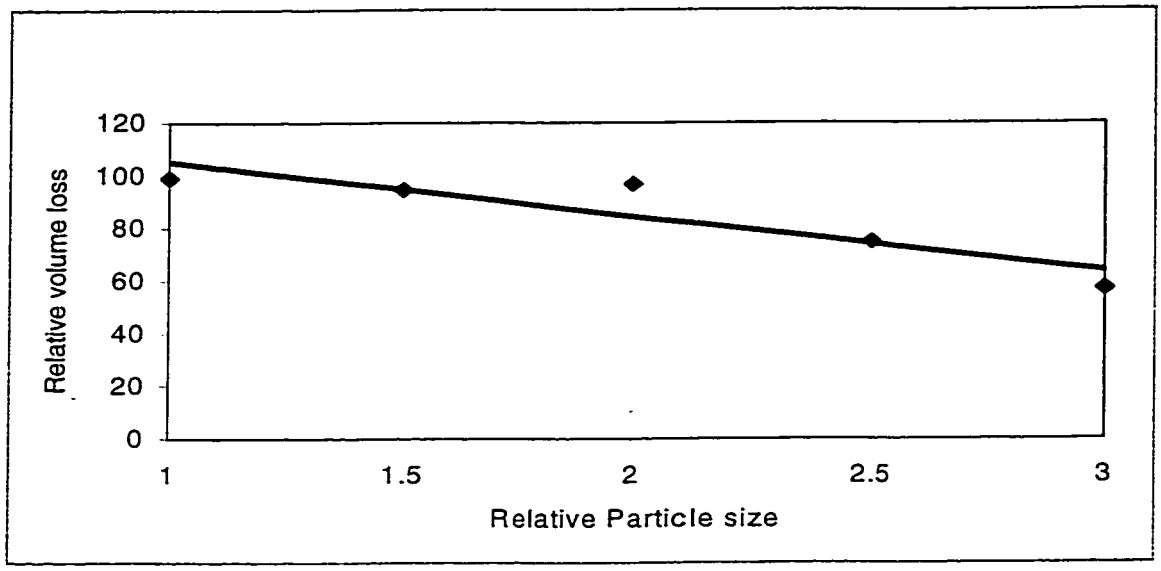

Figure 4-6. The effect of carbide size on the relative volume loss (under relative load L=2)

The preliminary MSDM modeling study on SiC/Al alloy composite provided the information on the wear behavior of this composite material. The agreement between the modeling and available experimental data manifests the capability of such an approach in simulating wear behavior of composite or multiphase materials. Further research is being conducted to refine this computational method for various tribological applications.

4.4. Conclusions

A dynamic wear model was developed to characterize wear processes and predict material performance at microscopic levels. This wear model is developed on fundamental physical laws, simple, flexible and easy to apply. In this model, a material system is mapped onto a discrete lattice and each lattice site represents a small volume of the material. Under the influence of an external force, a lattice site may move, governed

by Newton's law of motion. Final positions of all lattice sites reflect the response of the material to external force. Preliminary 2-dimensional simulation was conducted to study the abrasion behavior of SiC/Al alloy composite during an abrasive wear process that is similar to the Rubber-Wheel (ATSM G65) abrasion process. Effects of the applied load, the volume fraction of SiC particles, and the SiC particle size on the wear resistance of the composite were investigated. Good agreement between the modeling and available experimental results was found.

Acknowledgement

The authors are grateful for financial supports from the Natural Science and Engineering Research Council of Canada (NSERC) and Syncrude Canada Ltd.

Reference List for Chapter 4

1 S.M. Hsu, M.C. Shen and A.W. Ruff, "Wear Prediction for Metals", *Tribology International*, Vol. 30, No. 5, 1997, pp. 377-383.

2 J.M. Challen and P.L.B. Oxley, "An Explanation of The Different Regimes of Friction and wear using asperity deformation models", *Wear*, 1979, Vol. 53, pp. 229-243.

3 T. Wanheim and T. Abildgaard, "A mechanism for metallic friction", *Proc. 4th Int. Conf. On Production Engineering*, Tokyo, August 1980, pp. 122.

4 B. Avitzur, C.K. Huang and Y.D. Zhu, "A friction Model Based on the Upper-Bound approach to the Ridge and Sublayer Deformations", *Wear*, Vol. 95, 1984, pp. 59-77.

5 A. Azarkhin and M. L. Devenpeck, "Enhanced model of a plowing asperity", *Wear*, Vol. 206, 1997, pp. 147-155

6 K. Komvopoulos and D.H.Choi, "Elastic Finite Element Analysis of Multi-Asperity Contacts", *Journal of Tribology*, Vol. 114, 1992, pp. 823-831.

7 P. Põdra and S. Andersson, "Finite element analysis wear simulation of a conical spinning contact considering surface topography", *Wear*, Vol. 224, 1999, pp. 13-21.

8 H. Sui, H. Pohl, U. Schomburq, G. Upper, and S. Heine, "Wear and friction of PTFE seals", *Wear*, Vol. 224, 1999, pp. 175-182.

9 T. Xuefeng. and B. Bhushan., "A Numerical Three-dimensional Model for the Contact of Rough

Surfaces by Variational Principle", *Journal of Tribology*, Vol. 118, 1996, pp. 33-42.

10 F. F. Ling and C.H.T. Pan (ed.), "Approaches to Modeling of Friction and Wear", *(Proc. of the Workshop on the Use of Surface Deformation Models to Predict Tribology Behavior),* Springer-Verlag, New York, 1986.

11 M. O. Robbins and J. Krim, "Energy Dissipation in Interfacial Friction", *MRS Bulletin*, Vol. 23, 1998, pp. 23-26.

12 D. Y. Li, K. Elalem, M. J. Anderson and S. Chiovelli, "A microscale dynamical model for wear simulation" , *Wear*, Vol. 225, 1999, pp. 380-386.

13 N. P. Suh, *Tribophysics*, Prentice-Hall, Inc., Englewood Cliffs, New Jersey, USA, 1986, P.143.

14 K. Elalem and D.Y. Li, A Dynamical Simulation Model of Wear, *Journal of Computer Aided*

Materials Design, to be published.

15 W. D. Callister, Jr, *Materials Science and engineering an Introduction*, 4th ed., John Wiley & Sons, Inc., USA, 1997, pp. 401.

16 *ASM Handbook*, ASM international, USA, Vol. 18, 1992, pp. 801-811.

Chapter 5

Research Paper

Variations in wear loss with respect to load and sliding speed under dry sand/rubber-wheel abrasion condition: a modeling study

Accepted by Wear

5.1. Introduction

The dry sand/rubber-wheel abrasion test [1] is widely used to evaluate low-stress abrasive wear of materials, particularly for evaluating wear-resistant materials used in the mining, oilsand and agricultural machinery industries, e.g., those for mechanical components such as shovels, draglines, drilling systems, and agricultural tools [2]. Figure 5-1 illustrates a dry sand/rubber-wheel abrasion tester. During the abrasion test, a specimen is loaded against the rim of a rotating rubber wheel; a sand flow is directed to the gap between the wheel and specimen, abrading the specimen under an applied normal load at a certain sliding speed. Abrasion resistance of a material is evaluated by measuring its volume loss. A high wear-resistant material has a low volume loss. Reasonably good matching is usually found between the laboratory test and practice [3,4].

It is generally accepted that the volume loss of a material is proportional to the applied load. Materials are therefore often tested under a fixed load at a fixed sliding speed to have all materials tested under the same condition [3,5]. However, wear is a complex surface process and wear of a material differs from one to another and this makes the accuracy of the one-load testing procedure questionable.

Recent work on D2 tool steel has demonstrated that this material shows different response to variations in the applied load, not obeying a linear relationship between the load and wear loss [6]. The volume loss of the tool steel increases initially and then decreases as the load is increased. The D2 steel shows markedly better performance under high loads than under lower loads. This provides a good example to show that ranking materials using different loads could result in different conclusions. Haworth [7]

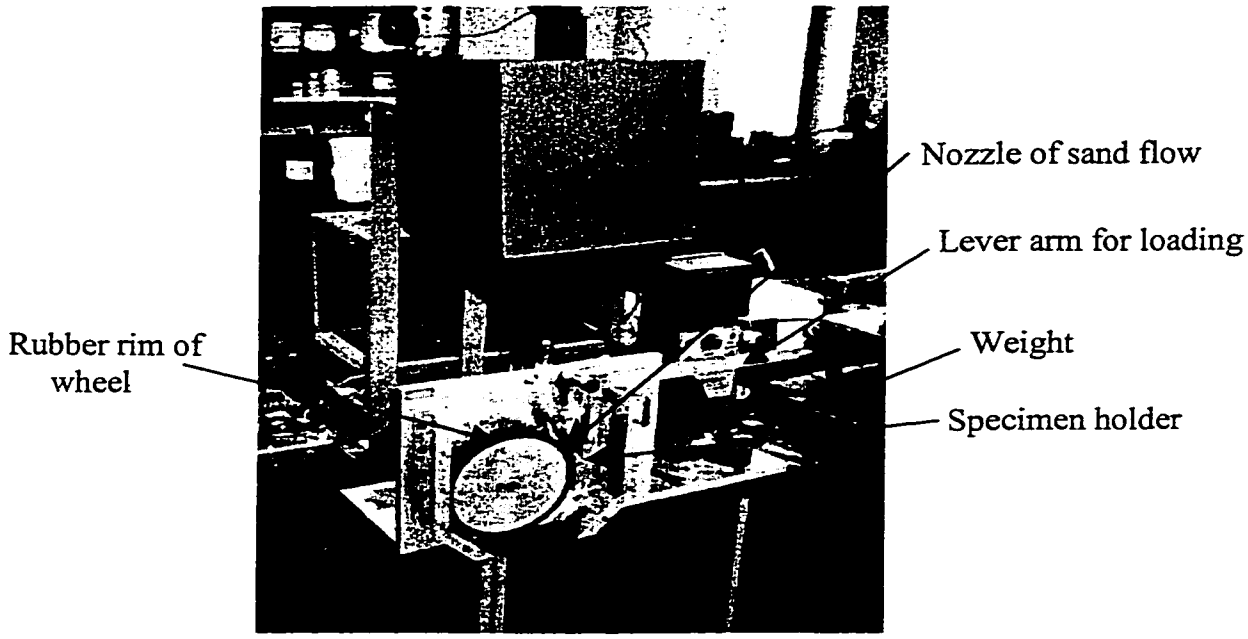

Figure 5-1. Rubber wheel test equipment

has also noticed that when the applied load is high, the wear rate of a material is greater than that expected and the linear relationship does not exist. The wear-load relation is also influenced by other factors such as the hardness of the rubber rim on the wheel [8] and the sand flow that is influenced by the load and the sliding speed. It is therefore needed to have a close look at the wear process under the dry sand/rubber-wheel abrasion condition, in order to adequately evaluate the wear behavior of materials and draw appropriate conclusions from the abrasion testing. However, the wear loss of a material is affected by the above-mentioned factors simultaneously and it is not easy to separate their effects experimentally.

Computer modeling provides an effective approach suitable for such a study, since this approach allows us to perform "computational" experiments under controllable

conditions and identify the predominant factors that determine the wear loss. In this work, abrasive wear of several engineering materials was investigated under the dry sand/rubber-wheel abrasion condition, with particular interest in the relation between the volume loss and the load as well as the sliding speed. A micro-scale dynamic model (MSDM) [5,9,10] was employed for this work. Several metallic materials, including Al alloy, Cu alloy, 17-4 PH stainless steel and D2 tool steel, were selected for the study.

5.2. Results and Discussions

- *The MSD model*

In order to make the article self-containing, a brief description of the MSD model is given here. In this approach, a material system was discretized and mapped onto a discrete lattice. Each lattice site represents a small volume of the material. During abrasion, a lattice site moves under the influence of both the external force and the interaction between the site and its adjacent sites. The site-site interaction is dependent on the mechanical properties of the material, such as the elastic modulus, yield strength, work-hardening and the fracture strain. Newton's law of motion is used to determine the movement of a lattice site. The strain between a pair of metal sites is recoverable within the elastic deformation range; otherwise plastic strain is generated. A site-site bond is broken when the total strain exceeds the fracture strain. A site or a cluster of sites is worn away if all bonds connecting the site or the cluster to its neighbors are broken. Good agreement between the MSD approach and experimental observations as well as finite element analysis has been found. Details of the model have been given elsewhere [5,9,10].

5.2.1. Effect of Load on Wear

Volume losses of several engineering materials as a function of load were predicted using the MSD model. Al alloy (Al 6061), copper alloy (Cu 110), 17-4 PH stainless steel and D2 tool steel were selected for the study. Mechanical properties of these materials were determined by tensile test using a tensile machine (Instron 8516) and the results are given in table 5-1. Figure 5-2 illustrates results of the modeling for which SiO_2 sand was used as the abrasive. It was demonstrated that the Al alloy exhibited the lowest resistance to abrasion, followed by the Cu alloy and PH-17 steel, and the D2 tool steel had the highest wear resistance. The modeling demonstrated that the volume loss increased as the load was increased. However, this situation changed when a material had a higher hardness, especially for the D2 steel. As shown in figure 5-2, the volume loss of D2 steel increased initially and then decreased as the load was continuously increased.

Table 5-1 - Mechanical properties of the materials under study

	E (GPa)	σ_y (Mpa)	σ_T (MPa)	ε_f (%)	Hardness (HRC)
Al 6061	66	300	349	15	21
Cu 110	107	278	302	17	40
PH-SS	201	1273	1375	14	46
D2 Steel	211	1772	1976	3.5	56
SiO_2	73	110	-	-	62

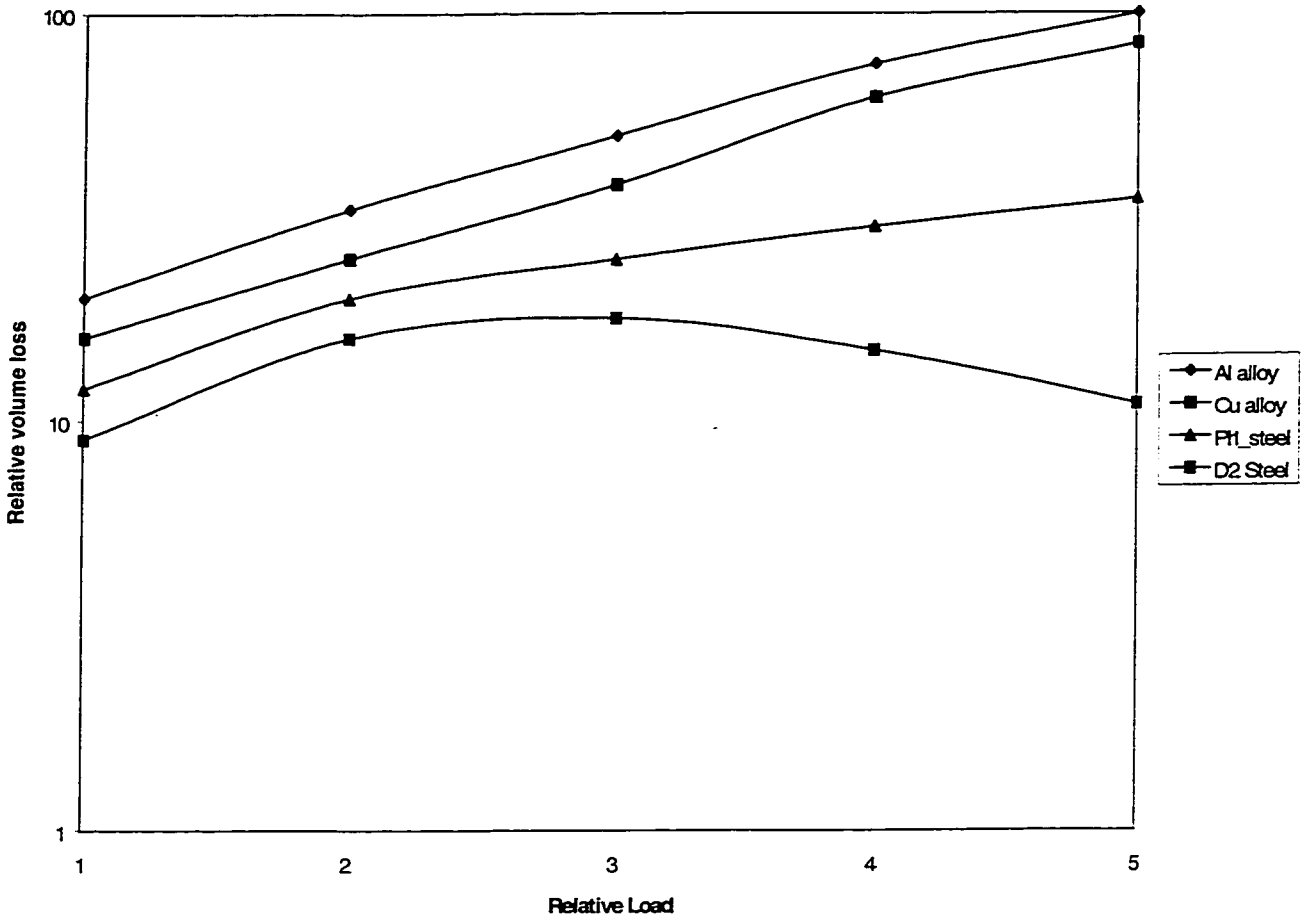

Figure 5-2. The effect of applied load on wear (modeling)

The wear losses of these materials were also experimentally evaluated using the dry sand/rubber-wheel abrasion tester as shown in figure 5-1. The testing procedure was similar to that described in ref. [6]. Figure 5-3 illustrates the experimental results. One may see that the experimental testing is consistent with the modeling. The experimental data is an average of three measurements. The variation of the data is about 5 %.

In order to explain the unusual abrasion behavior of D2 steel, we checked changes in the size of abrasive sand particles during abrasion test. Figure 5-4 gives the

information on the damage to sand during abrasion by counting the loss of sites of a sand particle under different loads.

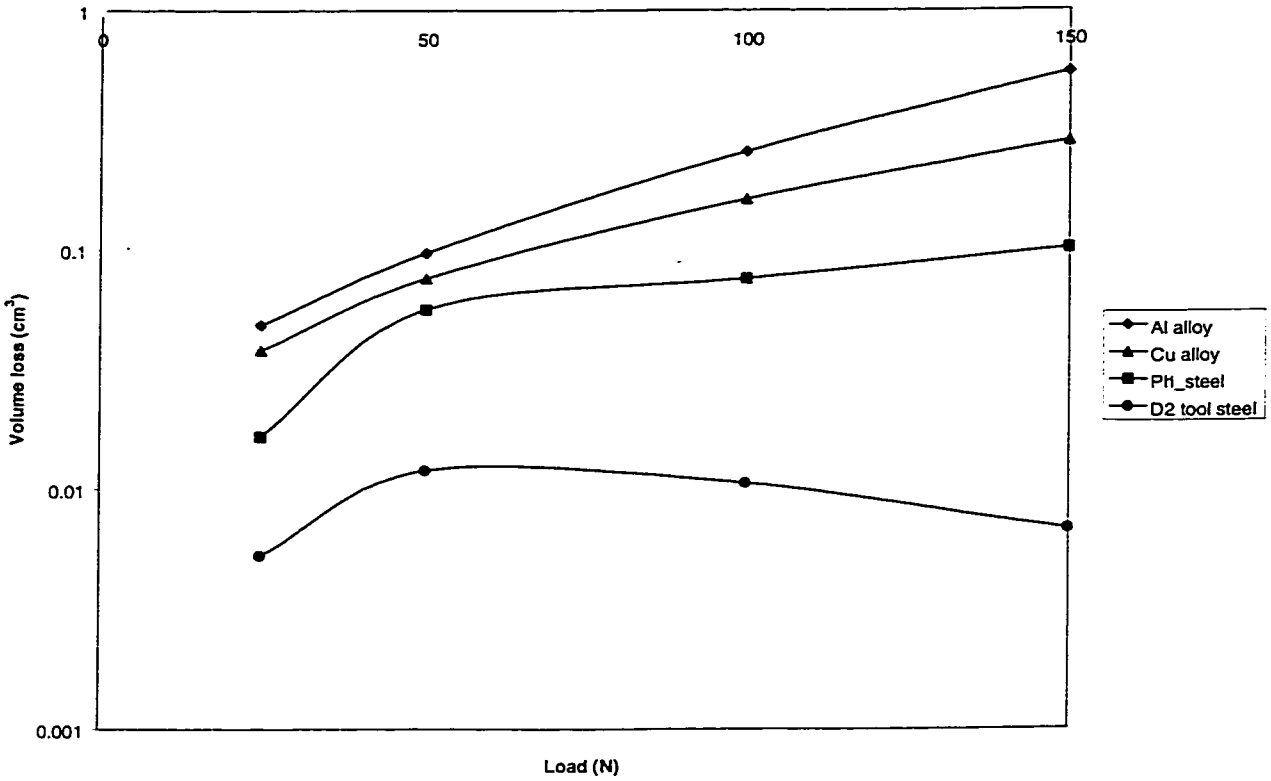

Figure 5-3. The effects of load on wear losses (experimentally)

It was demonstrated that as the hardness of the target material increased, the damage to sand increased and such damage was more severe under higher loads. In the case of D2 tool steel under higher loads, the damage to the sand particles considerably increased, leading to less wear of the tool steel. This result explains the variations in the relation between the wear losses of the tested materials and the applied load. As the hardness of the target material increased, the sand became less effective to abrade the material. In stead, the damage to the sand under high loads was so high that a decrease in

the volume loss of the target material could occur as the applied load was increased such as in the case of D2 tool steel.

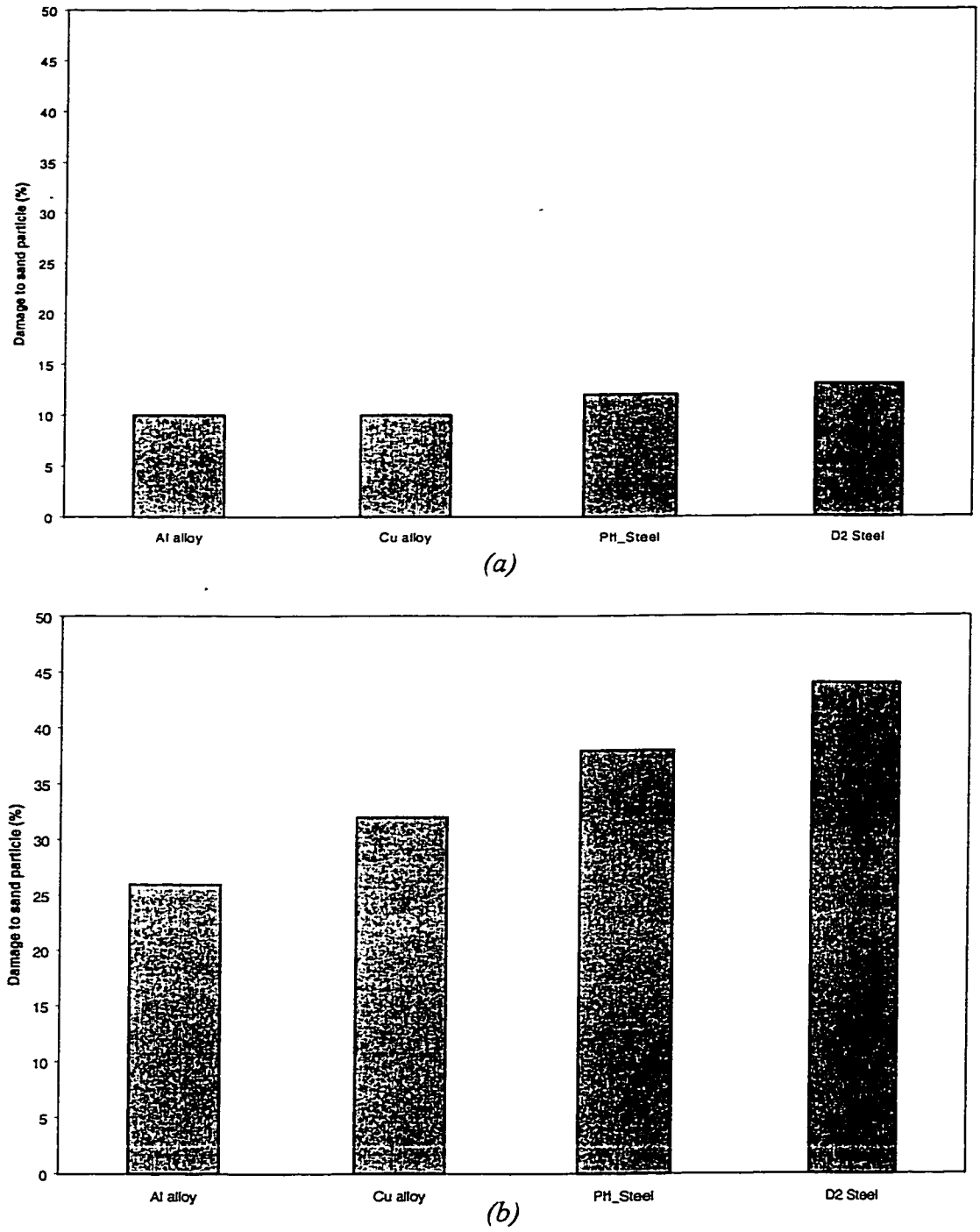

Figure 5-4. The percentage of site loss of an abrasive sand particle (a) under a low load (L=1), and (b) under a high load of (L=3), given by modeling

Previous work of SEM surface analysis [6] has demonstrated the damage to sand during abrasion test. It was shown that the surface of abrasive sand (SiO_2) was severe damaged when used to abrade D2 tool steel under high loads. When two asperities respectively on surfaces of the abrasive sand and the target material are in contact, break-up of the asperity on the sand would result in a decrease in wear of the target material. This may happen especially to those target materials having hardness closer to that of the abrasive sand. In addition, when asperities on sand are broken, the abrasive sand becomes less angular and this may cause additional decrease in wear. Figure 5-5 shows the SEM observation of sand surface morphologies before and after abrasion test under different loads, respectively. One may see that the original sand had relative smooth surface with some facets. After the wear test, the sand surface was damaged to some degree, depending on the applied load. Under the low-load abrasion condition, no significant changes in morphology were observed on sand surface (compare figure 5-5 (a) and (b)), meaning that the damage to the sand by wear was minor. Under the high-load condition, however, the surface damage was severe as figure 5-5 (c) illustrates. No facets comparable to those on the original sand surface were observed on the sand surface that experienced high-load abrasion. It is clear that although the SiO_2 sand did not crack during the wear test, severe surface failure was resulted under high loads when used for testing the D2 tool steel. In the cases of softer Al alloy, Cu alloy and 17-4 PH steel, the damage to the sand surface was markedly less, no matter the wear test was performed under which load level in the selected loading range. The surface analysis supports the present modeling work.

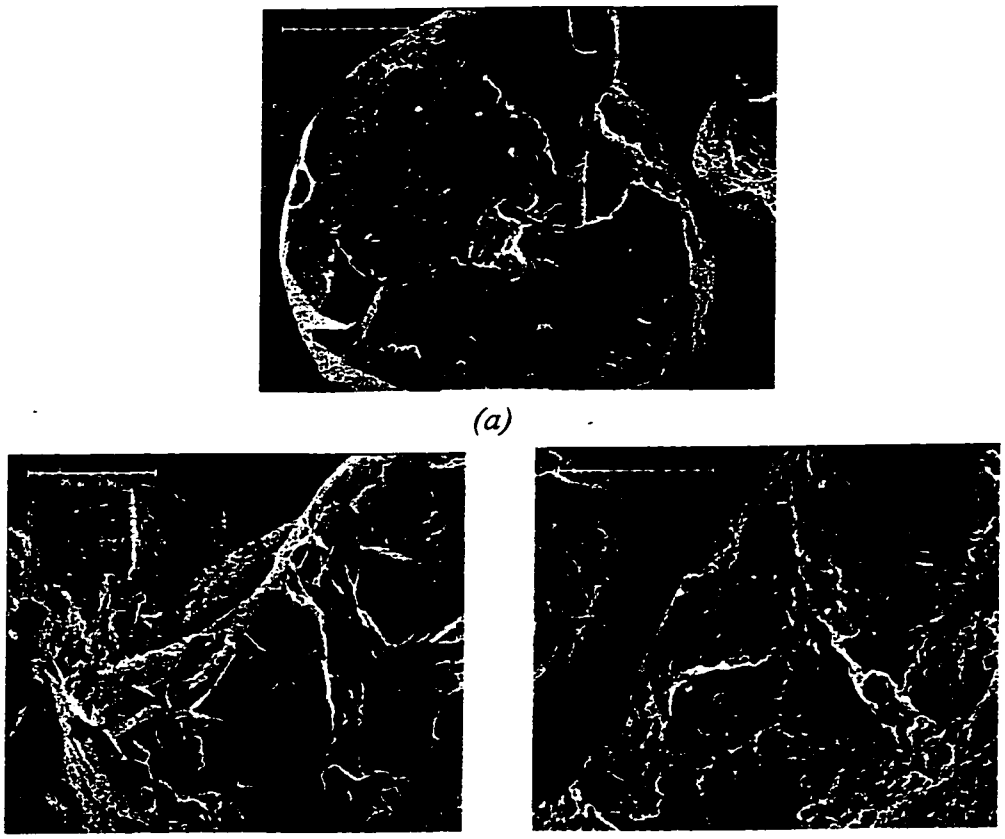

(a)

(b) (c)

Figure 5-5 (a) original sand, (b) worn sand after wear test under a load of 25N, and (c) worn sand after wear test under a higher load of 150N. The sliding speed=4 m/s (adapted from ref. [6])

5.2.2 Effect of Sliding Speed on Wear

Effects of the sliding speed on abrasion was also studied. Figure 5-6 illustrates wear losses of Al alloy (Al 6061), copper alloy (Cu 110), 17-4 PH stainless steel and D2 tool steel with respect to the sliding speed under a fixed load. The modeling demonstrated that no significant changes were observed for the Al alloy, Cu alloy and the 17-4 PH steel. However, the wear loss of D2 steel decreased after initial increase as the sliding

speed was increased. The result of modeling was confirmed by experimental abrasion test.

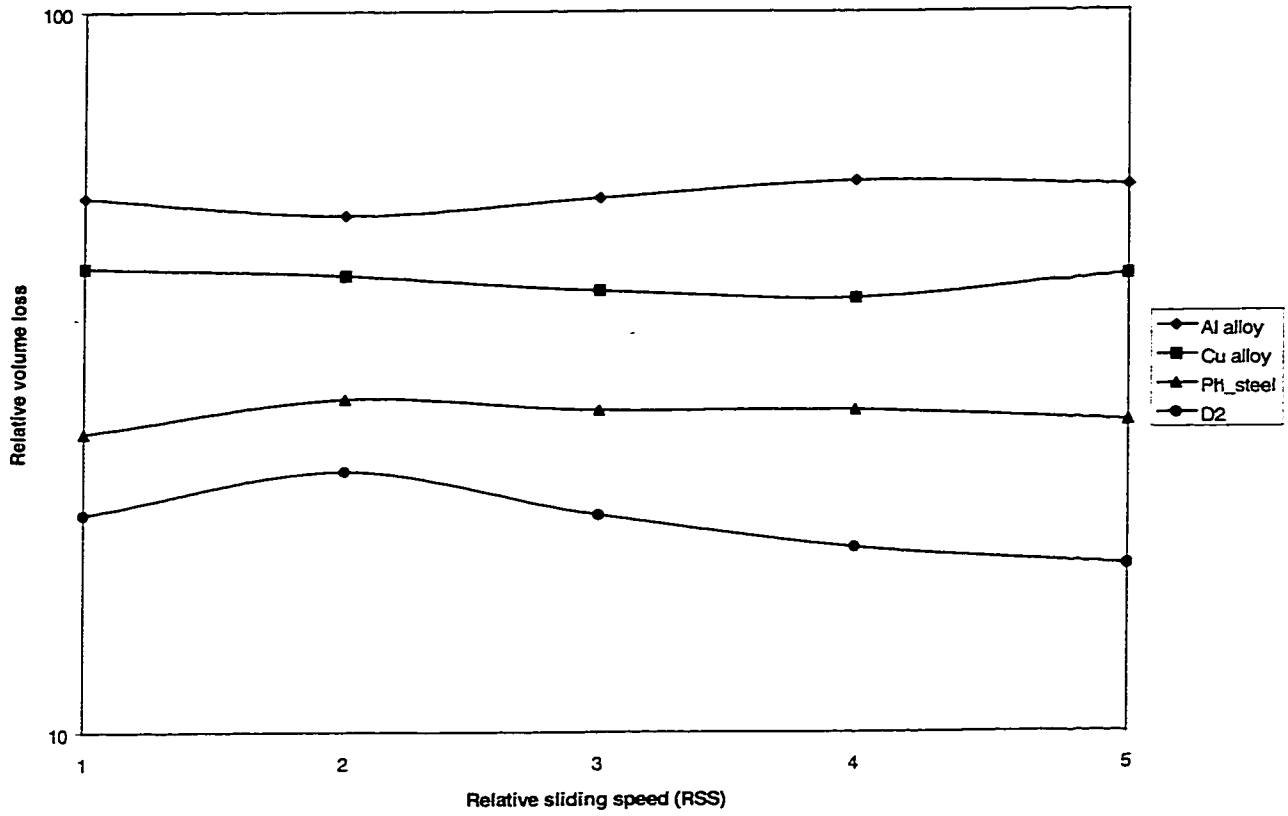

Figure 5-6. The effect of sliding speed on wear (modeling)

Figure 5-7 illustrates results of the abrasion test performed in the speed range from 1 to 5 m/s under a load of 100 N. The experimental result agreed with the modeling. It should, however, be mentioned that no initial increase in wear of D2 steel was shown in figure 5-7. This change should occur if the sliding speed was lower. The experimental data is an average of three measurements. The variation of the data is about 5 %. In the modeling, the damage to the abrasive sand was also determined by counting the site losses for different target materials at different sliding speeds. Figure 5-8 presents the volume losses of an abrasive sand particle after wear at different sliding speeds.

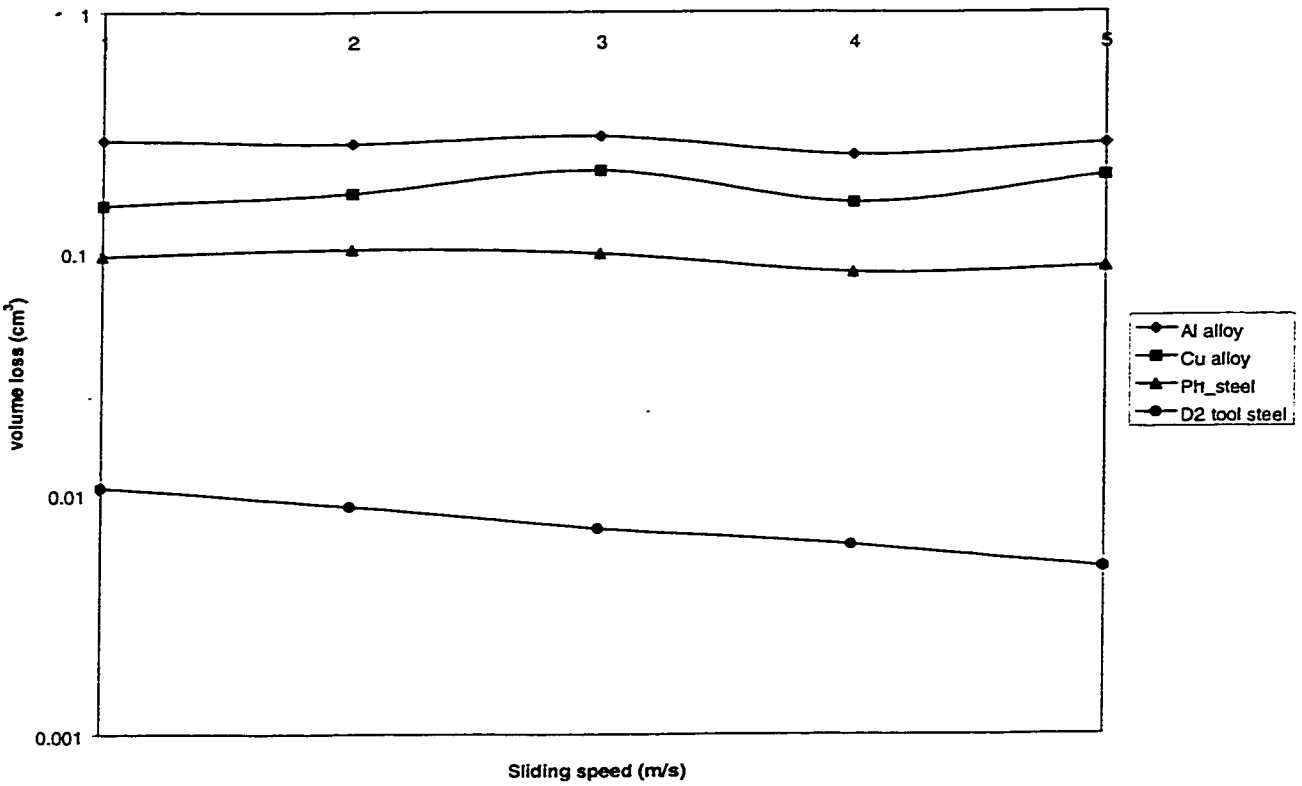

Figure 5-7. The effect of sliding speed on wear (experimentally)

One may see that the sand was damaged in all the cases. However, for the Al alloy, Cu alloy and 17-PH steel, there were no significant changes in the site loss when the sliding speed was changed from low to high. In the case of D2 steel, however, the damage to the abrasive sand was markedly increased at the higher sliding speed. The severe damage to the abrasive sand explains why at higher sliding speeds, the volume loss of D2 steel was lower than that at lower sliding speeds. This happened because the relatively brittle SiO_2 sand could not withstand increased impact at higher sliding speeds when interacted with hard but tougher D2 steel. Such a phenomena was not observed when the sand interacted with softer Al alloy, Cu alloy and 17-4 PH steel.

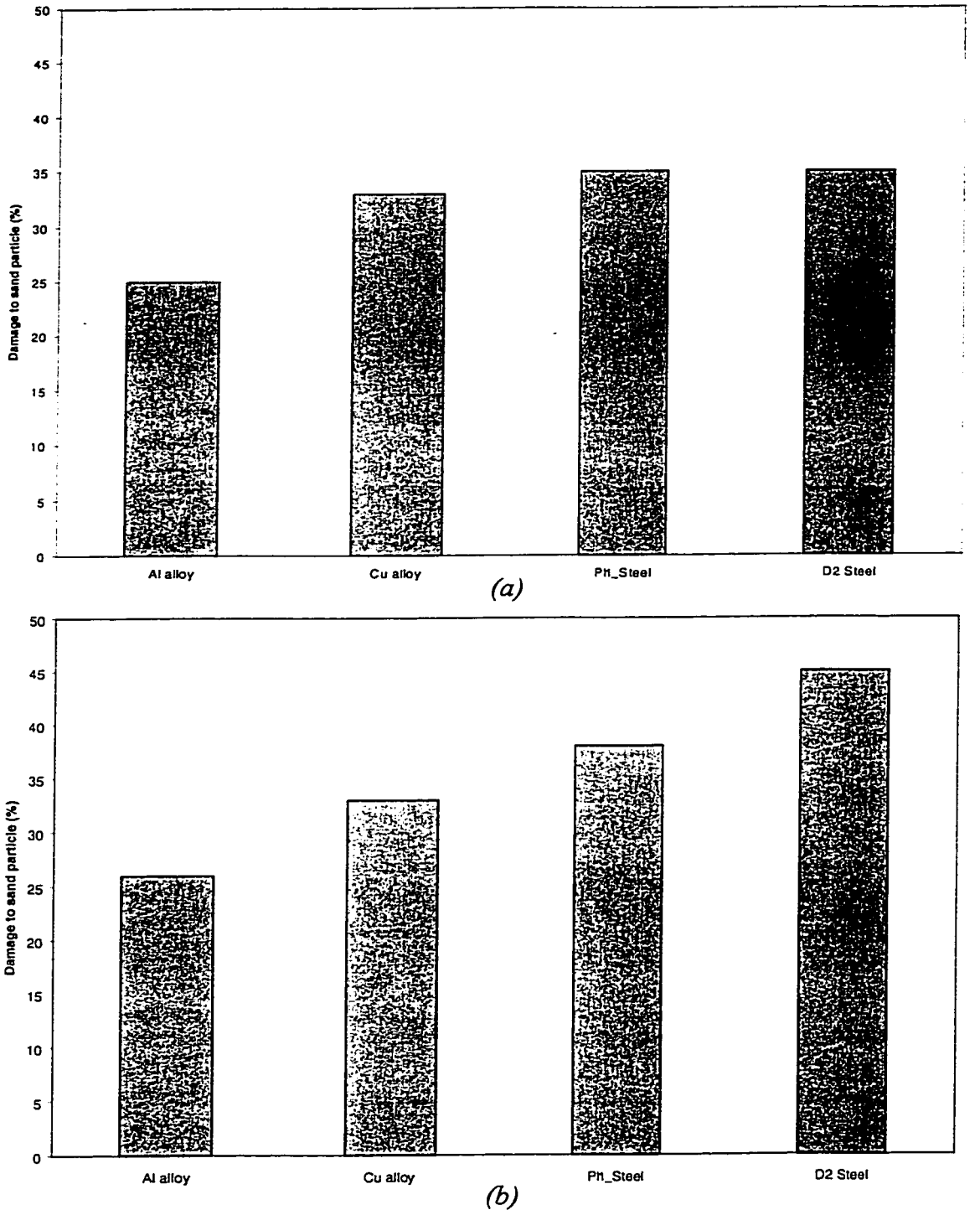

Figure 5-8. The damage to sand particle given by modeling (a) at a low sliding speed (RSS=1), and (b) at a higher sliding speed (RSS=5)

Remark Comments

In this work, the relationship between wear of several materials and the applied load as well as the sliding speed under the dry sand/rubber-wheel abrasion condition was investigated. In particular, the mechanism responsible for the unusual behavior of D2 tool steel was explored by analyzing the damage to the abrasive sand. It should be pointed out that the abrasive wear process is complex. Other factors may also influence this relationship, such as the sand flow and hardness of the rubber wheel. However, the present computational "experiments" were performed under the same condition for all materials. Therefore, these influences could be excluded. The consistence between the modeling and experimental observation as well as previous sand surface analysis imply that the damage to the abrasive sand should be the main factor responsible for the unusual wear response of D2 steel to variations in the load and sliding speed.

5.3. Conclusions

The relationships between the volume loss of a target material and the applied load as well as the sliding speed under the dry sand/rubber-wheel abrasion condition were studied, using a computer modeling approach. Four engineering materials, Al alloy (Al 6061), copper alloy (Cu 110), 17-4 PH stainless steel and D2 tool steel were investigated. It was demonstrated that the wear loss generally increased as the load was increased. However, such a trend may change oppositely above a certain load level when the target material had its hardness closer to that of the abrasive sand, such as the D2 tool steel. Regarding possible effects of sliding speed on abrasive wear, the wear loss of D2 steel

decreased (after an initial increase) as the sliding speed was increased in the tested speed range. However, the sliding speed did not show significant effect on wear losses of other materials. The modeling suggested that the increase in the damage of the abrasive sand was responsible for the unusual responses of D2 tool steel to high loads and high sliding speeds, respectively. Experiment was also performed under the dry sand/rubber-wheel abrasion condition. The modeling was consistent with experimental observations.

Acknowledgement

The authors are grateful for financial support from the Natural Science and Engineering Research Council of Canada (NSERC), Syncrude Canada Ltd. and Alberta Science and Research Authority (ASRA).

Reference List for Chapter 5

[1] ASTM G65-91, standard test method for measuring abrasion using the dry sand/rubber wheel apparatus in Annual Book of ASTM Standards Volume 03.02, ASTM, Philadelphia, PA, pp. 247-259

[2] M. Scholl, Conf. On wear of materials, Wear, 203-204 (March 1997) 57-64

[3] A.N.J. Stevenson and I.M. Hutchings, Wear, 195 (1996) 232-240.

[4] A.W. Ruff, ASM International, Materials Park, OH, USA, (1997) 22.

[5] K. Elalem and D.Y. Li, J. of Computer-aided Materials Design, 6 (1999) 185-193.

[6] X. Ma, R. Liu, and D. Y. Li, Wear, 2000, in press.

[7] R.D. Haworth, Jr., Trans, ASM, 41 (1949) 819-869.

[8] H.S. Avery, Proc. Int. Conf. On Wear of Materials, ASME, New York (1981) 367-378.

[9] Li, D. Y., Elalem, K., Anderson, M.J. and Chiovelli, S., Wear, 225-229, (1999), 380- 386.

[10] Elalem, K., Li, D. Y., Anderson, M.J., and Chiovelli, S., Hydraulic Failure Analysis: Fluids, Components, and Systems Effects, ASTM STP 1339, G. E. Totten, D. K. Wills, and D. Feldmann, Eds., American Society for Testing and Materials, West Conshohocken, PA, 2000. (in press)

Chapter 6

General Discussion and Conclusions

6.1. Summary of the Research Results Presented in Different Papers

This work has been reported in four papers, respectively. Three of them have been published in Wear, Journal of Computer-Aided Materials Design, and proceedings of International Conference on Powder Metallurgy, respectively; and one has been accepted for presentation in the International Conference "Wear of Materials 2001", and will be published in Wear.

Paper 1 mainly reports the development of the MSDM approach, and preliminary modeling of a few materials, including copper, steel, molybdenum and three different abrasion resistance (AR) steels. The result of modeling is compared to experimental data from literature and obtained by other researchers.

In paper 2, the model is further justified by analysis of stress/strain at the contact region using the MSDM approach in comparison with finite element analysis. This work shows good agreement between the MSDM and FEM. The modeling has also been justified by direct wear testing conducted by the author. The abrasive wear behaviour of four different materials, (aluminum alloy 6061, copper type 110, Hot rolled steel and 304 stainless steel) was determined using the MSDM based on their mechanical properties experimentally determined by the author. The wear behaviour of the materials was measured using a dry sand/rubber wheel tester in the wear/surface laboratory at the University of Alberta. Good agreement was found between the modeling, FEM analysis and the experimental work.

Paper 3 reports the application of the micro-scale dynamic approach to heterogeneous materials, composites. In this work, the mismatch in mechanical

properties between ceramic phase and the metal matrix was studied and accordingly the different interfacial interaction of ceramics-metal bonds was taken into account in the model. This part of work extends the capability of this model for wear prediction, particularly important for investigation of realistic wear-resistant materials. Preliminary simulation studies on composites were conducted using the MSDM; computational results are consistent with experimental observations.

In paper 4, the model is applied to investigation of a specific problem: unusual wear behaviour of D2 tool steel. The D2 tool steel shows "abnormal" wear responses to load and sliding speed during dry sand/rubber wheel abrasion test: its wear loss decreases as the load and sliding speed are increased. It is difficult to explain this phenomena based on the abrasion test. It is however easy to explore the mechanism of the unusual behaviour of D2 tool steel using the MSDM approach. This work provides a good example to demonstrate the capability of this model.

6.2. Some Technical Details of the Model that are not Given in the Papers

6.2.1. Flow Chart

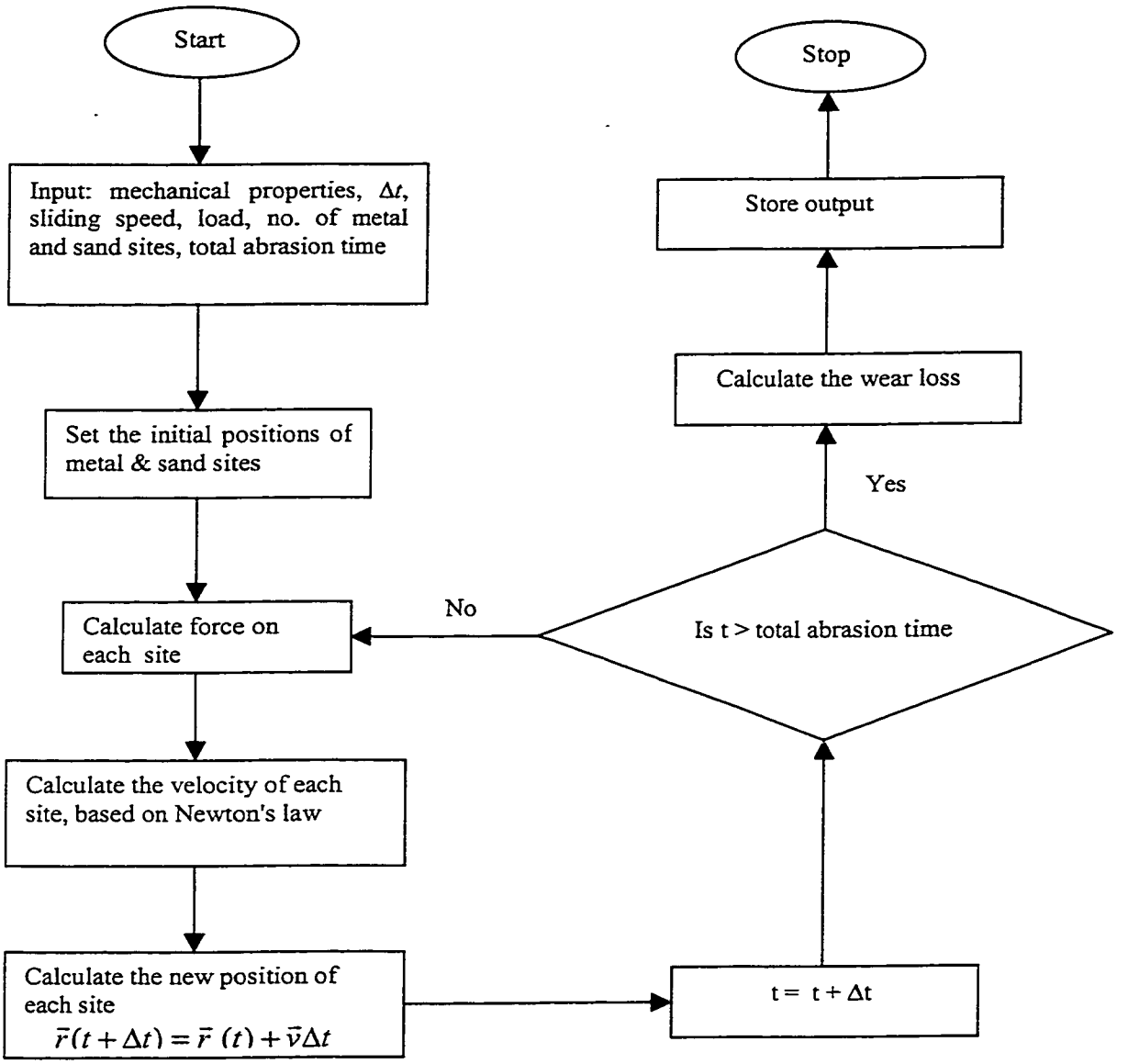

Figure 6-1. Flow chart of the MSDM

6.2.2. Interaction between Ceramic and Metal Phases

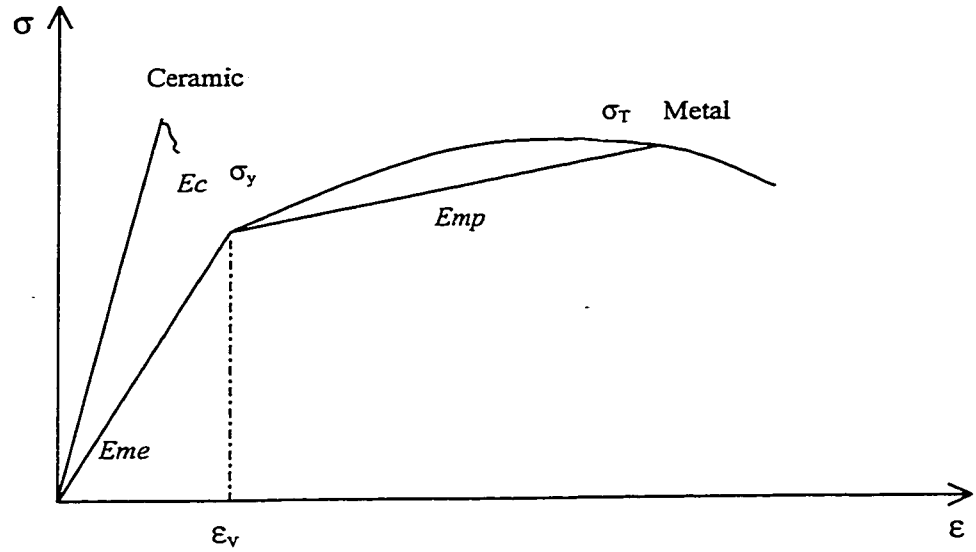

Figure 6-2. Schematic illustration of tensile curve of ceramic and metal materials

When under external force, the ceramic and metal phases in composite will experience different deformation due to their different mechanical properties. Figure 6-2 illustrates typical tensile curves of ceramic and metal materials. The difference in the mechanical behaviour makes the deformation of a ceramic-metal bond complicated. In the present work, it is assumed that the ceramic only experiences elastic deformation before fracture.

1) When only elastic deformation occurs

$$\Delta l = \Delta l_c + \Delta l_m$$

$$\because \quad f_{(c,m)} = Ec\,\varepsilon c l_o^2 = Ec\frac{\Delta lc}{\left(\frac{l_o}{2}\right)} l_o^2 = f_{(m,c)} = E_{me}\frac{\Delta l_m}{\left(\frac{l_o}{2}\right)} l_o^2 = E_{me}\varepsilon_m l_o^2$$

$$\therefore \Delta l_m = \frac{Ec}{E_{me}} \Delta lc$$

$$\because \Delta l = \Delta lc + \Delta l_m = \Delta lc + \frac{Ec}{E_{me}} \Delta lc = (1 + \frac{Ec}{E_{me}}) \Delta lc$$

$$\Delta lc = \frac{\Delta l}{1 + \frac{Ec}{E_{me}}}, \qquad \Delta l_m = \frac{\Delta l}{1 + \frac{E_{me}}{Ec}}$$

Let $l_0 = 1$

$$\therefore f_{(c,m)} = Ec \Delta lc = Ec \frac{2\Delta l}{1 + \frac{Ec}{E_{me}}} = \frac{2 E_{me} Ec}{E_{me} + Ec} \Delta l$$

$f_{(c,m)} = f_{(m,c)}$ (in opposite directions)

Since Δl is determined from previous force, the new force $f_{(c,m)}$ and $f_{(m,c)}$ can thus be calculated. Once $f_{(c,m)}$ and $f_{(m,c)}$ are obtained, one may predict next deformation. However, if ε_m is larger than ε_y, plastic deformation occurs. In this case, the force and deformation of a ceramic-metal bond may be calculated in the following way:

2) When plastic deformation takes place

let $\delta l = \Delta l_m - \Delta l_{my}$, $\Delta l = \Delta l_c + \Delta l_m$

$$\because \quad f_{(m,c)} = E_{me} \frac{\Delta l_{my}}{\left(\frac{l_o}{2}\right)} l_o^2 + E_{mp} \frac{\delta l}{\left(\frac{l_o}{2}\right)} l_o^2 = f_{(c,m)} = Ec \frac{\Delta lc}{\left(\frac{l_o}{2}\right)} l_o^2$$

$$\therefore \qquad E_{me}.\Delta l_{my} + E_{mp}(\Delta l - \Delta l_c - \Delta l_{my}) = Ec\Delta l_c$$

$$(E_{me} - E_{mp})\Delta l_{my} + E_{mp}\Delta l = (E_{mp} + Ec)\Delta l_c$$

$$\Delta lc = \frac{E_{mp}\Delta l + (E_{me} - E_{mp})\Delta l_{my}}{(E_{mp} + Ec)} = \frac{\Delta l - (1 - \frac{E_{me}}{E_{mp}})\Delta l_{my}}{(1 + \frac{Ec}{E_{mp}})}$$

and

$$\Delta l_m = \Delta l - \Delta l_c = \Delta l_c \frac{Ec}{Emp} + (1 - \frac{Eme}{Emp})\Delta lmy$$

Let $l_0 = 1$, we have

$$f_{(c,m)} = Ec\frac{\Delta lc}{\left(\frac{1}{2}\right)} = 2Ec\Delta lc = 2Ec\frac{\Delta l - (1 - \frac{E_{me}}{E_{mp}})\Delta l_{my}}{\left(1 + \frac{Ec}{E_{mp}}\right)} = f_{(m,c)}$$

6.2.3. Determination of the Time Interval (Δt)

The accuracy of the modeling is strongly influenced by the time interval (Δt). The selection of Δt is therefore important. For instance, if Δt is too large, large wear loss would be generated, since the bond length could exceed the critical length at fracture because of $\Delta l = V.\ \Delta t$, where V is the velocity of the site under study. As a result, a large jump in position will be given by the MSDM, which will lead to immediate breaking of bonds and thus extra wear loss. Very small Δt values can be used if the simulation time is not an issue. In the present work, the value of Δt was chosen to be small enough to provide reasonable results. The selection of Δt is based on the stability of wear results

predicted using different Δt in the range of the applied load and sliding speed for the present study. However, it is possible to determine the optimum Δt in a more quantitative manner. Such a possibility is currently under study. Figure 6-3 gives an example of the variation in wear versus Δt. In this case, wear is caused by only a few sand particles, so that the decrease in wear was caused by less contact between the target surface and a moving sand particle when Δt was increased.

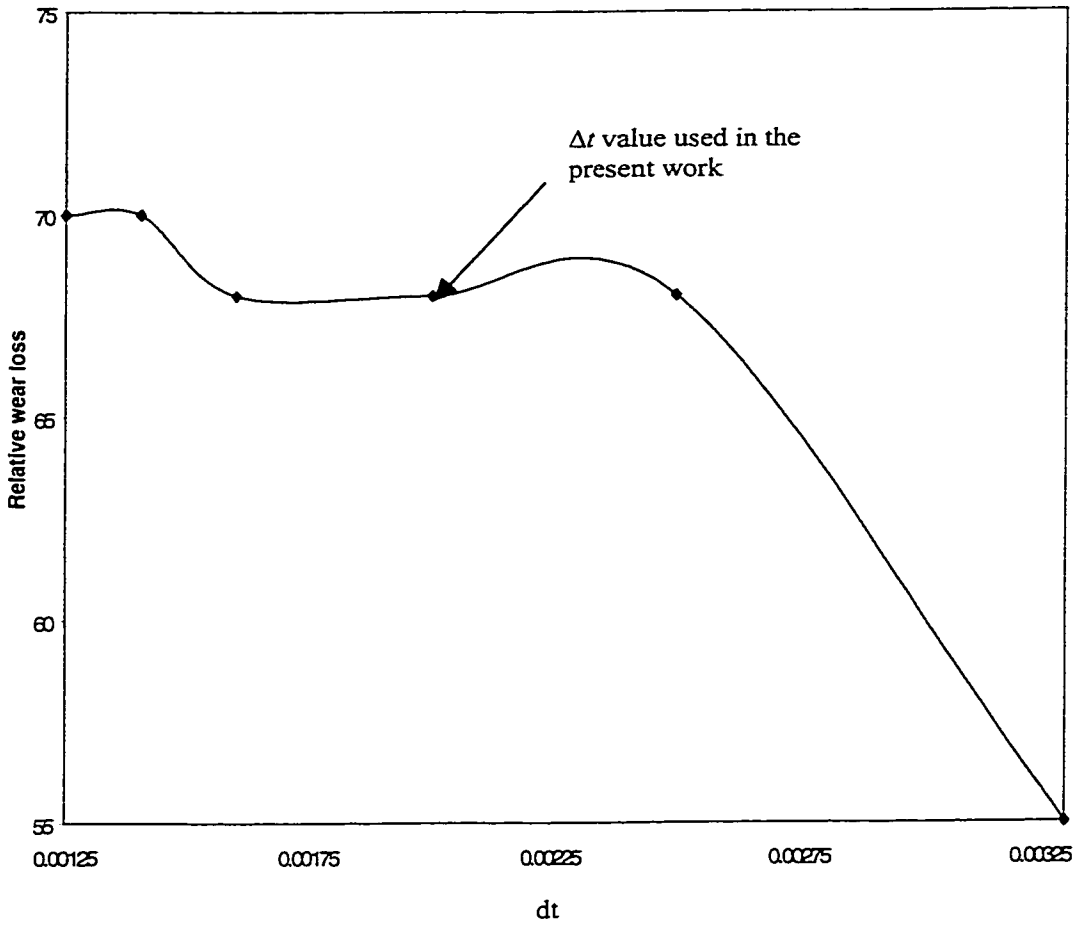

Figure 6-3. Variation in wear loss verses Δt

6.2.4. Simplification of the force on a sand particle from the rubber wheel

Under the dry sand/rubber-wheel abrasion condition, a sand particle is pushed onto the target metal by the rotating rubber wheel and thus scratch the metal surface. The force on the sand particle from the rubber wheel is rather complicated. In this initial model, the interaction between the rubber wheel and the sand particle is simplified by taking account of two force components, horizontal and vertical forces from the rubber wheel. A sand particle moves under the vertical and horizontal forces. The horizontal force is complicated because of the sand-rubber contact. However, the horizontal velocity of a sand particle is constant if the sand is not in contact with the target metal. To simplify the actual situation, the sand particle is given an average horizontal speed $\bar{v}$, which is equal to the wheel rotating speed. The actual horizontal velocity of a sand site is a sum of this average velocity and the one caused by the horizonal compoent of the sand-metal interaction. Vertical force $\bar{f}$ is applied on the sand particle to cause its vertical movement.

6.2.5. Interaction between sand and metal (surface interaction)

When sand and metal surfaces are in contact, a force is transferred from the sand particle into the metal. Figure 6-4 illustrated the contact between a sand site and a metal site. When the distance between the sand site and metal site is less than l_0, the original length of the sand or metal bond which is in stress-free condition, the sand and metal sites are in contact and results in the interaction forces on both the sites.

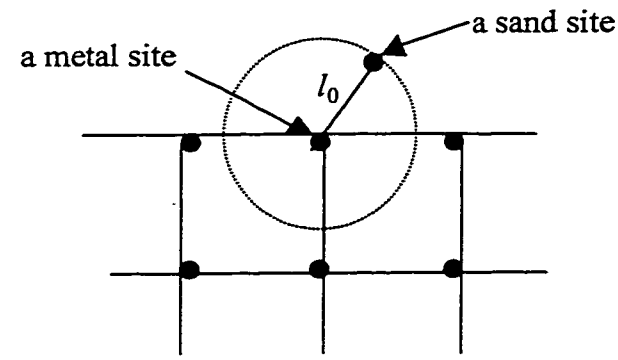

Figure 6-4. Sand-Metal interaction

The force due to the metal-sand interaction has been given in the section 6.2.2, that is

- In the case of elastic deformation,

$$f_{(c,m)} = \frac{2E_{me}Ec}{E_{me} + Ec}\Delta l$$

and

$$\Delta lc = \frac{\Delta l}{1 + \frac{Ec}{E_{me}}}, \qquad \Delta l_m = \frac{\Delta l}{1 + \frac{E_{me}}{Ec}}$$

where, $f_{(c,m)} = f_{(m,c)}$ (in opposite directions) represent the forces on the ceramic site and the metal site, respectively, Δlc and Δlm represent the deformation of the ceramic part and that of the metal part of the ceramic-metal bond respectively. In this case, Δlc and Δlm are negative.

- In the case of plastic deformation in the metal site,

$$f_{(c,m)} = 2Ec\frac{\Delta l - (1 - \frac{E_{me}}{E_{mp}})\Delta l_{my}}{\left(1 + \frac{Ec}{E_{mp}}\right)} = f_{(m,c)}$$

and

$$\Delta l_m = \Delta l_c \frac{Ec}{Emp} + (1 - \frac{Eme}{Emp})\Delta lmy$$

$$\Delta lc = \frac{\Delta l - (1 - \frac{E_{me}}{E_{mp}})\Delta l_{my}}{(1 + \frac{Ec}{E_{mp}})}$$

6.2.6. Discussion on mechanical properties used in the model

-The force coefficient, k

The force coefficient, k, reflects the strength of a bond and is related to the modulus *E*. The modulus *E* is either the elastic modulus or the plastic modulus as defined earlier, depending on if the deformation is elastic or plastic,

$$f = k \cdot \Delta l$$

$$\because \quad \sigma = E\varepsilon$$

$$\sigma = \frac{f}{l_\circ^2} = E.\frac{\Delta l}{l_\circ} = E\varepsilon$$

$$\therefore \quad f = E \cdot l_\circ \cdot \Delta l$$

$$\therefore \quad k = E \cdot l_\circ$$

-The tensile properties

Tensile properties, including the Young's modulus, yield strength, tensile strength, fracture strain and elongation are the basic mechanical properties used in the model to

simulate the wear behavior of a material. These properties are sufficient to describe and simulate the wear behaviour of the material. Traditionally, there are other mechanical properties, such as hardness and toughness, are often used to predict the wear resistance of a material. However, these properties are not basic mechanical properties and therefore not used as the input mechanical properties in this wear model, since they have been automatically taken into account due to their correlation with the basic ones.

6.3. Future Work

The MSDM has been demonstrated to be successful in modeling wear simulation and overcoming barriers of macro-modeling and atomistic modeling. However, this model is still in its infant stage and considerable work is needed to improve this new approach. The following are a few efforts, which should be made to enhance the capability of the MSDM.

1) Interfacial Bonding Strength

Almost all wear-resistant materials are multiphase materials or composites. The interfacial bonding strength is therefore of importance to the performance of the materials during wear. In the present study, the interfacial bonding in multiphase materials and composites is assumed to be perfect. This assumption is not true for all different cases. Atomic modeling technique (e.g., molecular dynamics simulation or monte carlo

modeling) would be incorporated to determine the interfacial bonding strength, which can be used as an input for modeling wear behaviour of multiphase and composite materials.

2) Visualization

It is of particular importance to obtain a direct view of a wear process for understanding the wear mechanism involved. Visualization should be the next step for improving the MSDM. By developing built- in code to the MSDM or by linking with a visualization commercial package, wear process simulated by the MSDM at any given time would be visualized.

3) Extension of MSDM for other wear modes

The MSDM approach developed in this work could be extended to simulate other wear processes such as erosion, impact wear, adhesive wear and corrosion wear. It is rather easy to apply this model to erosion and impact wear, since these wear processes only involve mechanical factors. For those wear modes involving temperature and electrochemical factors, more systematic work is necessary.

6.4. Conclusions

A dynamic model was developed to simulate wear processes and predict wear performance of materials at microscopic level. This model is simple, flexible and easy to

apply. In the model, a material system is mapped onto a discrete lattice or grid, each lattice site or node represents a small volume of the material. Under the influence of external force and the constraint from its neighbors, a lattice site may move obeying the Newton's second law of motion. Once a bond between this site and one of its neighbor sites exceeds a critical length at fracture, the bond is broken and local material failure occurs.

The model can provide information on the strain distribution in a contact region, in consistence with finite element analysis. This model was applied to single-phase and composite materials abraded under the dry sand/rubber-wheel abrasion condition. Good agreement between modeling and experiments was found. It has also been demonstrated that this model provides an effective tool to explain wear mechanisms, which may not be easily explained based on experimental observation.

Appendix

-The MSDM computer code

```
Program wear_1
(input,output,file,sandcdcu2,sandpocu2,metalcdcu2,metalpocu2,result6);
{this is for Unix}
const bl=' ';
const bll='     ';
const pi = 3.14159;

{Define Variables and Arrays}
var
sandcdcu2,sandpocu2,metalcdcu2,metalpocu2,result6,file:text;
KeyPressed : Boolean;

X: array [1..35] of real;
R0sx,R0sy,RNsx,RNsy,V0sx,V0sy,Fasx,Fasy,Fsx,Fsy,RX1,RX2,RX3,YYt: array
[1..6,1..6,1..6] of real;
dLsx1,dLsx2,dLsy1,dLsy2,inout,dLss,dLss1: array [1..6,1..6,1..6] of
integer;
V0mx,V0my,Famx,Famy,Fmx,Fmy: array [1..111,1..57] of real;
dLmx1,dLmx2,dLmy1,dLmy2 : array [1..111,1..57] of integer;
RNmx,RNmy,R0mx,R0my:array [1..111,1..57] of real;
Lx1,Lx2,Ly1,Ly2,L0x1,L0x2,L0y1,L0y2:array [1..111,1..57] of real;
Lx1y,Lx2y,Ly1y,Ly2y,Ax1,Ax2,Ay1,Ay2,Wx1,Wx2,Wy1,Wy2,ZF,ZFF,dZF:array
[1..111,1..57] of real;
Ms,Mm,Fnn,Fnx,Fny,Msd: real;
Vax,Vay,dx,dy: real;
Xs,Xm,Ys,Ym,Ees,Eem,Epm,Ro : real;
Vsx,Vsy,Vmx,Vmy,dt,dts,dtm,t,dL,dLx,dLy,d,EE,Fm :real;
Fx1,Fx2,Fx3,Fx4,Fy1,Fy2,Fy3,Fy4,Lx,Ly,V,Ar1,Ar2,Ar3,Ar4:real;
Lt0,ks,km,Kmp,Kmf,B,C,S,q,q1,E,Af,Lfm,Lcm,L,L0x,L0y,L0x11,L0y11:real;
dLx1,dLx2,dLy1,dLy2,Rr,O,p,ad,key,fs,RRT,RX4,Yt1,Yt2,a1,a2,a3,cs,hg,hg1
,hg2,tr,tr1,tr2: real;
i,j,ii,jj,NXs,NYs,qq,qq1,NXm,NYm,k,kk,Yt3,Gf,f,ff,fg,sn: integer;
pp,ppp,ZZ,cd,tt,g,gg,Yt,ed,add,ER,ab,bc,metal: integer;
p1,p2:real;


Procedure Inputs;
var
   i,j,ii,jj : integer;

begin
                    {open files for out put}
rewrite(sandpocu2);
rewrite(sandcdcu2);
rewrite(metalcdcu2);
rewrite(metalpocu2);
rewrite(result6);
```

```
reset (file);
                {read inputs..  normaly could be red from a separate
file}
readln (file,Eem,Epm,Km,Kmf,Ro);  {read material properties}
key:=6 {11.81};   { time}
fs:=0;
g:=0;
t:=0;
hg:=0;
hg1:=0;
hg2:=0;
tr:=0;
tr1:=0;
tr2:=0;
EE:=0;
Rr:=0.2;
Er:=0;
cd:=1;
pp:=1;
tt:= 6 {No. of sand particles};
ZZ:=1;
{writeln('Input Load');readln(Fnn);}
Fnn:=3.5 {4};
NXs:=3;  {when u change these values, make sure about what gonna happen
to Xp and fny...}
NYs:=3;
Fny:=0;
Fnx:=0;
Vax:=-8;
Vay:=0;
Xs:=2;  {be careful}
YS:=2;
{qq:=100;
qq1:=50;}

Ees:=0.7;                { sand properties}
ks:=1.033;
{
Ees:=4;
ks:=1.02;                  { metal properties}
Ees:=0.7;
ks:=1.0015;}
fg:=0;
sn:=1;
bc:=round(NXs/2);
ab:=round(NYs/2);
Ms:=0.3;
Mm:=0.07547*Ro;
f:=54;     {??????????????????}
ff:=28;
dx:=(Xs/(NXs-1));
dy:=(Ys/(NYs-1));
Xm:=Xs*f;
Ym:=Ys*ff;
NXm:=f*(NXs-1)+1;
NYm:=ff*(NYs-1)+1;
NXm:=109;
```

```
NYm:=57;
Xm:=108;
Ym:=56;
k:=100;
kk:=0;
RRT:=0;
RX4:=NXm/12;
{Yt1:=round(NYs/2);
Yt2:=Yt1+NYm;
Yt3:=round(Yt2-Yt1);}
E:=0;
ed:=0;
add:=0;
a1:=0; a2:=0;
ad:=Round(29*sqrt(Fnn));
{ad:=Round(45.434*sqrt(Fnn));
ad:=Round(27.26*sqrt(Fnn));}
Fm:=0;
{ Fm:=-0.8*sqrt(Fnn)/5;}
Fm:=-1.2*sqrt(Fnn)/5; {load}

O:=round(NXm/2);
qq:=round(O+ad);
qq1:=round(O-ad);
{ad:=qq-O;}
writeln('ad','=',ad:0:5);
{Fm:=((2*Fny)/(pi*ad))*cd;}
writeln('Fm','=',Fm:0:5);
writeln('key','=',key:0:3);
writeln('O','=',O:0:5);
writeln('ad','=',ad:0:5);
writeln('qq1','=',qq1:0);
writeln('qq','=',qq:0);
writeln('NXm','=',NXm:0);
writeln('NYm','=',NYm:0);
writeln('NXs','=',NXs:0);
writeln('NYs','=',NYs:0);

if ((2*ad) > NXm) then
begin
writeln('this is an error, Please reduce the value of Cd');
halt;
end;
Msd:=((2*Ees*Eem)/(Ees+Eem));
L0x:=dx;
L0y:=dy;
Lfm:=(dx*kmf);

Vsx:=0;
Vsy:=0;
pp:=1;
g:=0;
repeat
 g:=g+1;
for i := 1 to NXs do        {set arrays to zero}
      for j := 1 to NYs do
begin
```

```
    V0sx[pp,i,j]:=0;    R0sx[pp,i,j]:=0;
    V0sy[pp,i,j]:=0;    R0sy[pp,i,j]:=0;

    Fasx[pp,i,j]:=0;    Fsx[pp,i,j]:=0;    RNsx[pp,i,j]:=0;
    Fasy[pp,i,j]:=0;    Fsy[pp,i,j]:=0;    RNsy[pp,i,j]:=0;

    dLsx1[pp,i,j]:=0;   dLsy1[pp,i,j]:=0; dLsx2[pp,i,j]:=0;
    dLsy2[pp,i,j]:=0;   inout[pp,i,j]:=0;

    dLsx1[pp,i,j]:=1;   dLsy1[pp,i,j]:=1; dLsx2[pp,i,j]:=1;
    dLsy2[pp,i,j]:=1;
    inout[pp,i,j]:=1;

    RX1[pp,i,j]:=0;  RX2[pp,i,j]:=0;  RX3[pp,i,j]:=0;
    RX1[pp,i,j]:=((NYs/2)+0.5)+NYm;
    YYt[pp,i,j]:= (NYm+NYs-dy);
end;
pp:=pp+1;
until (g = tt);
g:=0;
pp:=1;

for i:= 1 to NXm do
  for j:= 1 to NYm do
  begin
    Lx1y[i,j]:=0;Lx2y[i,j]:=0;Ly1y[i,j]:=0;Ly2y[i,j]:=0;
    L0x1[i,j]:=0;L0y1[i,j]:=0;L0x2[i,j]:=0;L0y2[i,j]:=0;
    Lx1[i,j]:=0;Lx2[i,j]:=0;Ly1[i,j]:=0;Ly2[i,j]:=0;Wx1[i,j]:=0;
    Wx2[i,j]:=0;Wy1[i,j]:=0;Wy2[i,j]:=0;
  end;

for i:= 1 to NXm do
  for j:= 1 to NYm do
  begin
    Lx1y[i,j]:=(Km*dx); Lx2y[i,j]:=(Km*dx);  { We use that dx=dy}
    Ly1y[i,j]:=(Km*dy); Ly2y[i,j]:=(Km*dy);L0x1[i,j]:=dx;
    L0y1[i,j]:=dy;L0x2[i,j]:=dx; L0y2[i,j]:=dy;
  Wx1[i,j]:=Lx1y[1,1]-dx; Wx2[i,j]:=Lx2y[1,1]-dx;
  Wy1[i,j]:=Ly1y[1,1]-dy; Wy2[i,j]:=Ly2y[1,1]-dy;
  end;
L0x11:=sqrt(2);
L0y11:=sqrt(2);

Af:=Lfm-Lx1y[1,1];

for i := 1 to NXm do
      for j := 1 to NYm do
begin
   V0mx[i,j]:=0;    R0mx[i,j]:=0;  Famx[i,j]:=0;
   V0my[i,j]:=0;    R0my[i,j]:=0;  Famy[i,j]:=0;
   Fmx[i,j]:=0;     RNmx[i,j]:=0;  Fmy[i,j]:=0;
   RNmy[i,j]:=0;    dLmx1[i,j]:=1; dLmy1[i,j]:=1;
   dLmx2[i,j]:=1;   dLmy2[i,j]:=1;
   Ax1[i,j]:=0;Ax2[i,j]:=0;Ay1[i,j]:=0;Ay2[i,j]:=0;
end;

for j := 1 to NYm do
```

```
      dLmx1[NXm,j]:=0;
for i := 1 to NXm do
      dLmy2[i,NYm]:=0;

Vmx:=0; Vmy:=0;

dt:=dx/400;    {??????????}   {dt}
writeln('dt','=',dt:0:5);
S:=0;
B:=dx;
C:=0;
L0x:=dx;
L0y:=dy;
q:=((qq*dx)-dx);
q1:=((qq1*dx)-dx);
end;

Procedure outs;
var
   i,j,ii,jj : integer;
begin
for i:= 1 to NXm do
for j:=1 to NYm do
     begin
if (((i >= 0) and (i <= (0+RX4))) or ((i < 0) and (i >= (0-RX4))) and
(j >=(NYm-8))) or
(((i > (0+RX4)) and (i <= (0+(2*RX4)))) or ((i < (0-RX4)) and (i >= (0-
(2*RX4)))) and (j>= (NYm-6))) or
(((i > (0+(2*RX4))) and (i <= (0+(3*RX4)))) or ((i < (0-(2*RX4))) and
(i >= (0-(3*RX4)))) and (j>= (NYm-4))) or
(((i > (0+(3*RX4))) and (i <= (0+(4*RX4)))) or ((i < (0-(3*RX4))) and
(i >= (0-(4*RX4)))) and (j>= (NYm-2))) or
(((i > (0+(4*RX4))) and (i <= (0+(5*RX4)))) or ((i < (0-(4*RX4))) and
(i >= (0-(5*RX4)))) and (j>= (NYm-1))) or
(((i > (0+(5*RX4))) and (i <= (0+(6*RX4)))) or ((i < (0-(5*RX4))) and
(i >= (0-(6*RX4)))) and (j>= NYm)) then

begin
if (R0my[i,j] <= NYm) then
begin
if (dlmx1[i,j]=0) and (dlmx2[i,j]=0) and (dlmy1[i,j]=0) and
(dlmy2[i,j]=0) then
     ed:=ed+1;
end;
     end;
     end;
end;

procedure Small;  {set values to zero}
begin
Fx1:=0;Fx2:=0;Fy1:=0;Fy2:=0;
L:=0;dL:=0;dLx:=0;dLy:=0;dLx1:=0;dLy1:=0;dLx2:=0;dLy2:=0;
Lx:=0; Ly:=0;
end;

Procedure Small_2;
begin
```

```
L:=0;dL:=0;dLx:=0;dLy:=0;dLx1:=0;dLy1:=0;dLx2:=0;dLy2:=0;
Lx:=0; Ly:=0;
end;
Procedure In_face;                    {interface}
var
   i,j,ii,jj : integer;
begin
for i := 1 to NXs do
    for j:= 1 to NYs do
    for ii:= qq1 to qq do
          for jj:= 1 to (NYm-1) do
           begin
           if (R0sx[pp,3,1] >= qq1) then
           begin
           if (R0my[ii,jj] <= NYm) then
           begin
Small;
           Lx:= (R0sx[pp,i,j]-R0mx[ii,jj]);
           Ly:= (R0sy[pp,i,j]-R0my[ii,jj]);
           L:=sqrt(sqr(Lx)+sqr(Ly));
      if (L <= L0y) then
  begin
      dL:=(L-L0y);
      dLx:=Lx*(dL/L);
      dLy:=Ly*(dL/L);
      Fx1:=(Msd*dLx);
      Fy1:=(Msd*dLy);

           Fasx[pp,i,j]:=Fasx[pp,i,j]-Fx1;    {-}
           Fasy[pp,i,j]:=Fasy[pp,i,j]-Fy1;

           Famx[ii,jj]:=Famx[ii,jj]+Fx1;      {+}
           Famy[ii,jj]:=Famy[ii,jj]+Fy1;
              Fx1:=0; Fy1:=0;
              end;
         end;
      end;
end;
    for i:= 1 to NXm do
    for j:= 1 to NYm do
                    begin
                         Famx[i,j]:=Famx[i,j]+Fmx[i,j];
                         Famy[i,j]:=Famy[i,j]+Fmy[i,j];
                         Fmx[i,j]:=0; Fmy[i,j]:=0;
                     end;
    for i:= 1 to NXs do
    for j:= 1 to NYs do
                    begin
                         Fasx[pp,i,j]:=Fasx[pp,i,j]+Fsx[pp,i,j];
                         Fasy[pp,i,j]:=Fasy[pp,i,j]+Fsy[pp,i,j];
                         Fsx[pp,i,j]:=0;
                         Fsy[pp,i,j]:=0;
                     end;
end;

procedure Metal_Calculations;              {calculation for metal}
var
```

```
   i,j,ii,jj : integer;
begin
In_face;

    for i := 1 to NXm do
    for j := 1 to NYm do
                        begin
                  if (R0my[i,j] <= NYm) then
           begin
   RNmx[i,j]:=0;     RNmy[i,j]:=0;
                     end;
    end;

   Vmx:=0;           Vmy:=0;

    for i := 1 to NXm do
    for j := 1 to NYm do
                         begin
           if (R0my[i,j] <= NYm) then
           begin
     Vmx:= (((Famx[i,j]*dt)/Mm)+V0mx[i,j]);
     Vmy:= (((Famy[i,j]*dt)/Mm)+V0my[i,j]);  {the equations}
     V0mx[i,j]:=Vmx;
     V0my[i,j]:=Vmy;
     RNmx[i,j]:=(R0mx[i,j]+(Vmx*dt));
     RNmy[i,j]:=(R0my[i,j]+(Vmy*dt));
     Vmx:=0; Vmy:=0;
                       end;
                         end;
    for i := 1 to NXm do
    for j := 1 to NYm do
                         begin
Famx[i,j]:=0;
Famy[i,j]:=0;
       Fmx[i,j]:=0;
       Fmy[i,j]:=0;
                         end;

      for i:=1 to NXm do
      for j :=1 to NYm do
begin
           if (R0my[i,j] <= NYm) then
           begin

if (i=1) and (j=1) then
                                  begin
dLmx2[i,j]:=0;
dLmy1[i,j]:=0;

     RNmx[i,j]:=R0mx[i,j];
     RNmy[i,j]:=R0my[i,j];
                                   end;

if (i=1) and ((j>1) and (j<NYm)) then
                                  begin
dLmx2[i,j]:=0;
     RNmx[i,j]:=R0mx[i,j];
```

```
      RNmy[i,j]:=R0my[i,j];
                                    end;

if ((i>1) and (i<NXm)) and (j=1) then
                                  begin
dLmy1[i,j]:=0;
Small;
   if (L0x1[i,j] >= Lfm) then dLmx1[i,j]:=0;
   if (dLmx1[i,j]=1) then
    begin
      Lx:= (RNmx[i+1,j]-RNmx[i,j]);
      Ly:= (RNmy[i+1,j]-RNmy[i,j]);
      Lx1[i,j]:=sqrt(sqr(Lx)+sqr(Ly));
      if ((Lx1[i,j]>=L0x1[i,j]) and (Lx1[i,j]<=Lx1y[i,j])) and
(dLmx1[i,j]=1) then
      begin
      dL:=(Lx1[i,j]-L0x1[i,j]);
      dLx:=Lx*(dL/Lx1[i,j]);
      dLy:=Ly*(dL/Lx1[i,j]);
      Fx1:=Eem*dLx;
      Fy1:=Eem*dLy;
      end;
      if (Lx1[i,j]< L0x1[i,j]) then
      begin
      dL:=(Lx1[i,j]-L0x1[i,j]);
      dLx:=Lx*(dL/Lx1[i,j]);
      dLy:=Ly*(dL/Lx1[i,j]);
      Fx1:=Eem*dLx;
      Fy1:=Eem*dLy;
      end;
      if (Lx1[i,j] > Lfm) then
      begin
      Fx1:=0;
      Fy1:=0;
      dLmx1[i,j]:=0;
      end;
      if ((Lx1[i,j] > Lx1y[i,j]) and (Lx1[i,j] <=Lfm)) and
(dLmx1[i,j]=1) then
      begin
      Ax1[i,j]:=(Lx1[i,j]-Lx1y[i,j]);
      Wx1[i,j]:=Wx1[i,j]+((Epm/Eem)*Ax1[i,j]);
      dL:=(Lx1[i,j]-L0x1[i,j]);
      dLx:=Lx*(dL/Lx1[i,j]);
      dLy:=Ly*(dL/Lx1[i,j]);
      dLx1:=((dLx*Wx1[i,j])/dL);
      dLx2:=((dLx*Ax1[i,j])/dL);
      dLy1:=((dLy*Wx1[i,j])/dL);
      dLy2:=((dLy*Ax1[i,j])/dL);
      Fx1:=((Eem*dLx1)+(Epm*dLx2));
      Fy1:=((Eem*dLy1)+(Epm*dLy2));
      L0x1[i,j]:=L0x1[i,j]+Ax1[i,j];
      Lx1y[i,j]:=L0x1[i,j]+Wx1[i,j];
      Lx1[i,j]:=0;
      end;
   end;
Small_2;
      if (L0x2[i,j] >= Lfm) then dLmx2[i,j]:=0;
```

```
        if (dLmx2[i,j]=1) then
        begin
        Lx:= (RNmx[i-1,j]-RNmx[i,j]);
        Ly:= (RNmy[i-1,j]-RNmy[i,j]);
        Lx2[i,j]:=sqrt(sqr(Lx)+sqr(Ly));
        if ((Lx2[i,j] >= L0x2[i,j]) and (Lx2[i,j] <= Lx2y[i,j])) and
 (dLmx2[i,j]=1) then
        begin
        dL:=(Lx2[i,j]-L0x2[i,j]);
        dLx:=Lx*(dL/Lx2[i,j]);
        dLy:=Ly*(dL/Lx2[i,j]);
        Fx2:=Eem*dLx;
        Fy2:=Eem*dLy;
        end;
        if (Lx2[i,j]< L0x2[i,j]) then
        begin
        dL:=(Lx2[i,j]-L0x2[i,j]);
        dLx:=Lx*(dL/Lx2[i,j]);
        dLy:=Ly*(dL/Lx2[i,j]);
        Fx2:=Eem*dLx;
        Fy2:=Eem*dLy;
        end;
        if (Lx2[i,j] > Lfm) then
        begin
        Fx2:=0;
        Fy2:=0;
        dLmx2[i,j]:=0;
        end;
        if ((Lx2[i,j] > Lx2y[i,j]) and (Lx2[i,j] <= Lfm)) and
 (dLmx2[i,j]=1) then
        begin
        Ax2[i,j]:=(Lx2[i,j]-Lx2y[i,j]);
        Wx2[i,j]:=Wx2[i,j]+((Epm/Eem)*Ax2[i,j]);
        dL:=(Lx2[i,j]-L0x2[i,j]);
        dLx:=Lx*(dL/Lx2[i,j]);
        dLy:=Ly*(dL/Lx2[i,j]);
        dLx1:=((dLx*Wx2[i,j])/dL);
        dLx2:=((dLx*Ax2[i,j])/dL);
        dLy1:=((dLy*Wx2[i,j])/dL);
        dLy2:=((dLy*Ax2[i,j])/dL);
        Fx2:=((Eem*dLx1)+(Epm*dLx2));
        Fy2:=((Eem*dLy1)+(Epm*dLy2));
        L0x2[i,j]:=L0x2[i,j]+Ax2[i,j];
        Lx2y[i,j]:=L0x2[i,j]+Wx2[i,j];
        Lx2[i,j]:=0;
        end;
    end;
Small_2;
     if (L0y2[i,j] >= Lfm) then dLmy2[i,j]:=0;
     if (dLmy2[i,j]=1) then
     begin
       Lx:= (RNmx[i,j+1]-RNmx[i,j]);
       Ly:= (RNmy[i,j+1]-RNmy[i,j]);
       Ly2[i,j]:=sqrt(sqr(Lx)+sqr(Ly));
       if ((Ly2[i,j]>=L0y2[i,j]) and (Ly2[i,j]<=Ly2y[i,j])) and
 (dLmy2[i,j]=1) then
       begin
```

```
        dL:=(Ly2[i,j]-L0y2[i,j]);
        dLx:=Lx*(dL/Ly2[i,j]);
        dLy:=Ly*(dL/Ly2[i,j]);
        Fx3:=Eem*dLx;
        Fy3:=Eem*dLy;
        end;
        if (Ly2[i,j]< L0y2[i,j]) then
        begin
        dL:=(Ly2[i,j]-L0y2[i,j]);
        dLx:=Lx*(dL/Ly2[i,j]);
        dLy:=Ly*(dL/Ly2[i,j]);
        Fx3:=Eem*dLx;
        Fy3:=Eem*dLy;
        end;
        if (Ly2[i,j] > Lfm) then
        begin
        Fx3:=0;
        Fy3:=0;
        dLmy2[i,j]:=0;
        end;
        if ((Ly2[i,j] > Ly2y[i,j]) and (Ly2[i,j] <=Lfm)) and
(dLmy2[i,j]=1) then
        begin
        Ay2[i,j]:=(Ly2[i,j]-Ly2y[i,j]);
        Wy2[i,j]:=Wy2[i,j]+((Epm/Eem)*Ay2[i,j]);
        dL:=(Ly2[i,j]-L0y2[i,j]);
        dLx:=Lx*(dL/Ly2[i,j]);
        dLy:=Ly*(dL/Ly2[i,j]);
        dLx1:=((dLx*Wy2[i,j])/dL);
        dLx2:=((dLx*Ay2[i,j])/dL);
        dLy1:=((dLy*Wy2[i,j])/dL);
        dLy2:=((dLy*Ay2[i,j])/dL);
        Fx3:=((Eem*dLx1)+(Epm*dLx2));
        Fy3:=((Eem*dLy1)+(Epm*dLy2));
        L0y2[i,j]:=L0y2[i,j]+Ay2[i,j];
        Ly2y[i,j]:=L0y2[i,j]+Wy2[i,j];
        Ly2[i,j]:=0;
        end;
        Fmx[i,j]:=Fx1+Fx2+Fx3;
        Fmy[i,j]:=Fy1+Fy2+Fy3;
        Ax2[i,j]:=0;
        Ax1[i,j]:=0;
        Ay2[i,j]:=0;
end;
                                    end;
if (i=NXm) and (j=1) then
                                     begin
dLmx1[i,j]:=0;
dLmy1[i,j]:=0;
      RNmx[i,j]:=R0mx[i,j];
      RNmy[i,j]:=R0my[i,j];
                                      end;

if (i=NXm) and ((j>1) and (j<NYm)) then
                                     begin
dLmx1[i,j]:=0;
      RNmx[i,j]:=R0mx[i,j];
```

```
      RNmy[i,j]:=R0my[i,j];
                                    end;
if (i=NXm) and (j=NYm) then
                                  begin
dLmx1[i,j]:=0;
dLmy2[i,j]:=0;
      RNmx[i,j]:=R0mx[i,j];
      RNmy[i,j]:=R0my[i,j];
                                   end;

if ((i>1) and (i<NXm)) and (j=NYm) then
                                  begin
dLmy2[i,j]:=0;
      RNmx[i,j]:=R0mx[i,j];
      RNmy[i,j]:=R0my[i,j];

                                  end;
if ((i>1) and (i<NXm)) and ((j>1) and (j<NYm)) then
                                  begin
if (Lx1y[i,j] > Lfm ) then Lx1y[i,j] := Lfm;
if (Lx2y[i,j] > Lfm ) then Lx2y[i,j] := Lfm;
if (Ly1y[i,j] > Lfm ) then Ly1y[i,j] := Lfm;
if (Ly2y[i,j] > Lfm ) then Ly2y[i,j] := Lfm;

Small;
   if (L0x1[i,j] >= Lfm) then dLmx1[i,j]:=0;
   if (dLmx1[i,j]=1) then
    begin
      Lx:= (RNmx[i+1,j]-RNmx[i,j]);
      Ly:= (RNmy[i+1,j]-RNmy[i,j]);
      Lx1[i,j]:=sqrt(sqr(Lx)+sqr(Ly));
      if ((Lx1[i,j]>=L0x1[i,j]) and (Lx1[i,j]<=Lx1y[i,j])) and
(dLmx1[i,j]=1) then
      begin
      dL:=(Lx1[i,j]-L0x1[i,j]);
      dLx:=Lx*(dL/Lx1[i,j]);
      dLy:=Ly*(dL/Lx1[i,j]);
      Fx1:=Eem*dLx;
      Fy1:=Eem*dLy;
      end;
      if (Lx1[i,j]< L0x1[i,j]) then
      begin
      dL:=(Lx1[i,j]-L0x1[i,j]);
      dLx:=Lx*(dL/Lx1[i,j]);
      dLy:=Ly*(dL/Lx1[i,j]);
      Fx1:=Eem*dLx;
      Fy1:=Eem*dLy;
      end;
      if (Lx1[i,j] > Lfm) then
      begin
      Fx1:=0;
      Fy1:=0;
      dLmx1[i,j]:=0;
      end;
      if ((Lx1[i,j] > Lx1y[i,j]) and (Lx1[i,j] <= Lfm)) and
(dLmx1[i,j]=1) then
      begin
```

```
        Ax1[i,j]:=(Lx1[i,j]-Lx1y[i,j]);
        Wx1[i,j]:=Wx1[i,j]+((Epm/Eem)*Ax1[i,j]);
        dL:=(Lx1[i,j]-L0x1[i,j]);
        dLx:=(Lx*(dL/Lx1[i,j]));
        dLy:=(Ly*(dL/Lx1[i,j]));
        dLx1:=((dLx*Wx1[i,j])/dL);
        dLx2:=((dLx*Ax1[i,j])/dL);
        dLy1:=((dLy*Wx1[i,j])/dL);
        dLy2:=((dLy*Ax1[i,j])/dL);
        Fx1:=((Eem*dLx1)+(Epm*dLx2));
        Fy1:=((Eem*dLy1)+(Epm*dLy2));
        L0x1[i,j]:=L0x1[i,j]+Ax1[i,j];
        Lx1y[i,j]:=L0x1[i,j]+Wx1[i,j];
        Lx1[i,j]:=0;
        end;
        end;
Small_2;
    if (L0x2[i,j] >= Lfm) then dLmx2[i,j]:=0;
    if (dLmx2[i,j]=1) then
     begin
        Lx:= (RNmx[i-1,j]-RNmx[i,j]);
        Ly:= (RNmy[i-1,j]-RNmy[i,j]);
        Lx2[i,j]:=sqrt(sqr(Lx)+sqr(Ly));
        if ((Lx2[i,j] >= L0x2[i,j]) and (Lx2[i,j] <= Lx2y[i,j])) and
(dLmx2[i,j]=1) then
        begin
        dL:=(Lx2[i,j]-L0x2[i,j]);
        dLx:=Lx*(dL/Lx2[i,j]);
        dLy:=Ly*(dL/Lx2[i,j]);
        Fx2:=Eem*dLx;
        Fy2:=Eem*dLy;
        end;
        if (Lx2[i,j]< L0x2[i,j]) then
        begin
        dL:=(Lx2[i,j]-L0x2[i,j]);
        dLx:=Lx*(dL/Lx2[i,j]);
        dLy:=Ly*(dL/Lx2[i,j]);
        Fx2:=Eem*dLx;
        Fy2:=Eem*dLy;
        end;
        if (Lx2[i,j] > Lfm) then
        begin
        Fx2:=0;
        Fy2:=0;
        dLmx2[i,j]:=0;
        end;
        if ((Lx2[i,j] > Lx2y[i,j]) and (Lx2[i,j] <= Lfm)) and
(dLmx2[i,j]=1) then
        begin
        Ax2[i,j]:=(Lx2[i,j]-Lx2y[i,j]);
        Wx2[i,j]:=Wx2[i,j]+((Epm/Eem)*Ax2[i,j]);
        dL:=(Lx2[i,j]-L0x2[i,j]);
        dLx:=Lx*(dL/Lx2[i,j]);
        dLy:=Ly*(dL/Lx2[i,j]);
        dLx1:=((dLx*Wx2[i,j])/dL);
        dLx2:=((dLx*Ax2[i,j])/dL);
        dLy1:=((dLy*Wx2[i,j])/dL);
```

```
        dLy2:=((dLy*Ax2[i,j])/dL);
        Fx2:=((Eem*dLx1)+(Epm*dLx2));
        Fy2:=((Eem*dLy1)+(Epm*dLy2));
        L0x2[i,j]:=L0x2[i,j]+Ax2[i,j];
        Lx2y[i,j]:=L0x2[i,j]+Wx2[i,j];
        Lx2[i,j]:=0;
        end;
        end;
Small_2;
    if (L0y1[i,j] >= Lfm) then dLmy1[i,j]:=0;
    if (dLmy1[i,j]=1) then
    begin
      Lx:= (RNmx[i,j-1]-RNmx[i,j]);
      Ly:= (RNmy[i,j-1]-RNmy[i,j]);
      Ly1[i,j]:=sqrt(sqr(Lx)+sqr(Ly));
      if ((Ly1[i,j] >= L0y1[i,j]) and (Ly1[i,j] <= Ly1y[i,j])) and
(dLmy1[i,j]=1) then
      begin
      dL:=(Ly1[i,j]-L0y1[i,j]);
      dLx:=Lx*(dL/Ly1[i,j]);
      dLy:=Ly*(dL/Ly1[i,j]);
      Fx3:=Eem*dLx;
      Fy3:=Eem*dLy;
      end;
      if (Ly1[i,j]< L0y1[i,j]) then
      begin
      dL:=(Ly1[i,j]-L0y1[i,j]);
      dLx:=Lx*(dL/Ly1[i,j]);
      dLy:=Ly*(dL/Ly1[i,j]);
      Fx3:=Eem*dLx;
      Fy3:=Eem*dLy;
      end;
      if (Ly1[i,j] > Lfm) then
      begin
      Fx3:=0;
      Fy3:=0;
      dLmy1[i,j]:=0;
      end;
      if ((Ly1[i,j] > Ly1y[i,j]) and (Ly1[i,j] <= Lfm)) and
(dLmy1[i,j]=1) then
      begin
      Ay1[i,j]:=(Ly1[i,j]-Ly1y[i,j]);
      Wy1[i,j]:=Wy1[i,j]+(Epm/Eem)*Ay1[i,j];
      dL:=(Ly1[i,j]-L0y1[i,j]);
      dLx:=Lx*(dL/Ly1[i,j]);
      dLy:=Ly*(dL/Ly1[i,j]);
      dLx1:=((dLx*Wy1[i,j])/dL);
      dLx2:=((dLx*Ay1[i,j])/dL);
      dLy1:=((dLy*Wy1[i,j])/dL);
      dLy2:=((dLy*Ay1[i,j])/dL);
      Fx3:=((Eem*dLx1)+(Epm*dLx2));
      Fy3:=((Eem*dLy1)+(Epm*dLy2));
      L0y1[i,j]:=L0y1[i,j]+Ay1[i,j];
      Ly1y[i,j]:=L0y1[i,j]+Wy1[i,j];
      Ly1[i,j]:=0;
      end;
      end;
```

```
Small_2;
    if (L0y2[i,j] >= Lfm) then dLmy2[i,j]:=0;
    if (dLmy2[i,j]=1) then
    begin
      Lx:= (RNmx[i,j+1]-RNmx[i,j]);
      Ly:= (RNmy[i,j+1]-RNmy[i,j]);
      Ly2[i,j]:=sqrt(sqr(Lx)+sqr(Ly));
      if ((Ly2[i,j] >= L0y2[i,j]) and (Ly2[i,j] <= Ly2y[i,j])) and
(dLmy2[i,j]=1) then
      begin
      dL:=(Ly2[i,j]-L0y2[i,j]);
      dLx:=Lx*(dL/Ly2[i,j]);
      dLy:=Ly*(dL/Ly2[i,j]);
      Fx4:=Eem*dLx;
      Fy4:=Eem*dLy;
      end;
      if (Ly2[i,j]< L0y2[i,j]) then
      begin
      dL:=(Ly2[i,j]-L0y2[i,j]);
      dLx:=Lx*(dL/Ly2[i,j]);
      dLy:=Ly*(dL/Ly2[i,j]);
      Fx4:=Eem*dLx;
      Fy4:=Eem*dLy;
      end;
      if (Ly2[i,j] > Lfm) then
      begin
      Fx4:=0;
      Fy4:=0;
      dLmy2[i,j]:=0;
      end;
      if ((Ly2[i,j] > Ly2y[i,j]) and (Ly2[i,j] <= Lfm)) and
(dLmy2[i,j]=1) then
      begin
      Ay2[i,j]:=(Ly2[i,j]-Ly2y[i,j]);
      Wy2[i,j]:=Wy2[i,j]+((Epm/Eem)*Ay2[i,j]);
      dL:=(Ly2[i,j]-L0y2[i,j]);
      dLx:=Lx*(dL/Ly2[i,j]);
      dLy:=Ly*(dL/Ly2[i,j]);
      dLx1:=((dLx*Wy2[i,j])/dL);
      dLx2:=((dLx*Ay2[i,j])/dL);
      dLy1:=((dLy*Wy2[i,j])/dL);
      dLy2:=((dLy*Ay2[i,j])/dL);
      Fx4:=((Eem*dLx1)+(Epm*dLx2));
      Fy4:=((Eem*dLy1)+(Epm*dLy2));
      L0y2[i,j]:=L0y2[i,j]+Ay2[i,j];
      Ly2y[i,j]:=L0y2[i,j]+Wy2[i,j];
      Ly2[i,j]:=0;
      end;
      end;
      Fmx[i,j]:=Fx1+Fx2+Fx3+Fx4;
      Fmy[i,j]:=Fy1+Fy2+Fy3+Fy4;
      Ax1[i,j]:=0;
      Ax2[i,j]:=0;
      Ay1[i,j]:=0;
      Ay2[i,j]:=0;
                              end;
    R0mx[i,j]:=0;
```

```
      R0my[i,j]:=0;

      R0mx[i,j]:=RNmx[i,j];
      R0my[i,j]:=RNmy[i,j];
end;
end;

for i:= 1 to NXm do
for j:= 1 To NYm do
begin
 if ((RNmy[i,j] > NYm) and (R0my[i,j]<>1000)) or (RNmx[i,j] < 1)  then
 begin
KK:=KK+1;
R0mx[i,j]:=1000;
R0my[i,j]:=1000;
RNmx[i,j]:=1000;
RNmy[i,j]:=1000;
dlmx1[i,j]:=0;
dlmy2[i,j]:=0;
end;
end;
end;

Procedure Metal_Positions; {initial positions for metal}
var
   i,j,ii,jj : integer;
begin
S:=0;
B:=dx;
C:=0;
for  i:=1 to NXm do
begin
   for  j:=1 to NYm do
                  begin
                      if (i=1)  then
                                  begin
                                      R0mx[i,j]:=dx;
                                      R0my[i,j]:=(NYm-S);
                                      S:=(S+dY);
                                    end;
                           If (i >=2)  then
                         begin
    R0mx[i,j]:=(dx+B);
    R0my[i,j]:=(NYm-C);
    C:=(C+dY);
                          end;
                     end;
If (i >=2)  then B:=(B+dX);
 C:=0;
end;
end;

Procedure Sand_Positions; {initial positions for sand}
var
   i,j,ii,jj : integer;
begin
g:=0;
```

```
pp:=1;
repeat
g:=g+1;
S:=0;
B:=dx;
C:=0;
for  i:=1 to NXs do
begin
   for  j:=1 to NYs do
                  begin
                      if (i=1)  then
                                    begin
                                        R0sx[pp,i,j]:=qq;
                                        R0sy[pp,i,j]:=((NYs-S)+NYm);
                                        S:=(S+dY);
                                      end;
                            If (i >=2)  then
                           begin
    R0sx[pp,i,j]:=(qq+B);
    R0sy[pp,i,j]:=((NYs+NYm)-C);
    C:=(C+dY);
                             end;
                       end;
If (i >=2)  then B:=(B+dX);
 C:=0;
end;
pp:=pp+1;
until (g = tt);
pp:=1;
g:=0;
end;
{1
Procedure extra;  {write out puts}
var
   i,j,ii,jj : integer;
label 110,120,130;
begin

writeln(metalpocu2,NXm:0);
writeln(metalpocu2,NYm:0);

for j := 1 to NYm do
begin
for i := 1 to NXm do
begin
write(metalpocu2,R0mx[i,j]:0:7,',',' ',R0my[i,j]:0:7,',',' ');
if ((R0my[i,j] >= 1) and (R0my[i,j] <= NYm)) and ((R0mx[i,j] >= 1) and
(R0mx[i,j] <= NXm)) then
begin
writeln(metalpocu2,'1');
goto 110;
end;
dlmx1[i,j]:=0;
dlmy2[i,j]:=0;
dlmx2[i,j]:=0;
dlmy1[i,j]:=0;
writeln(metalpocu2,'0');
```

```
110: end;
end;
  1}

{
for j := 1 to NYm do
for i := 1 to NXm do
begin

check it out ..if (R0mx[i+1,j] > NYm) or (R0mx[i,j] < 1) or (R0mx[i,j]
> NXm) then
dLmx1[i,j]:=0;
 }
 {
if (R0mx[i,j] < 1) or (R0mx[i,j] > NXm) or (R0my[i,j] > NYm) then
begin
dLmx1[i,j]:=0;
dLmy2[i,j]:=0;
end;
end;}
{2
for j := 1 to NYm do
      dLmx1[NXm,j]:=0;
for i := 1 to NXm do
      dLmy2[i,NYm]:=0;

for j:=1 to NYm do
begin
for i:= 1 to NXm do
begin
if (dLmx1[i,j]=1) then write (metalcdcu2,'1',',',' ');
if (dLmx1[i,j]=0) then write (metalcdcu2,'0',',',' ');
if (dLmy2[i,j]=1) then writeln (metalcdcu2,'1');
if (dLmy2[i,j]=0) then writeln (metalcdcu2,'0');
end;
end;

for j := 1 to NYs do
      dLsx1[1,NXs,j]:=0;

 for i := 1 to NXs do
     dLsy2[1,i,NYs]:=0;
for j:=1 to NYs do
begin
for i:= 1 to NXs do
begin
if (dLsx1[1,i,j]=1) then write (sandcdcu2 ,'1',',',' ');
if (dLsx1[1,i,j]=0) then write (sandcdcu2,'0',',',' ');
if (dLsy2[1,i,j]=1) then writeln (sandcdcu2,'1');
if (dLsy2[1,i,j]=0) then writeln (sandcdcu2,'0');
end;
end;
writeln(sandpocu2,NXs:0);
writeln(sandpocu2,NYs:0);

for j := 1 to NYs do
begin
```

```
for i := 1 to NXs do
begin
write(sandpocu2,R0sx[1,i,j]:2:2,',',' ',R0sy[1,i,j]:2:2,',',' ');
if (R0sy[1,i,j] <= (NYs+NYm)) and (inout[1,i,j]=1) and ((R0sx[1,i,j]
>=qq1) and (R0sx[1,i,j] <= qq)) then
begin
writeln(sandpocu2,'1',' ');
goto 120;
end;
writeln(sandpocu2,'0',' ');
120:end;
end;
130:writeln;
writeln(sandpocu2);
k:=0;
end;
 2}

Procedure Sand_Calculations; {calculatios for sand}
var
   i,j,ii,jj,pp : integer;
label 100,200,300,400;
begin
pp:=1;
g:=0;
repeat
pp:=1;
g:=0;
       V:=(L0x*ks);                { here L0x=L0y}
repeat
g:=g+1;
                                  {taking care of thye eleptical shape of
the rubber wheel}
     Vsx:=0; Vsy:=0;
    for i:= 1 to NXs do
    for j:= 1 to NYs do
                     begin
        RNsx[pp,i,j]:=0; RNsy[pp,i,j]:=0;
                    end;

if ((R0sx[pp,1,1] >= O) and (R0sx[pp,1,1] <= (O+RX4))) or
   ((R0sx[pp,1,1] < O) and (R0sx[pp,1,1] >= (O-RX4))) then Yt:= (NYm-
8);
if ((R0sx[pp,1,1] > (O+RX4)) and (R0sx[pp,1,1] <= (O+(2*RX4)))) or
   ((R0sx[pp,1,1] < (O-RX4)) and (R0sx[pp,1,1] >= (O-(2*RX4)))) then Yt
:= (NYm-6);
if ((R0sx[pp,1,1] > (O+(2*RX4))) and (R0sx[pp,1,1] <= (O+(3*RX4)))) or
   ((R0sx[pp,1,1] < (O-(2*RX4))) and (R0sx[pp,1,1] >= (O-(3*RX4))))
then Yt := (NYm-4);
if ((R0sx[pp,1,1] > (O+(3*RX4))) and (R0sx[pp,1,1] <= (O+(4*RX4)))) or
   ((R0sx[pp,1,1] < (O-(3*RX4))) and (R0sx[pp,1,1] >= (O-(4*RX4))))
then Yt := (NYm-2);
if ((R0sx[pp,1,1] > (O+(4*RX4))) and (R0sx[pp,1,1] <= (O+(5*RX4)))) or
   ((R0sx[pp,1,1] < (O-(4*RX4))) and (R0sx[pp,1,1] >= (O-(5*RX4))))
then Yt := (NYm-1);
if ((R0sx[pp,1,1] > (O+(5*RX4))) and (R0sx[pp,1,1] <= (O+(6*RX4)))) or
```

```
   ((R0sx[pp,1,1] < (O-(5*RX4))) and (R0sx[pp,1,1] >= (O-(6*RX4))))
then Yt := NYm;

Fny:=0;
X[pp]:=0;
X[pp]:=(R0sx[pp,1,3]-O);
Fny:=Fm*sqrt(1-(sqr(X[pp])/sqr(ad)))*((4/9)*sqr(dx));    {load 0 to max}

300:for i:=1 to NXs do
begin
   if (dlsx1[pp,i,sn]=0) and (dlsx2[pp,i,sn]=0)
    and (dlsy1[pp,i,sn]=0) and (dlsy2[pp,i,sn]=0) then
      begin
         fg:=fg+1;
         if (fg=NXs) and (sn<NYs) then
             begin
                 fg:=0;
                 sn:=sn+1;
              goto 300;
              end;
                  if (sn=NYs) then goto 400;
       end;
end;

 for i:=1 to NXs do
   begin
   if (dlsx1[pp,i,sn]=1) or (dlsx2[pp,i,sn]=1)
   or (dlsy1[pp,i,sn]=1) or (dlsy2[pp,i,sn]=1) and (sn<NYs) then
  begin
    if (R0sy[pp,i,sn] > Yt) then
    Fasy[pp,i,sn]:=Fasy[pp,i,sn]+(Fny/(NXs-fg));
    end;
 end;

400:sn:=1;
    for i := 1 to NXs do
    for j := 1 to NYs do
      begin
     Vsx:= (((Fasx[pp,i,j]*dt)/Ms)+V0sx[pp,i,j]);          {main
equations}
     Vsy:= (((Fasy[pp,i,j]*dt)/Ms)+V0sy[pp,i,j]);
     V0sx[pp,i,j]:=Vsx;
     V0sy[pp,i,j]:=Vsy;
     RNsx[pp,i,j]:=(R0sx[pp,i,j]+((Vsx+Vax)*dt));
     RNsy[pp,i,j]:=(R0sy[pp,i,j]+((Vsy+Vay)*dt));
     Vsx:=0; Vsy:=0;
     end;

 for i := 1 to NXs do
    for j := 1 to NYs do
      begin
Fasx[pp,i,j]:=0;
Fasy[pp,i,j]:=0;
Fsx[pp,i,j]:=0;
Fsy[pp,i,j]:=0;
   end;
```

```
if (R0sx[tt,2,1] < qq1) then
begin
writeln('broken error 200');
writeln('tt','=',tt:0);
goto 200
end;
      for i:=1 to NXs do
      for j:=1 to NYs do
begin
{if (RNsx[pp,1,1] >= R0sx[pp,1,1]) then
begin
for ii:= 1 to 5 do
writeln('Chang Vx');
end;}

{if (R0sx[pp,1,1] < qq1) then
begin
writeln('Shit 100');
goto 100
end; }

if (i=1) and (j=1) then
                                  begin
dLsx2[pp,i,j]:=0;
dLsy1[pp,i,j]:=0;
Small;
      Lx:= (RNsx[pp,i+1,j]-RNsx[pp,i,j]);
      Ly:= (RNsy[pp,i+1,j]-RNsy[pp,i,j]);
      L:=sqrt(sqr(Lx)+sqr(Ly));
      V:=(L0x*ks);
      if ((L>=L0x) and (L<= V)) and (dLsx1[pp,i,j]=1) then
      begin
      dL:=(L-L0x);
      dLx:=Lx*(dL/L);
      dLy:=Ly*(dL/L);
      Fx1:=Ees*dLx;
      Fy1:=Ees*dLy;
      end;
      if (L > V) then
      begin
      Fx1:=0;
      Fy1:=0;
      dLsx1[pp,i,j]:=0;
      dLsx2[pp,i+1,j]:=0;
      end;
      if (L< L0x) then
      begin
      dL:=(L-L0x);
      dLx:=Lx*(dL/L);
      dLy:=Ly*(dL/L);
      Fx1:=Ees*dLx;
      Fy1:=Ees*dLy;
      end;
Small_2;
      Lx:= (RNsx[pp,i,j+1]-RNsx[pp,i,j]);
      Ly:= (RNsy[pp,i,j+1]-RNsy[pp,i,j]);
      L:=sqrt(sqr(Lx)+sqr(Ly));
```

```
        V:=(L0y*ks);
        if ((L>=L0y) and (L <= V)) and (dLsy2[pp,i,j]=1) then
                              begin
        dL:=(L-L0y);
        dLx:=Lx*(dL/L);
        dLy:=Ly*(dL/L);
        Fx2:=Ees*dLx;
        Fy2:=Ees*dLy;
                               end;
        if (L > V) then
                            begin
        Fx2:=0;
        Fy2:=0;
        dLsy2[pp,i,j]:=0;
        dLsy1[pp,i,j+1]:=0;
                               end;

        if (L< L0y) then
                               begin
        dL:=(L-L0y);
        dLx:=Lx*(dL/L);
        dLy:=Ly*(dL/L);
        Fx2:=Ees*dLx;
        Fy2:=Ees*dLy;
                               end;

        Fsx[pp,i,j]:=Fx1+Fx2;
        Fsy[pp,i,j]:=Fy1+Fy2;

        end;

if (i=1) and ((j>1) and (j<NYs)) then
                                    begin
dLsx2[pp,i,j]:=0;
Small;
        Lx:= (RNsx[pp,i+1,j]-RNsx[pp,i,j]);
        Ly:= (RNsy[pp,i+1,j]-RNsy[pp,i,j]);
        L:=sqrt(sqr(Lx)+sqr(Ly));
        V:=(L0x*ks);
        if ((L>=L0x) and (L <= V)) and (dLsx1[pp,i,j]=1) then
                              begin
        dL:=(L-L0x);
        dLx:=Lx*(dL/L);
        dLy:=Ly*(dL/L);
        Fx1:=Ees*dLx;
        Fy1:=Ees*dLy;
                               end;
        if (L > V) then
                            begin
        Fx1:=0;
        Fy1:=0;
        dLsx1[pp,i,j]:=0;
        dLsx2[pp,i+1,j]:=0;
                               end;
        if (L < L0x ) then
                               begin
        dL:=(L-L0x);
```

```
        dLx:=Lx*(dL/L);
        dLy:=Ly*(dL/L);
        Fx1:=Ees*dLx;
        Fy1:=Ees*dLy;
                          end;
Small_2;
        Lx:= (RNsx[pp,i,j-1]-RNsx[pp,i,j]);
        Ly:= (RNsy[pp,i,j-1]-RNsy[pp,i,j]);
        L:=sqrt(sqr(Lx)+sqr(Ly));
        V:=(L0y*ks);
        if ((L>=L0y) and (L <= V)) and (dLsy1[pp,i,j]=1) then
                          begin
        dL:=(L-L0y);
        dLx:=Lx*(dL/L);
        dLy:=Ly*(dL/L);
        Fx2:=Ees*dLx;
        Fy2:=Ees*dLy;
                        end;
        if (L > V) then
                         begin
        Fx2:=0;
        Fy2:=0;
        dLsy1[pp,i,j]:=0;
        dLsy2[pp,i,j-1]:=0;
                          end;

        if (L < L0y) then
                          begin
        dL:=(L-L0y);
        dLx:=Lx*(dL/L);
        dLy:=Ly*(dL/L);
        Fx2:=Ees*dLx;
        Fy2:=Ees*dLy;

                          end;
Small_2;
        Lx:= (RNsx[pp,i,j+1]-RNsx[pp,i,j]);
        Ly:= (RNsy[pp,i,j+1]-RNsy[pp,i,j]);
        L:=sqrt(sqr(Lx)+sqr(Ly));
        V:=(L0y*Ks);
        if ((L>=L0y) and (L <= V)) and (dLsy2[pp,i,j]=1) then
                          begin
        dL:=(L-L0y);
        dLx:=Lx*(dL/L);
        dLy:=Ly*(dL/L);
        Fx3:=Ees*dLx;
        Fy3:=Ees*dLy;
                      end;
        if (L > V) then
                         begin
        Fx3:=0;
        Fy3:=0;
        dLsy2[pp,i,j]:=0;
        dLsy1[pp,i,j+1]:=0;
                          end;
        if (L < L0y) then
                          begin
```

```
        dL:=(L-L0y);
        dLx:=Lx*(dL/L);
        dLy:=Ly*(dL/L);
        Fx3:=Ees*dLx;
        Fy3:=Ees*dLy;
                    end;

        Fsx[pp,i,j]:=Fx1+Fx2+Fx3;
        Fsy[pp,i,j]:=Fy1+Fy2+Fy3;

                                end;

if ((i>1) and (i<NXs)) and (j=1) then
                               begin
dLsy1[pp,i,j]:=0;
Small;
        Lx:= (RNsx[pp,i+1,j]-RNsx[pp,i,j]);
        Ly:= (RNsy[pp,i+1,j]-RNsy[pp,i,j]);
        L:=sqrt(sqr(Lx)+sqr(Ly));
        V:=(L0x*ks);
        if ((L>=L0x) and (L <= V)) and (dLsx1[pp,i,j]=1) then
                            begin
        dL:=(L-L0x);
        dLx:=Lx*(dL/L);
        dLy:=Ly*(dL/L);
        Fx1:=Ees*dLx;
        Fy1:=Ees*dLy;
                                        end;
        if (L > V) then
                          begin
        Fx1:=0;
        Fy1:=0;
        dLsx1[pp,i,j]:=0;
        dLsx2[pp,i+1,j]:=0;
                                    end;

        if (L < L0x) then
                            begin
        dL:=(L-L0x);
        dLx:=Lx*(dL/L);
        dLy:=Ly*(dL/L);
        Fx1:=Ees*dLx;
        Fy1:=Ees*dLy;
                                        end;
Small_2;
        Lx:= (RNsx[pp,i-1,j]-RNsx[pp,i,j]);
        Ly:= (RNsy[pp,i-1,j]-RNsy[pp,i,j]);
        V:=(L0x*ks);
        if ((L>=L0x) and (L <= V)) and (dLsx2[pp,i,j]=1) then
                            begin
        L:=sqrt(sqr(Lx)+sqr(Ly));
        dL:=(L-L0x);
        dLx:=Lx*(dL/L);
        dLy:=Ly*(dL/L);
        Fx2:=Ees*dLx;
        Fy2:=Ees*dLy;
                      end;
```

```
        if (L > V) then
                        begin
        Fx2:=0;
        Fy2:=0;
        dLsx2[pp,i,j]:=0;
        dLsx1[pp,i-1,j]:=0;
                         end;
        if (L < L0x) then
                         begin
        L:=sqrt(sqr(Lx)+sqr(Ly));
        dL:=(L-L0x);
        dLx:=Lx*(dL/L);
        dLy:=Ly*(dL/L);
        Fx2:=Ees*dLx;
        Fy2:=Ees*dLy;
                    end;
Small_2;
        Lx:= (RNsx[pp,i,j+1]-RNsx[pp,i,j]);
        Ly:= (RNsy[pp,i,j+1]-RNsy[pp,i,j]);
        L:=sqrt(sqr(Lx)+sqr(Ly));
        V:=(L0y*ks);
        if ((L>=L0y) and (L <= V)) and (dLsy2[pp,i,j]=1) then
                         begin
        dL:=(L-L0y);
        dLx:=Lx*(dL/L);
        dLy:=Ly*(dL/L);
        Fx3:=Ees*dLx;
        Fy3:=Ees*dLy;
                    end;
        if (L > V) then
                        begin
        Fx3:=0;
        Fy3:=0;
        dLsy2[pp,i,j]:=0;
        dLsy1[pp,i,j+1]:=0;
                         end;
        if (L < L0y) then
                         begin
        dL:=(L-L0y);
        dLx:=Lx*(dL/L);
        dLy:=Ly*(dL/L);
        Fx3:=Ees*dLx;
        Fy3:=Ees*dLy;
                    end;

        Fsx[pp,i,j]:=Fx1+Fx2+Fx3;
        Fsy[pp,i,j]:=Fy1+Fy2+Fy3;
                                end;

if (i=NXs) and (j=1) then
                                begin
dLsx1[pp,i,j]:=0;
dLsy1[pp,i,j]:=0;
Small;
        Lx:= (RNsx[pp,i-1,j]-RNsx[pp,i,j]);
        Ly:= (RNsy[pp,i-1,j]-RNsy[pp,i,j]);
        L:=sqrt(sqr(Lx)+sqr(Ly));
```

```
        V:=(L0x*ks) ;
        if ((L>=L0x) and (L <= V)) and (dLsx2[pp,i,j]=1) then
                              begin
        dL:=(L-L0x);
        dLx:=Lx*(dL/L);
        dLy:=Ly*(dL/L);
        Fx1:=Ees*dLx;
        Fy1:=Ees*dLy;
                               end;
        if (L > V) then
                            begin
        Fx1:=0;
        Fy1:=0;
        dLsx2[pp,i,j]:=0;
        dLsx1[pp,i-1,j]:=0;
                               end;
        if (L < L0x) then
                             begin
        dL:=(L-L0x);
        dLx:=Lx*(dL/L);
        dLy:=Ly*(dL/L);
        Fx1:=Ees*dLx;
        Fy1:=Ees*dLy;
                               end;
Small_2;
        Lx:= (RNsx[pp,i,j+1]-RNsx[pp,i,j]);
        Ly:= (RNsy[pp,i,j+1]-RNsy[pp,i,j]);
        L:=sqrt(sqr(Lx)+sqr(Ly));
        V:=(L0y*ks) ;
        if ((L>=L0y) and (L <= V)) and (dLsy2[pp,i,j]=1) then
                             begin
        dL:=(L-L0y);
        dLx:=Lx*(dL/L);
        dLy:=Ly*(dL/L);
        Fx2:=Ees*dLx;
        Fy2:=Ees*dLy;
                               end;
        if (L > V) then
                            begin
        Fx2:=0;
        Fy2:=0;
        dLsy2[pp,i,j]:=0;
        dLsy1[pp,i,j+1]:=0;
                               end;

        if (L < L0y) then
                             begin
        dL:=(L-L0y);
        dLx:=Lx*(dL/L);
        dLy:=Ly*(dL/L);
        Fx2:=Ees*dLx;
        Fy2:=Ees*dLy;
                                  end;
        Fsx[pp,i,j]:=Fx1+Fx2;
        Fsy[pp,i,j]:=Fy1+Fy2;
                                end;
```

```
if (i=NXs) and ((j>1) and (j<NYs)) then
                              begin
dLsx1[pp,i,j]:=0;
Small;
      Lx:= (RNsx[pp,i-1,j]-RNsx[pp,i,j]);
      Ly:= (RNsy[pp,i-1,j]-RNsy[pp,i,j]);
      L:=sqrt(sqr(Lx)+sqr(Ly));
      V:=(L0x*ks) ;
      if ((L>=L0x) and (L <= V)) and (dLsx2[pp,i,j]=1) then
                           begin
      dL:=(L-L0x);
      dLx:=Lx*(dL/L);
      dLy:=Ly*(dL/L);
      Fx1:=Ees*dLx;
      Fy1:=Ees*dLy;
                     end;
      if (L > V) then
                          begin
      Fx1:=0;
      Fy1:=0;
      dLsx2[pp,i,j]:=0;
      dLsx1[pp,i-1,j]:=0;
                           end;
      if (L < L0x) then
                           begin
      dL:=(L-L0x);
      dLx:=Lx*(dL/L);
      dLy:=Ly*(dL/L);
      Fx1:=Ees*dLx;
      Fy1:=Ees*dLy;
                     end;
Small_2;
      Lx:= (RNsx[pp,i,j-1]-RNsx[pp,i,j]);
      Ly:= (RNsy[pp,i,j-1]-RNsy[pp,i,j]);
      L:=sqrt(sqr(Lx)+sqr(Ly));
      V:=(L0y*ks);
      if ((L>=L0y) and (L <= V)) and (dLsy1[pp,i,j]=1) then
                           begin
      dL:=(L-L0y);
      dLx:=Lx*(dL/L);
      dLy:=Ly*(dL/L);
      Fx2:=Ees*dLx;
      Fy2:=Ees*dLy;
                           end;
      if (L > V) then
                          begin
      Fx2:=0;
      Fy2:=0;
      dLsy1[pp,i,j]:=0;
      dLsy2[pp,i,j-1]:=0;
                           end;
      if (L < L0y) then
                           begin
      dL:=(L-L0y);
      dLx:=Lx*(dL/L);
      dLy:=Ly*(dL/L);
      Fx2:=Ees*dLx;
```

```
        Fy2:=Ees*dLy;
                              end;
Small_2;
        Lx:= (RNsx[pp,i,j+1]-RNsx[pp,i,j]);
        Ly:= (RNsy[pp,i,j+1]-RNsy[pp,i,j]);
        L:=sqrt(sqr(Lx)+sqr(Ly));
        V:=(L0y*ks) ;
        if ((L>=L0y) and (L <= V)) and (dLsy2[pp,i,j]=1) then
                             begin
        dL:=(L-L0y);
        dLx:=Lx*(dL/L);
        dLy:=Ly*(dL/L);
        Fx3:=Ees*dLx;
        Fy3:=Ees*dLy;
                           end;
        if (L > V) then
                            begin
        Fx3:=0;
        Fy3:=0;
        dLsy2[pp,i,j]:=0;
        dLsy1[pp,i,j+1]:=0;
                             end;

        if (L < L0y) then
                             begin
        dL:=(L-L0y);
        dLx:=Lx*(dL/L);
        dLy:=Ly*(dL/L);
        Fx3:=Ees*dLx;
        Fy3:=Ees*dLy;
                           end;

        Fsx[pp,i,j]:=Fx1+Fx2+Fx3;
        Fsy[pp,i,j]:=Fy1+Fy2+Fy3;
                                end;

if (i=NXs) and (j=NYs) then
                                  begin
dLsx1[pp,i,j]:=0;
dLsy2[pp,i,j]:=0;
Small;
        Lx:= (RNsx[pp,i-1,j]-RNsx[pp,i,j]);
        Ly:= (RNsy[pp,i-1,j]-RNsy[pp,i,j]);
        L:=sqrt(sqr(Lx)+sqr(Ly));
        V:=(L0x*ks) ;
        if ((L>=L0x) and (L<= V)) and (dLsx2[pp,i,j]=1) then
                             begin
        dL:=(L-L0x);
        dLx:=Lx*(dL/L);
        dLy:=Ly*(dL/L);
        Fx1:=Ees*dLx;
        Fy1:=Ees*dLy;
                           end;
        if (L > V) then
                             begin
        Fx1:=0;
        Fy1:=0;
```

```
        dLsx2[pp,i,j]:=0;
        dLsx1[pp,i-1,j]:=0;
                          end;
        if (L< L0x) then
                         begin
        dL:=(L-L0x);
        dLx:=Lx*(dL/L);
        dLy:=Ly*(dL/L);
        Fx1:=Ees*dLx;
        Fy1:=Ees*dLy;
                     end;
Small_2;
        Lx:= (RNsx[pp,i,j-1]-RNsx[pp,i,j]);
        Ly:= (RNsy[pp,i,j-1]-RNsy[pp,i,j]);
        L:=sqrt(sqr(Lx)+sqr(Ly));
        V:=(L0y*ks);
        if ((L>=L0y) and (L <= V)) and (dLsy1[pp,i,j]=1) then
                         begin
        dL:=(L-L0y);
        dLx:=Lx*(dL/L);
        dLy:=Ly*(dL/L);
        Fx2:=Ees*dLx;
        Fy2:=Ees*dLy;
                        end;
        if (L > V) then
                        begin
        Fx2:=0;
        Fy2:=0;
        dLsy1[pp,i,j]:=0;
        dLsy2[pp,i,j-1]:=0;
                         end;

        if (L < L0y) then
                         begin
        dL:=(L-L0y);
        dLx:=Lx*(dL/L);
        dLy:=Ly*(dL/L);
        Fx2:=Ees*dLx;
        Fy2:=Ees*dLy;
                        end;

        Fsx[pp,i,j]:=Fx1+Fx2;
        Fsy[pp,i,j]:=Fy1+Fy2;
                              end;
if ((i>1) and (i<NXs)) and (j=NYs) then
                                begin
dLsy2[pp,i,j]:=0;
Small;
        Lx:= (RNsx[pp,i+1,j]-RNsx[pp,i,j]);
        Ly:= (RNsy[pp,i+1,j]-RNsy[pp,i,j]);
        L:=sqrt(sqr(Lx)+sqr(Ly));
        V:=(L0x*ks) ;
        if ((L>=L0x) and (L <= V)) and (dLsx1[pp,i,j]=1) then
                        begin
        dL:=(L-L0x);
        dLx:=Lx*(dL/L);
        dLy:=Ly*(dL/L);
```

```
        Fx1:=Ees*dLx;
        Fy1:=Ees*dLy;
                              end;
        if (L > V) then
                            begin
        Fx1:=0;
        Fy1:=0;
        dLsx1[pp,i,j]:=0;
        dLsx2[pp,i+1,j]:=0;
                             end;
        if (L < L0x) then
                            begin
        dL:=(L-L0x);
        dLx:=Lx*(dL/L);
        dLy:=Ly*(dL/L);
        Fx1:=Ees*dLx;
        Fy1:=Ees*dLy;
                             end;
small_2;
        Lx:= (RNsx[pp,i-1,j]-RNsx[pp,i,j]);
        Ly:= (RNsy[pp,i-1,j]-RNsy[pp,i,j]);
        L:=sqrt(sqr(Lx)+sqr(Ly));
        V:=(L0x*ks) ;
        if ((L>=L0x) and (L <= V)) and (dLsx2[pp,i,j]=1) then
                            begin
        dL:=(L-L0x);
        dLx:=Lx*(dL/L);
        dLy:=Ly*(dL/L);
        Fx2:=Ees*dLx;
        Fy2:=Ees*dLy;
                            end;
        if (L > V) then
                           begin
        Fx2:=0;
        Fy2:=0;
        dLsx2[pp,i,j]:=0;
        dLsx1[pp,i-1,j]:=0;
                            end;
        if (L < L0x) then
                            begin
        dL:=(L-L0x);
        dLx:=Lx*(dL/L);
        dLy:=Ly*(dL/L);
        Fx2:=Ees*dLx;
        Fy2:=Ees*dLy;
                            end;
small_2;
        Lx:= (RNsx[pp,i,j-1]-RNsx[pp,i,j]);
        Ly:= (RNsy[pp,i,j-1]-RNsy[pp,i,j]);
        L:=sqrt(sqr(Lx)+sqr(Ly));
        V:=(L0y*ks) ;
        if ((L>=L0y) and (L <= V)) and (dLsy1[pp,i,j]=1) then
                            begin
        dL:=(L-L0y);
        dLx:=Lx*(dL/L);
        dLy:=Ly*(dL/L);
        Fx3:=Ees*dLx;
```

```
        Fy3:=Ees*dLy;
                          end;
        if (L > V) then
                        begin
        Fx3:=0;
        Fy3:=0;
        dLsy1[pp,i,j]:=0;
        dLsy2[pp,i,j-1]:=0;
                            end;
        if (L < L0y) then
                          begin
        dL:=(L-L0y);
        dLx:=Lx*(dL/L);
        dLy:=Ly*(dL/L);
        Fx3:=Ees*dLx;
        Fy3:=Ees*dLy;
                          end;

        Fsx[pp,i,j]:=Fx1+Fx2+Fx3;
        Fsy[pp,i,j]:=Fy1+Fy2+Fy3;

                             end;
if ((i>1) and (i<NXs)) and ((j>1) and (j<NYs)) then
                             begin
Small;
        Lx:= (RNsx[pp,i+1,j]-RNsx[pp,i,j]);
        Ly:= (RNsy[pp,i+1,j]-RNsy[pp,i,j]);
        L:=sqrt(sqr(Lx)+sqr(Ly));
        V:=(L0x*ks) ;
        if ((L>=L0x) and (L <= V)) and (dLsx1[pp,i,j]=1) then
                          begin

        dL:=(L-L0x);
        dLx:=Lx*(dL/L);
        dLy:=Ly*(dL/L);
        Fx1:=Ees*dLx;
        Fy1:=Ees*dLy;
                                    end;
        if (L > V) then
                                  begin
        Fx1:=0;
        Fy1:=0;
        dLsx1[pp,i,j]:=0;
        dLsx2[pp,i+1,j]:=0;
                           end;

        if (L < L0x) then
                          begin

        dL:=(L-L0x);
        dLx:=Lx*(dL/L);
        dLy:=Ly*(dL/L);
        Fx1:=Ees*dLx;
        Fy1:=Ees*dLy;
                                    end;
small_2;
        Lx:= (RNsx[pp,i-1,j]-RNsx[pp,i,j]);
```

```
        Ly:= (RNsy[pp,i-1,j]-RNsy[pp,i,j]);
        L:=sqrt(sqr(Lx)+sqr(Ly));
        V:=(L0x*ks);
        if ((L>=L0x) and (L <= V)) and (dLsx2[pp,i,j]=1) then
                          begin
        dL:=(L-L0x);
        dLx:=Lx*(dL/L);
        dLy:=Ly*(dL/L);
        Fx2:=Ees*dLx;
        Fy2:=Ees*dLy;
                        end;
        if (L > V) then
                         begin
        Fx2:=0;
        Fy2:=0;
        dLsx2[pp,i,j]:=0;
        dLsx1[pp,i-1,j]:=0;
                          end;
        if (L < L0x) then
                          begin

        dL:=(L-L0x);
        dLx:=Lx*(dL/L);
        dLy:=Ly*(dL/L);
        Fx2:=Ees*dLx;
        Fy2:=Ees*dLy;
                        end;
small_2;
        Lx:= (RNsx[pp,i,j-1]-RNsx[pp,i,j]);
        Ly:= (RNsy[pp,i,j-1]-RNsy[pp,i,j]);
        L:=sqrt(sqr(Lx)+sqr(Ly));
        V:=(L0y*ks);
        if ((L>=L0y) and (L <= V)) and (dLsy1[pp,i,j]=1) then
                          begin
        dL:=(L-L0y);
        dLx:=Lx*(dL/L);
        dLy:=Ly*(dL/L);
        Fx3:=Ees*dLx;
        Fy3:=Ees*dLy;
                        end;
        if (L > V) then
                         begin
        Fx3:=0;
        Fy3:=0;
        dLsy1[pp,i,j]:=0;
        dLsy2[pp,i,j-1]:=0;
                          end;
        if (L < L0y) then
                          begin
        dL:=(L-L0y);
        dLx:=Lx*(dL/L);
        dLy:=Ly*(dL/L);
        Fx3:=Ees*dLx;
        Fy3:=Ees*dLy;
                        end;
small_2;
        Lx:= (RNsx[pp,i,j+1]-RNsx[pp,i,j]);
```

```
        Ly:= (RNsy[pp,i,j+1]-RNsy[pp,i,j]);
        L:=sqrt(sqr(Lx)+sqr(Ly));
        V:=(L0y*ks);
        if ((L>=L0y) and (L <= V)) and (dLsy2[pp,i,j]=1) then
                          begin

        dL:=(L-L0y);
        dLx:=Lx*(dL/L);
        dLy:=Ly*(dL/L);
        Fx4:=Ees*dLx;
        Fy4:=Ees*dLy;
                         end;
        if (L > V) then
                         begin
        Fx4:=0;
        Fy4:=0;
        dLsy2[pp,i,j]:=0;
        dLsy1[pp,i,j+1]:=0;
                           end;
        if (L < L0y) then
                          begin
        dL:=(L-L0y);
        dLx:=Lx*(dL/L);
        dLy:=Ly*(dL/L);
        Fx4:=Ees*dLx;
        Fy4:=Ees*dLy;
                         end;

        Fsx[pp,i,j]:=Fx1+Fx2+Fx3+Fx4;
        Fsy[pp,i,j]:=Fy1+Fy2+Fy3+Fy4;
                            end;
if (i=1) and (j=NYs) then
                               begin
dLsy2[pp,i,j]:=0;
dLsx2[pp,i,j]:=0;
Small;
        Lx:= (RNsx[pp,i+1,j]-RNsx[pp,i,j]);
        Ly:= (RNsy[pp,i+1,j]-RNsy[pp,i,j]);
        L:=sqrt(sqr(Lx)+sqr(Ly));
        V:=(L0x*ks);
        if ((L>=L0x) and (L <= V)) and (dLsx1[pp,i,j]=1) then
                          begin

        dL:=(L-L0x);
        dLx:=Lx*(dL/L);
        dLy:=Ly*(dL/L);
        Fx1:=Ees*dLx;
        Fy1:=Ees*dLy;
                         end;
        if (L > V) then
                         begin
        Fx1:=0;
        Fy1:=0;
        dLsx1[pp,i,j]:=0;
        dLsx2[pp,i+1,j]:=0;
                           end;
        if (L < L0x) then
```

```
                        begin

        dL:=(L-L0x);
        dLx:=Lx*(dL/L);
        dLy:=Ly*(dL/L);
        Fx1:=Ees*dLx;
        Fy1:=Ees*dLy;
                        end;
small_2;
        Lx:= (RNsx[pp,i,j-1]-RNsx[pp,i,j]);
        Ly:= (RNsy[pp,i,j-1]-RNsy[pp,i,j]);
        L:=sqrt(sqr(Lx)+sqr(Ly));
        V:=(L0y*ks);
        if ((L>=L0y) and (L<= V)) and (dLsy1[pp,i,j]=1) then
                        begin
        dL:=(L-L0y);
        dLx:=Lx*(dL/L);
        dLy:=Ly*(dL/L);
        Fx2:=Ees*dLx;
        Fy2:=Ees*dLy;
                        end;
        if (L > V) then
                        begin
        Fx2:=0;
        Fy2:=0;
        dLsy1[pp,i,j]:=0;
        dLsy2[pp,i,j-1]:=0;
                        end;
        if (L< L0y) and (dLsy1[pp,i,j]=0) then
                        begin
        dL:=(L-L0y);
        dLx:=Lx*(dL/L);
        dLy:=Ly*(dL/L);
        Fx2:=Ees*dLx;
        Fy2:=Ees*dLy;
                        end;
        Fsx[pp,i,j]:=Fx1+Fx2;
        Fsy[pp,i,j]:=Fy1+Fy2;
                        end;
      RX2[pp,i,j]:=R0sy[pp,i,j]-RNsy[pp,i,j];
      YYt[pp,i,j]:=YYt[pp,i,j]-RX2[pp,i,j];
      R0sx[pp,i,j]:=0;  R0sy[pp,i,j]:=0;
      R0sx[pp,i,j]:=RNsx[pp,i,j];
      R0sy[pp,i,j]:=RNsy[pp,i,j];

 end;
{regid;}
Metal_calculations;
100:pp:=pp+1;
until (g = ZZ);
pp:=1;
g:=0;

 if (EE = dt) and (ZZ < tt) then
  begin
  EE:=0;
  ZZ:=ZZ+1;
```

```
  end;
k:=k+1;
E:=E+dt;
EE:=EE+dt;
t:=t+dt;
fs:=fs+dt;
RRT:=RRT+dt;
{if ((t>=0.1) and (t< (0.1+dt))) then
begin
extra;
halt;
end;}
until {(t >= key) or} (R0sx[tt,1,1] <= 1);    {end of the calculation}
{extra;}
200:writeln;
end;
                              { The Main Program }
begin
inputs;
Sand_positions;
Metal_positions;
Sand_Calculations;
outs;
close(sandpocu2);
close(sandcdcu2);
close(metalcdcu2);
close(metalpocu2);
close(result6);
close (file);

end.
```